1992

Performance improvements study of steam turbine exhaust hoods

Sinan ðCelen
Lehigh University

AUTHOR:

Celen, Sinan

TITLE:

Performance Study of Steam Turbine Exhaust Hoods.

DATE: January 17, 1993

Performance Improvement Study of Steam Turbine Exhaust Hoods

by

Sinan Çelen

A Thesis

Presnted to the Graduate and Research Committee

of Lehigh University

in Candidacy for the Degree of

Master of Science

in

Mechanical Engineering

Lehigh University

December 1992

This thesis is accepted and approved in partial fulfillment of the requirements for the degree of Master of Science.

November 25, 1992

Date

Thesis Advisor

Chairperson of Department

To my parents

ACKNOWLEDGEMENTS

The author would like to thank Prof. Jerzy Owczarek of Mechanical Engineering Department at Lehigh University for his help and motivation during the course of this study. Invaluable help throughout this work was also provided by Dr. Art Warnock.

The author is grateful to Behzat Türegün who initiated this work by designing the test loop and the generic model.

Special thanks to Yeşim Erke and Özgür Akın for their care and friendship.

Finally the author would like to express his deepest gratitudes to his parents and his brother for their continous support.

TABLE OF CONTENTS

LIST OF TABLES

LIST OF FIGURES

NOMENCLATURE

A	cross-sectional area, hood annulus length
AR	area ratio, A_2/A_1
B	blocked area fraction, hood length
$C_{LOSS,DIFF}$	non-dimensional diffuser loss coefficient
C_p	specific heat at constant pressure, pressure coefficient
$\underline{C}_P$	pressure coefficient (equation (35))
C_{PR}	pressure recovery coefficient
C_{pi}	ideal pressure recovery coefficient
d	venturi meter pipe diameter
D	hood width
H	total energy loss, hood height
h	specific enthalpy, inlet annulus height in diffuser
H_L	total pressure loss coefficient
HL	hood loss
(H+C)L	hood and condenser neck loss
L	last stage rotor blade height, wall length of diffuser
LL	leaving loss
L_v	axial length of guide vane
M, M_{AN}	annulus Mach number
N	diffuser length

P	static pressure
P_{AN}	average annulus static pressure
$P_{T,AN}$	average annulus total pressure
q	dynamic head based on mass averaged velocity ($\rho V^2/2$)
R	radius, gas constant
Re	Reynolds number
S	specific humidity
s	specific entropy
T	temperature
V	mass averaged velocity
W	mass flow rate, width of a two-dimensional diffuser

Greek Symbols

α	kinetic-energy-flux velocity-profile parameter
ß	diameter ratio of venturi meter
γ	ratio of specific heats
δ^*	boundary layer displacement thickness
ϵ	overall effectiveness of a diffuser
ν	dynamic viscosity
ρ	fluid density
ϕ	channel divergence half angle
Ψ	swirl angle

Subscripts

air	air
AN	annulus
ATM	atmospheric conditions
AVE	average
C	condenser
FL	flange
H	hub
i	inner, inlet
IDEAL	ideal conditions; no losses
lab	test lab conditions
LOC	particular location on the hub or the shroud in the annulus
MAX	maximum
o	outer, outlet
T	total conditions
t	throat
v	vapor
vent	value obtained at the venturi meter
∞	far downstream or upstream
1	diffuser inlet, anuulus
2	diffuser exit, flange

ABSTRACT

The exhaust hood loss represents the energy loss due to friction and the inability of the hood to properly diffuse the flow. The current performance of old low pressure turbine exhaust hoods is less than optimum. Little, if any, of the available kinetic energy in the steam exiting from the last row of blades of the low pressure turbine is recovered by diffusion. The objective of this study was to carry out an experimental investigation using air model tests to gather the data needed to optimize the design of the low pressure turbine hood and condenser neck for a range of large steam turbine designs. A generic model design was used to study the effect of the hood size relative to the last rotating blade height on the exhaust hood loss.

An annular diffuser review is given to form a basis for design of a diffusing type exhaust hood. Equations for computing the exhaust hood loss coefficient and dimensionless parameters affecting the performance of a turbine exhaust hood are discussed. The experimental procedure is described, and the results of the experiments for two different generic model configurations are presented.

1. INTRODUCTION

The continuing increase in the cost of fuel combined with the decrease in the availability of energy sources emphasize the importance of increasing the efficiency of the existing steam power plants. The manufacturers of individual components of the power plants make effort to improve their performance, but the overall improvements are difficult to achieve because they depend on the interaction between a number of components.

In a steam power plant the low pressure steam leaving the turbine enters the condenser through an exhaust hood. The turbine exhaust hood includes the inlet annulus, the flow guide, the bearing cone, the outer shell, the supporting struts, and the inlet flange to the condenser neck. A schematic drawing of an exhaust hood is shown in figure 1. The structural part located between the exhaust hood (or condenser) flange and the condenser tube bundles is called the condenser neck. It includes the flange, reinforcing structural beams for the condenser neck, feedwater heaters, and associated extraction piping.

In most large utility steam turbines, the steam flowing out axially from the last row of blades of a low pressure (LP) turbine has to turn 90° in order to flow downward into the condenser. The kinetic energy of the steam exiting the last row of blades is called the leaving loss. The leaving loss per unit mass of the flowing steam is equal to one-half of the exit velocity squared ($V^2/2$). It represents a part of the available energy of the steam which is not converted into useful work in a turbine. The hood loss is

defined as the isentropic enthalpy drop from the exit of the last row of blades to the condenser flange. When, as a result of diffusion, $P_{AN} < P_{FL}$, the hood loss is said to be negative. The condenser neck loss corresponds to the isentropic enthalpy drop from the flange pressure, P_{FL}, to the pressure above the condenser tube, P_C. The hood and condenser neck losses depend on the overall geometry of the exhaust hood and the condenser neck, on the average Mach number at the exit from the last stage, and on the kinetic energy of the steam leaving the last row of blades. Figure 2 indicates these losses on an enthalpy-entropy diagram. The frictional losses have the effect of increasing the static pressure at the exit of last row of blades, P_{AN}, above the static pressure at the condenser flange, P_{FL}. The hood and condenser neck losses can be reduced by modifications in the geometry of the exhaust hood and condenser neck. Reduced losses result in a lowering of the static pressure at the exit of the last row of blades, P_{AN}, and a power gain for the turbine generator unit.

2. ANNULAR DIFFUSERS:

A diffusing type exhaust hood is said to have negative hood loss. In such case the last stage exit annulus pressure, P_{AN}, is lower than the condenser flange pressure, P_{FL}. In a study of performance of exhaust hoods, it is important to understand the performance characteristics of diffusers. Since the flow passage cross section at the last stage annulus of a turbine has an annular shape, the performance of annular type diffusers will now be discussed.

2.1. Performance Parameters:

There is no satisfactory analytical method for predicting the performance of a diffuser with an arbitrary shape and inlet flow velocity distribution. The only way to learn about the performance of diffusers with different geometries and inlet conditions is to perform systematic experiments.

The most important quantity describing the performance of a diffuser is the static pressure rise in it. Experiments show that, without swirl in the flow, the static pressure is fairly uniform over any cross section of the diffuser, although the velocity generally varies .

When representing a diffuser performance, the measured pressure rise is compared to the maximum value that could be theoretically obtained at the particular flow rate, which corresponds to an infinite area ratio, or zero exit velocity. The pressure recovery coefficient is defined as

$$C_{PR}=\frac{\Delta P_{ACTUAL}}{\Delta P_{MAX}}=\frac{\Delta P_{ACTUAL}}{\frac{\rho V_1^2}{2}}=\frac{P_{2,ACT}-P_1}{\frac{\rho V_1^2}{2}} \quad (1)$$

where, $P_{2,ACT}$ denotes the actual exit pressure and P_1 denotes the inlet pressure.

Another useful diffuser performance parameter is one based on an ideal, inviscid and uniform fluid flow. Writing the Bernoulli equation for uniform, incompressible flow without any losses and change in elevation:

$$\frac{P_1}{\rho}+\frac{V_1^2}{2}=\frac{P_2}{\rho}+\frac{V_2^2}{2} \quad (2)$$

where subscripts 1 and 2 refer to inlet and exit sections respectively, and the continuity equation:

$$V_2=V_1\frac{A_1}{A_2} \quad (3)$$

we obtain the expression for the ideal pressure recovery coefficient which is only a function of the area ratio, AR, of a diffuser:

$$\frac{(P_2-P_1)_{IDEAL}}{\frac{\rho V_1^2}{2}}=1-\frac{1}{AR^2}=C_{pi} \quad (4)$$

where the area ratio, $AR=A_2/A_1$.

For annular diffusers, the geometric area ratio of the diffusers is dependent on the divergence angles of the inner and outer walls, ϕ_2 and ϕ_1, on the ratio of the wall length to the inlet annulus height, L/h, and on the ratio of the annulus radius at the diffuser

entry, R_i/R_o.

$$AR=1+2\frac{L}{h}\frac{\left(\sin\phi_1+\frac{R_i}{R_o}\sin\phi_2\right)}{\left(1+\frac{R_i}{R_o}\right)}+\frac{L^2}{h^2}\frac{\left(1-\frac{R_i}{R_o}\right)\left(\sin^2\phi_1-\sin^2\phi_2\right)}{\left(1+\frac{R_i}{R_o}\right)} \tag{5}$$

see reference[2].

A straight-cone annular diffuser has a central cone angle, ϕ_2, equal to zero. For straight cone annular diffuser, the expression for the area ratio becomes,[2]:

$$AR=1+\frac{2L\sin\phi}{h\left(1+\frac{R_i}{R_o}\right)}+\frac{L^2\sin^2\phi}{h^2}\frac{\left(1-\frac{R_i}{R_o}\right)}{\left(1+\frac{R_i}{R_o}\right)} \tag{6}$$

The simplest case for annular diffusers is the one having equal inner and outer cone angles ($\phi_1=\phi_2$). For such diffusers the expression for the area ratio becomes:

$$AR=1+2\frac{L}{h}\sin\phi \tag{7}$$

Equi-angular annular and straight cone annular diffusers are shown in figure 3.

The overall diffuser effectiveness relates actual pressure rise to that achievable from same geometry with an ideal one-dimensional, or 1-D, flow at the same flow rate:

$$\epsilon=\frac{\Delta P}{\Delta P_i}=\frac{\Delta P/\Delta P_{MAX}}{\Delta P_i/\Delta P_{MAX}}=\frac{C_{PR}}{C_{pi}} \tag{8}$$

The total energy loss in a diffuser, H, for a real incompressible flow

$$H=\left(\frac{P_1}{\rho}+\frac{1}{2}V_1^2\right)-\left(\frac{P_2}{\rho}+\frac{1}{2}V_2^2\right) \tag{9}$$

can be expressed in terms of the non-dimensional diffuser loss coefficient, $C_{LOSS,DIF}$, defined as:

$$C_{LOSS,DIF}=\frac{H}{\frac{1}{2}V_1^2}=\frac{\left(\frac{1}{2}\left(V_2^2-V_1^2\right)\right)-\left(\frac{P_2-P_1}{\rho}\right)}{\frac{1}{2}V_1^2} \tag{10}$$

or,

$$C_{LOSS,DIF}=1-AR^2-\left(\frac{P_2-P_1}{\frac{\rho V_1^2}{2}}\right) \tag{11}$$

It can be represented by equation:

$$C_{LOSS,DIF}=C_{pi}-C_{PR} \tag{12}$$

2.2. Flow Regimes and Performance Characteristics:

In most applications, diffusers are used in turbomachines such as compressors and turbines. When another turbomachine is placed downstream of a diffuser, the uniformity and steadiness of diffuser discharge is extremely important because it has a direct effect on the performance of the neighbouring turbomachine.

Kline, Abbot and Fox [3] related the overall geometric characteristics of two-dimensional, or 2-D, diffusers to the occurrences of unsteadiness and non-uniformities of discharge flow. The results show that four diffuser flow regimes exist:

2.2.1. Region of No Appreciable Stall. It corresponds to well-behaved, steady and fairly uniform, unseparated flow. In such flow pressure increases along the diffuser, although the magnitude of the pressure rise is very small. This type of flow should be expected when the area ratio of the diffuser is small and the diffuser has a relatively long length. Due to small pressure rise, the pressure recovery coefficient is also small. In this flow the ideal and actual pressure recovery coefficients are close to each other resulting in a high effectiveness, ϵ.

2.2.2. Region of Transitory Stall. This is an unsteady and non-uniform flow. In this regime the separation varies in size, intensity and position with time. For a given diffuser length, the area ratio of a diffuser operating in the transitory stall regime is greater than that of the diffuser operating in a non-appreciable stall regime. Therefore, the ideal pressure recovery coefficient is also greater.

2.2.3. Fully-Developed Stall Regime. This is a reasonably steady, but very non-uniform flow. In this flow a major portion of the diffuser is filled with a recirculation region extending from a position close to the inlet and continuing to the exit of the diffuser. This regime occurs when the pressure gradient becomes too large to support flow wholly attached to diffuser walls. Pressure recovery coefficients and effectiveness are small in this flow because of large losses.

2.2.4. Jet Flow Regime. This is a reasonably steady, but very non-uniform flow.

In the jet flow regime, the main flow is completely separated from the walls. The pressure recovery coefficients and the effectiveness are low.

Figure 4 shows the schematic diagram of diffuser flow regimes, and figure 5 illustrates the performance characteristics of 2-D diffusers.

Howard, Henseler and Thornton-Trump [2], observed the flow regimes for equiangular and straight core type annular diffusers. The results for equiangular case are compared with data on 2-D diffusers in figure 6. The positions of first appreciable stall for all diffusers are compared in figure 7.

Howard, Henseler and Thornton-Trump have found that in annular diffusers, the stall forms always on the outer cone and commonly over a limited circumferential region. Figure 6 shows that, for annular diffusers, the first stall line *a-a*, is close to that for 2-D diffusers, but the fully developed stall line *b-b* is significantly lower. That is, for annular diffusers a fully developed stall occurs at smaller diffuser divergence angles, 2ϕ.

2.3. Effect of Inlet Conditions on Performance:

2.3.1. Effect of Inlet Turbulence:

Since the turbulent boundary layers are more resistant to separation than the laminar boundary layers, pressure recovery of diffusers can be improved by increasing the inlet turbulence. In addition, the turbulent flow velocity profile is more flat than the laminar flow velocity profile. This reduction in velocity profile distortion and the delay of separation with increased inlet turbulence improve the pressure recovery.

2.3.2. Effect of Swirl at Inlet:

In a flow downstream of a pump or turbine, some swirl is usually present. The

effects of swirling flow must be always kept in mind when designing a diffuser. The effects of swirling inlet flow on pressure recovery coefficient depend on the flow regime of the diffuser that would exist for axial inlet flow. Swirling inlet flow can improve the performance of diffusers by delaying flow separation. For flows without any separation, the swirling inlet flow does not provide any improvement.

Several tests have been performed for different swirl angles. Figure 8 shows the effect of inlet swirl angle Ψ and inner cant angle ϕ_i on the pressure recovery. For diffusers with negative inner cant angle, ϕ_i, swirl at inlet reduces pressure recovery. On the other hand, for diffusers with positive inner cant angle, ϕ_i, swirl at inlet increases pressure recovery (The cant angle is negative when the cross section of hub decreases in the flow direction).

2.3.3. Effect of Inlet Boundary Layer Thickness:

Figure 9 shows schematically the boundary layer blockage concept. If α is defined as the ratio of the actual kinetic energy flux to the kinetic energy flux for flow with uniform velocity profile at the same cross section and flow rate ($\alpha=V^2/\bar{V}^2$), and q is defined as the dynamic head ($\rho V^2/2$), then the mass averaged total pressure of an incompressible internal flow at any cross section can be expressed as:

$$P_T=P+\alpha q \tag{13}$$

The pressure rise can be expressed as:

$$\Delta P=P_2 - P_1=(\alpha_1 q_1-\alpha_2 q_2)-(P_{T,1}-P_{T,2}) \tag{14}$$

Defining the total pressure loss coefficient as:

$$H_L = \frac{(P_{T,1} - P_{T,2})}{q} \tag{15}$$

the expression for the effectiveness can be written as:

$$\epsilon = \frac{\Delta P}{\Delta P_i} = \frac{C_{PR}}{C_{pi}} = \frac{\alpha_1 - \alpha_2 \frac{1}{AR^2}}{C_{pi}} - \frac{H_L}{C_{pi}} \tag{16}$$

2.3.4. Effect of Mach Number:

When the flow Mach number is greater than unity, shock-boundary layer interactions may cause flow separation, degrading the performance of the diffuser.

3. METHOD OF EXHAUST LOSS EVALUATION

3.1. Equations for the Hood Loss Coefficient:

Figure 2 illustrates the exhaust hood loss and the leaving losss on an h-s diagram. The hood loss, as defined on this h-s diagram, and the isentropic gas dynamic relations obtained from the energy and continuity equations of an ideal compressible fluid form the basis for the following methodology for analysis of exhaust hood performance that has been developed by Prof. J.A.Owczarek [1]. This methodology allows determination of the hood loss coefficient from the experimentally measured values of the exhaust hood model annulus total and static pressures, total temperature, and model flange static pressure.

The expression for the leaving loss is,

$$LL=\frac{V_{AN}^{2}}{2}=h_{T,AN}-h_{AN} \tag{17}$$

Since air is used as the working fluid and the temperature variation is small, ideal gas equation of state and constant specific heats can be used. As a result, the leaving loss can be expressed as,

$$LL=\frac{V_{AN}^{2}}{2}=C_pT_{T,AN}\left(1-\frac{T_{AN}}{T_{T,AN}}\right)=C_pT_{T,AN}\left[1-\left(\frac{P_{AN}}{P_{T,AN}}\right)^{\frac{\gamma-1}{\gamma}}\right] \tag{18}$$

The hood loss corresponds to the enthalpy difference between the states 1 and 2' shown in figure 2, because $h_1=h_{AN}$. The hood loss is non-dimensionalized using the

leaving loss by introducing the hood loss coefficient, HL/LL.The equation for the hood loss coefficient becomes:

$$\frac{HL}{LL}=\frac{(h_{T,AN}-h_2')-LL}{LL}=\frac{C_pT_{T,AN}\left(1-\frac{T_2'}{T_{T,AN}}\right)}{C_pT_{T,AN}\left[1-\left(\frac{P_{AN}}{P_{T,AN}}\right)^{\frac{\gamma-1}{\gamma}}\right]}-1 \tag{19}$$

Since

$$\frac{T_2'}{T_{T,AN}}=\left(\frac{P_{FL}}{P_{T,AN}}\right)^{\frac{\gamma-1}{\gamma}} \tag{20}$$

we obtain

$$\frac{HL}{LL}=\frac{\left(\frac{P_{AN}}{P_{T,AN}}\right)^{\frac{\gamma-1}{\gamma}}-\left(\frac{P_{FL}}{P_{T,AN}}\right)^{\frac{\gamma-1}{\gamma}}}{1-\left(\frac{P_{AN}}{P_{T,AN}}\right)^{\frac{\gamma-1}{\gamma}}} \tag{21}$$

The term $(P_{AN}/P_{T,AN})$ is a function of the annulus flow Mach number, M_{AN}:

$$\frac{P_{AN}}{P_{T,AN}}=\left(1+\frac{\gamma-1}{2}M_{AN}^2\right)^{-\frac{\gamma}{\gamma-1}} \tag{22}$$

The ratio $P_{FL}/P_{T,AN}$ is determined from the air model tests for varying flow rates and annulus flow Mach numbers, M_{AN}. For a given exhaust hood, the hood loss coefficient depends on the Reynolds and Mach numbers. In our air test the Reynolds number is quite close to that in the steam turbine whose exhaust hood is being modeled.

For a typical turbine unit modeled, the Reynolds number based on the flow speed in the exit annulus of the LP turbine and the last blade height, at M_{AN}=0.6, is $12.3x10^5$ for steam, and $4.5x10^5$ for the air model. For this reason, the hood loss coefficient obtained from our tests is considered to be only a function of the annulus Mach number, M_{AN}:

$$\frac{HL}{LL}=f_1(M_{AN}) \tag{23}$$

The hood loss coefficient, HL/LL, can be obtained graphically at various annulus Mach numbers, M_{AN}, by plotting the terms

$$\left(\frac{P_{AN}}{P_{T,AN}}\right)^{\frac{\gamma-1}{\gamma}} \quad \text{and} \quad \left(\frac{P_{FL}}{P_{T,AN}}\right)^{\frac{\gamma-1}{\gamma}}$$

versus the Mach number, M_{AN}, as shown in figure 10. The dimensionless hood loss coefficient, HL/LL is represented by the ratio

$$\frac{HL}{LL}=\frac{C}{D} \tag{24}$$

where C and D are the numerator and denominator of the equation (21) respectively. That is,

$$C=\left(\frac{P_{AN}}{P_{T,AN}}\right)^{\frac{\gamma-1}{\gamma}} - \left(\frac{P_{FL}}{P_{T,AN}}\right)^{\frac{\gamma-1}{\gamma}} \tag{25}$$

and,

$$D=1-\left(\frac{P_{AN}}{P_{T,AN}}\right)^{\frac{\gamma-1}{\gamma}} \tag{26}$$

The symbols P_{AN}, P_{FL}, and $P_{T,AN}$ represent the (flow) averaged static pressure in the annulus, average static pressure at the flange, and the (flow) averaged total pressure at the annulus, respectively. The Mach number in the annulus, M_{AN}, can be determined from the equation (22) knowing the average values of $P_{T,AN}$ and P_{AN}, which are experimentally determined.

Measuring the flow rate in the annulus allows the use of a second approach to obtain the Mach number in the annulus. (This Mach number will be referred to as M_{AN}'). In the air model tests the mass flow rate, W, is measured using a standard venturi meter.

The function,

$$\frac{W\sqrt{RT_{T,AN}}}{A_{AN}P_{T,AN}} = \sqrt{\gamma} M'_{AN} \left(1 + \frac{\gamma - 1}{2} M'^{2}_{AN}\right)^{-\frac{\gamma+1}{2(\gamma-1)}} \qquad (27)$$

is tabulated in Air Tables. Knowing W, $T_{T,AN}$, A_{AN} and $P_{T,AN}$, the non-dimensional mass flow rate can be calculated which directly gives the Mach number in the annulus, M_{AN}'. In the text which follows, the superscript ' will refer to a quantity determined using the value of M_{AN}'.

A good agreement between the values of M_{AN} and M_{AN}' indicates reliable total and static pressure measurements in the annulus. A second estimate for the hood loss coefficient, (HL/LL)' can be determined using the M_{AN}' value. First the ratio $(P_{AN}/P_{T,AN})'$ is calculated substituding M_{AN}' into equation (22), which then will give (HL/LL)' when introduced into equation (21).

The measure of the exhaust hood loss can also be expressed using the pressure coefficient,

$$C_p = \frac{P_{AN} - P_{FL}}{\left(\frac{\rho V^2}{2}\right)_{AN}} \qquad (28)$$

instead of the hood loss coefficient HL/LL.

A general remark should be made concerning the (flow) averaged value of the annulus static pressure, P_{AN}. The average static pressure in the last stage annulus, P_{AN}, is not exactly equal to the (flow) averaged value of the local static pressures measured on the hub and the shroud in the annulus. This is so, because the Mach number lines in the annulus followed by a diffuser are curved lines, and not straight radial lines perpendicular to the turbine shaft axis. The curvature of the Mach number lines is influenced by the shape of the diffuser vane near the shroud. It is also influenced by the curvature of the streamlines near the hub, caused by the tendency of the fluid to flow around the hub.

The pressure coefficient, C_p, when used with the average annulus static pressure, P_{AN}, gives a value which is not much different than the hood loss coefficient HL/LL. This can be shown as follows. From

$$Tds = dh - \frac{1}{\rho} dP \qquad (29)$$

it follows that, for an isentropic change of state from 1 to 2', shown in figure 2,

$$\frac{1}{\rho}dP=dh \tag{30}$$

Therefore,

$$\frac{P_{AN}-P_{FL}}{\rho_{AN}^{FL}}=h_{AN}-h_{FL}=h_1-h_2'=HL \tag{31}$$

where the quantity ρ_{AN}^{FL} represents the average fluid density between the annulus and the flange of the exhaust hood for an isentropic process. Recalling that $LL=V^2/2$,

$$\frac{HL}{LL}\cong\frac{P_{AN}-P_{FL}}{\rho_{AN}^{FL}\frac{V^2}{2}}\cong C_P \tag{32}$$

Using the relation,

$$\frac{\rho V^2}{2P_T}=\frac{\gamma M^2}{2}\left(1+\frac{\gamma-1}{2}M^2\right)^{\frac{-\gamma}{\gamma-1}} \tag{33}$$

the expression for the pressure coefficient, C_P, can be written as:

$$C_P=\frac{\frac{P_{AN}}{P_{T,AN}}-\frac{P_{FL}}{P_{T,AN}}}{\frac{\gamma M_{AN}^2}{2}\left(1+\frac{\gamma-1}{2}M_{AN}^2\right)^{-\frac{\gamma}{\gamma-1}}} \tag{34}$$

Another common definition for the pressure coefficient, which will be referred as $\underline{C}_P$, is

$$\underline{C_P} = \frac{P_{AN} - P_{FL}}{P_{T,AN} - P_{AN}} = \frac{\frac{P_{AN}}{P_{T,AN}} - \frac{P_{FL}}{P_{T,AN}}}{1 - \frac{P_{AN}}{P_{T,AN}}} \qquad (35)$$

It can also be used to express the hood loss.

The two different Mach numbers: M_{AN}, which is obtained from the average static and total pressures at the exit annulus of the last stage, and M_{AN}', which is obtained from the mass flow rate, average total pressure, total temperature and the area of the last stage annulus allow determination of four different values for the pressure coefficient, namely, C_p, C_p', $\underline{C}_P$ and $\underline{C}_P$'. As a result, from the air model tests one can obtain six different values of exhaust hood performance parameters: HL/LL, (HL/LL)', C_P, C_P', $\underline{C}_P$ and $\underline{C}_P$'.

3.2. Calculation of Hood Loss Coefficient Using Test Data:

3.2.1. Input Data:

- Total pressure values (in volts) for 31 points for each of the 7 different traverses in the last stage annulus indicated in figure 11.
- Static pressure values (in volts) for 12 different locations positioned circumferentially at the hub and shroud in the last stage annulus. These locations are indicated by symbols H1 to H12, and S1 to S12, in figure 11.
- The atmospheric pressure in the test room, in inches of mercury.
- The atmospheric temperature (in °F) in the test room during the test.
- The relative humidity in the test room during the test.
- The static pressure at the inlet to the venturi meter (in psig).

- The pressure difference across the venturi meter (in inches of H_2O).
- The total temperature, $T_{T,AN}$(in °F) measured at the inlet to the model.
- The static pressure values (in volts) for 28 different locations on the exit flange.

3.2.2. Arranging of the Units of Data:

- **Atmospheric Pressure:**

The specific weight of mercury is determined from a table for the known atmospheric temperature. The table used is given in the appendix C. Then, the atmospheric pressure in psia, is calculated using the relation:

P_{ATM}(in lb_f/in^2) = P_{ATM}(in inches of Hg) x Specific weight of Hg at T_{ATM}(lb_f/in^3)

- **Static and Total Pressure Data:**

The pressure data in volts is first converted into psig units using calibration charts obtained for the pressure transducers (The calibration charts for the transducers are updated from time to time, to ensure reliability of the test data). The pressure data in psig is converted into psia units by adding the atmospheric pressure.

P (in volts) → Calibration Chart → P (in psig) → Add P_{ATM}(in psia) → P (in psia)

- **Total Temperature in °R:**

T_T(in °R) = T_T(in °F) + 459.67

- **3.2.3. Static Pressure Values:**

The static pressure in the annulus is measured at 12 different locations positioned circumferentially at the hub and shroud. These locations are referred as H1 to H12 (hub), and S1 to S12 (shroud), in figure 11.

The static pressure values at the traverse points are estimated using the values at

the hub and the shroud, following the procedure described below.

Using the circumferential variation of static pressure at the hub and shroud, the static pressure values at the walls (hub and shroud) corresponding to the location of a given traverse are found for each of the seven traverses. The static pressure is assumed to vary linearly in the radial direction, from hub to shroud. Therefore a straight line is fit through the hub and shroud static pressure values, from which the corresponding static pressure value for each traverse point in the annulus can be calculated. The increment used for the traverse is constant (0.050 inches); therefore a formula can be derived to calculate the radial distance of each of the 31 data points from the hub. 1st point is the data point at the hub and the 31st point is the data point at the shroud, as shown in figure 12. The distance of n^{th} traverse point from the hub, x_n (in inches), is calculated from equation:

$$x_n=(n-1)\ 0.050$$

Then, the static pressure value for n^{th} traverse point, P_n, is interpolated between the static pressure values at the walls, P_{HUB} and P_{SHR} (in psig).

$$P_n=P_{HUB}-\left(\frac{x_n}{1.5}(P_{HUB}-P_{SHR})\right) \tag{36}$$

The distance between hub and the shroud is 1.5 inches. After calculating the static pressure values at all the traverse points in psig, atmospheric pressure is added to convert the units to psia.

◎ 3.2.4. Mass-Averaging of the Static and Total Pressure Values in the Annulus:

The static and total pressures obtained for the 217 points (31 points for each 7 traverses) in the annulus are mass-flow averaged. For example, the average value of the total pressure is obtained using the formula:

$$P_{T,AN}=\frac{\int (P_{T,AN})_i \rho V dA}{\int \rho V dA} \tag{37}$$

or,

$$P_{T,AN}=\frac{\int (P_{T,AN})_i \frac{W}{A_{AN}}\, dA}{\int \frac{W}{A_{AN}}\, dA}=\frac{\int f(r)\, dr}{\int g(r)\, dr} \tag{38}$$

where r denotes the radius in the annulus and W the mass flow rate. $(P_{T,AN})_i$ represents the total pressure for each traverse point. The integration is done by *Simpson's Method.* For *n* points, the integral between *a* and *b* can be determined from equation,

$$\int_a^b f(x)dx=\frac{h}{3}\left(f(x_1)+4f(x_2)+2f(x_3)+.....+2f(x_{n-2})+4f(x_{n-1})+f(x_n)\right) \tag{39}$$

with h=(b-a)/(n-1).

In our case the integral becomes,

$$\int (P_{T,AN})_i \frac{W}{A_{AN}} \frac{2\pi r}{12} dr \tag{40}$$

The area element *dA* is expressed as $(2\pi rdr/12)$, because the annulus is divided into 12

equal area segments (see figure 11). No swirl is introduced into the flow. Therefore, the values of P_{AN} and $P_{T,AN}$ for area segments 8, 9, 10, 11 and 12 correspond to that of area segments 4, 2, 1, 6 and 5, respectively.

Similarly, the denominator of equation (38) becomes,

$$\int \frac{W}{A_{AN}} \frac{2\pi r}{12} dr \tag{41}$$

Since

$$\frac{W\sqrt{RT_{T,AN}}}{A_{AN}P_{T,AN}} = \sqrt{\gamma} M_{AN} \left(1 + \frac{\gamma - 1}{2} M_{AN}^2\right)^{-\frac{\gamma+1}{2(\gamma-1)}} \tag{42}$$

and

$$M_{AN} = \left[\frac{2}{\gamma - 1}\left(\left(\frac{P_{AN}}{P_{T,AN}}\right)^{\frac{\gamma-1}{-\gamma}} - 1\right)\right]^{1/2} \tag{43}$$

substituting the expression for Mach number, M_{AN}, into equation (42) gives,

$$\frac{W}{A_{AN}} = \frac{P_{T,AN}}{\sqrt{RT_{T,AN}}} \sqrt{\frac{2\gamma}{\gamma - 1}\left[\left(\frac{P_{AN}}{P_{T,AN}}\right)^{2/\gamma} - \left(\frac{P_{AN}}{P_{T,AN}}\right)^{\frac{\gamma+1}{\gamma}}\right]} \tag{44}$$

Taking $\gamma = 1.4$ and $R = 53.35$ (lb_f-ft/lb_m-°R) for air, and rearranging the units, one obtains,

$$\frac{W}{A_{AN}}\left(\frac{lb_m}{ft^2 sec}\right) = 111.8273 \times \frac{P_{T,AN}}{\sqrt{T_{T,AN}}} \sqrt{7.0\left[\left(\frac{P_{AN}}{P_{T,AN}}\right)^{2/1.4} - \left(\frac{P_{AN}}{P_{T,AN}}\right)^{2.4/1.4}\right]} \tag{45}$$

where $P_{T,AN}$ is in lb_f/in^2 and $T_{T,AN}$ is in °R.

Substituting the expression for the mass flow rate per unit area, W/A_{AN}, into equations (40) and (41), the functions $f(r)$ and $g(r)$ of equation (38), that are to be integrated can be expressed as,

$$f(r_i)=111.8273\frac{(P_{T,AN_i})^2}{\sqrt{T_{T,AN}}}\sqrt{7.0\left[\left(\frac{P_{AN_i}}{P_{T,AN_i}}\right)^{2/1.4}-\left(\frac{P_{AN_i}}{P_{T,AN_i}}\right)^{\frac{2.4}{1.4}}\right]}x\frac{2\pi r_i}{12} \qquad (46)$$

and,

$$g(r_i)=111.8273\frac{P_{T,AN_i}}{\sqrt{T_{T,AN}}}\sqrt{7.0\left[\left(\frac{P_{AN_i}}{P_{T,AN_i}}\right)^{2/1.4}-\left(\frac{P_{AN_i}}{P_{T,AN_i}}\right)^{2.4/1.4}\right]}x\frac{2\pi r_i}{12} \qquad (47)$$

These functions are integrated using the *Simpson's Method.*

In the last two equations $(P_{T,AN})_i$ represents the total pressure and r_i the radius corresponding to each traverse point. The expression used for r_i is,

$$r_i=1.5+(n-1)0.050 \quad \text{(inches)}$$

where 1.5 inches is the hub outer radius.

The mass-averaged static pressure in the annulus, P_{AN}, is calculated similarly, by replacing $(P_{T,AN})_i$ by $(P_{AN})_i$ in equation (38).

3.2.5. Averaging of the Static Pressure at the Exit Flange:

The average static pressure at the exit flange, P_{FL}, is calculated by taking the arithmetic mean of the 28 static pressure data obtained.

3.2.6. Calculation of the Hood Loss Coefficient:

Knowing the average values for $P_{T,AN}$, P_{AN} and P_{FL}, the hood loss coefficient,

HL/LL, is calculated using equation (21),

$$\frac{HL}{LL}=\frac{\left(\frac{P_{AN}}{P_{T,AN}}\right)^{0.4/1.4}-\left(\frac{P_{FL}}{P_{T,AN}}\right)^{0.4/1.4}}{1-\left(\frac{P_{AN}}{P_{T,AN}}\right)^{0.4/1.4}} \tag{48}$$

or graphically, as explained on page 14.

3.2.7. Calculation of the Mass Flow Rate from Venturi Meter Data:

The mass flow rate through the venturi meter, W, in lb_m/sec, is calculated using the following expression:

$$W_{vent}(lb_m/sec)=45.285\times C\times Y\times F_a\times\sqrt{\rho_1(lb_m/ft^3)\times\Delta P_{vent}(psi)} \tag{49}$$

where ρ_1 represents the corrected density at the inlet to the meter corrected for specific humidity. The value of ρ_1 is determined using the expression

$$\rho_1=(1+S)\frac{P-P_v}{P}\rho_d \tag{50}$$

where P_v represents the vapor pressure and ρ_d the density of dry air which can be determined from the equation:

$$\rho_d(lb_m/ft^3)=\frac{P}{R_{air}T}=\frac{P(lb_f/in^2)}{53.35\left(\frac{lb_f\ ft}{lb_m\ ^\circ R}\right)T(^\circ R)}\times 144(in^2/ft^2) \tag{51}$$

Therefore,

$$\rho_1(lb_m/ft^3)=2.6991(1+S)\frac{(P-P_v)(psi)}{T(^\circ R)} \tag{52}$$

The expression for the specific humidity, S, is,

$$S=0.622\frac{P_v}{P-P_v} \tag{53}$$

Therefore, knowing the dry bulb and wet bulb temperatures one can obtain the relative humidity, ϕ, from the *Psychrometric Chart*. The steam tables can be used to get the saturation temperature, P_g, knowing the dry bulb temperature. Once P_g and ϕ are obtained, vapor pressure, P_v, can be calculated using the expression for the relative humidity, $\phi=P_v/P_g$.

Assuming no moisture condensation between the venturi meter and the lab ($S_{vent}=S_{lab}$), the specific humidity is calculated from equation:

$$S=0.622\frac{P_v}{P_{lab}-P_v} \tag{54}$$

where $P_{lab}=P_{ATM}$. Subsequently, ρ_1 is calculated from equation (52).

The variation of the discharge coefficient, C, with the Reynolds number, R_{ed}, is given in Appendix C. The compressibility expansion factor, Y, and thermal expansion factor, F_a are obtained from the charts for the used *Fluidic Venturi Meter*.

Note that ΔP_{vent} is measured in inches of H_2O, and must be converted into psi units, by multiplying with the specific weight of H_2O at the temperature recorded in the laboratory.

4. EXPERIMENTAL SET-UP

Air Test Loop:

A schematic diagram of the air test loop is shown in figure 13. A *Hoffman* compressor model *67106A* is used providing 10,000 scfm at 12.5 psig maximum. A three phase electric motor with a capacity of 800 HP at 3600 rpm is used to drive the compressor. Air is taken through an inlet filter. Silencers are mounted at both the intake and discharge sides. Air exiting the compressor at about 250 °F is cooled to 100 °F by an aftercooler.

After the aftercooler, a 36 inches long flow straightener section is placed. The length of the flow straightener is determined according to ASME recommendation. A *Fluidic* venturimeter is placed downstream of the flow straightener. The venturi meter has a diameter ratio of 0.5281 and is designed to produce a differential pressure of 20 inches of water column at a maximum flow rate of 11,000 scfm, with a coefficient of discharge of 0.9950 . A manometer is used to measure the static pressure difference between the inlet and throat of the venturimeter. The manometer is placed in the test room and the connection is provided by a one piece long copper tubing to prevent any leakages through connecting elements.

Flow leaving the venturi, turns 90° in the horizontal plane via a large radius elbow, and enters a diffuser having an area ratio of 1.78 . After the diffuser, the flow turns another 90°, to a vertical position, through an elbow having turning vanes designed to produce a uniform flow at the exit. The pressure drop in the elbow was estimated to

be 0.034 psi [8].

After the elbow, the flow enters a contraction duct, which has a length of 19.3 inches and provides an area contraction ratio of 16. Air, upon leaving the contraction duct, flows over an elliptical bullet-nosed center body and enters the exhaust hood model. A round-wire-screen is placed 1.25 inches upstream of the annulus section where the total pressure traverses are done. The screen is used because without it, at low Mach numbers, the major portion of the mass flow tends to bypass the upper half of the hood model. Such flow pattern differs from that in an actual steam turbine and results in an incorrect value of hood loss coefficient. The use of a screen helps to make the flow in the model annulus circumferentially uniform. The solidity of the screen that is used is 10%. (The solidity of a screen is defined as the ratio of the total projected screen wire area to the total cross sectional area). A round-wire-screen having a solidity of 10% chokes the air flow when the inlet Mach number is equal or greater than 0.693. Therefore, for Mach numbers greater than 0.693, the tests without the screen were run. For high Mach numbers, the tendency to bypass the upper half of the hood is low because the flow close to choking tends to fill the whole annulus uniformly.

At a distance of 1.25 inches downstream of the screen, total pressure measurements are taken at five angular positions using 1/8" *Kiel Probes*, manufactured by *United Sensors*. Figure 11 shows the circumferential positioning of total pressure probes. No swirl is introduced into the flow. Therefore, the total pressure at sections 8, 9, 10, 11 and 12 are taken to be equal to the total pressure at sections 4, 2, 1, 6 and 5, respectively (see figure 11).

Five different traverse actuators manufactured by *Rotadata* are used (*Rotadata Mini Traverse Actuator RTM 025A*) for total pressure traverses. The actuators use 200-pole stepper motors to move probes in a series of small increments to give very precise positioning. The actuators have an accuracy of plus or minus 0.05 mm (0.002 in) over 300 mm in linear axis or 0.25 degree in yaw. The actuators are connected to a compact 2-axis controller (*Rotadata C2A5*) placed in the test room, which makes it possible to remotely control the total pressure traverses.

At a distance of 0.3 inches downstream of the total pressure probes, static pressure holes of 1/32" diameter are located at 12 angular positions at the hub and the shroud of the annulus, as shown in figure 11.

The total pressure probes and the static pressure taps are connected to a *15 psid Scanivalve Pressure Transducer* placed in the test room. The connections are made using tygon tubing. The pressure transducer has 48 ports available, allowing a quick access of static and total pressure tubes.

Positioned circumferentially on the exit flange are 28 static pressure holes of 1/32" diameter as shown in figure 14. These static pressure taps are connected to a *2.5 psid Scanivalve Pressure Transducer*. Signals from the pressure transducers are amplified through *SCSG2 Signal Conditioners* to provide a high level analog output. The outputs are recorded using voltmeters.

5. GENERIC MODEL

The size of the generic model was chosen to be able to attain a maximum average annulus Mach number of 0.75 without using a screen. The required model annulus height came out to be 1.5 inches.

Determination of Minimum Hood Size for Significant Diffusion:

The following analysis has been developed by Prof J.A.Owczarek for the experimental improvement study of LP turbine exhaust hoods[9]. Figure 15 illustrates the most important variables having the dimensions of area and length, which control the geometry and size of an exhaust hood. The following dimensionless parameters can be used to define the geometry and relative exhaust hood size:

$$\frac{R_H}{L} = \frac{\text{last blade root radius}}{\text{last blade height (annulus height)}}$$

$$\frac{H}{L} = \frac{\text{hood height}}{\text{last blade height}}$$

$$\frac{B}{L} = \frac{\text{hood length}}{\text{last blade height}}$$

$$\frac{D}{L} = \frac{\text{hood width}}{\text{last blade height}}$$

$$\frac{A}{B} = \frac{\text{annulus advance}}{\text{hood length}}$$

$$\frac{A_{CF}}{\frac{1}{2}A_{AN}} = \frac{\text{centerline flange open area}}{\frac{1}{2}(\text{annulus area})}$$

$$\frac{A_{FL}}{A_{AN}} = \frac{\text{condenser flange open area}}{\text{annulus area}}$$

The large number of parameters defining the relative hood size and geometry makes it very difficult to examine their effect by systematic testing. However, not all of these parameters are of equal importance. In large steam turbines some of the parameters do not vary by much from one design to another. For example the ratio of last blade root radius to last blade height, R_H/L, ranges between 1.0 and 1.3. Similarly, the parameter A/B ranges between 0.3 and 0.5, whereas B/L is between 4.0 and 4.6. For the generic model of the exhaust hood, the chosen values for R_H/L, A/B and B/L are 1.0, 0.5 and 4.4 respectively. The two variable parameters are the dimensionless hood height H/L, and width, D/L. The reason why the parameter D/L has been chosen rather than the parameter B/L is because a change in the value of the parameter B/L would require a complicated model design.

The parameter $A_{CF}/\frac{1}{2}A_{AN}$ can be expressed as (see figure 15):

$$\frac{A_{CF}}{\frac{1}{2}A_{AN}} \approx \frac{[D-2(L+R_H)]B}{\frac{1}{2}\pi(2R_H+L)L} = \frac{2\left[\frac{D}{L}-2-\frac{2R_H}{L}\right]\frac{B}{L}}{\pi\left[2\frac{R_H}{L}+1\right]} = 0.933\frac{D}{L}-3.73 \qquad (55)$$

for $R_H/L=1.0$ and $B/L=4.4$. For constant values of R_H/L and B/L, the parameter $A_{CF}/\frac{1}{2}A_{AN}$ depends only on the dimensionless hood width D/L. This parameter indicates whether the flow from the upper half of the annulus can diffuse or not. If $A_{CF}/\frac{1}{2}A_{AN}$ is less than 1.0, the flow cannot diffuse. In practice this parameter should be quite large, since the fluid from upper half of the annulus flows mainly through the centerline flange area near the front wall (see figure 15c).

The parameter A_{FL}/A_{AN} can be expressed as:

$$\frac{A_{FL}}{A_{AN}} = \frac{BD}{\pi(2R_H+L)L} = \frac{\frac{B}{L}\frac{D}{L}}{\pi\left[2\frac{R_H}{L}+1\right]} \cong 0.467\frac{D}{L} \qquad (56)$$

for $R_H/L=1.0$ and $B/L=4.4$.

In reality, the actual flange flow area, A_{FL}, is much smaller than the flange open area BxD, because of the blockage by the turbine cylinder and the beams and struts in the condenser flange. Therefore, the ratio of the effective condenser flange area to annulus area, $A_{FL,EFF}/A_{AN}$, is much smaller than the value obtained from equation (56). The effective flange area ratio can be estimated from equation:

$$\frac{A_{FL,EFF}}{A_{AN}} \cong \frac{BD-2(R_H+L)(A+L_v)}{\pi(2R_H+L)L} \qquad (57)$$

where L_v denotes the axial length of the guide vane.

The generic exhaust hood model has variable width, D, and height, H, only. With the use of wooden inserts nine different configurations can be created, with three different values for both height and width. Table 1 shows the characteristic dimensionless lengths for the nine different configurations of the generic model.

6. TEST PROCEDURE

Nine different configurations of the generic model were tested. Each configuration was tested with and without screen. In addition, configurations 1, 8, and 9 were tested without the guide vane. The configurations 3, 4 and 5 were also tested with a smaller size flange. For each case four tests were run at different annulus Mach numbers. The total number of tests was 108.

The procedure described below was followed for each test.

- The configuration that was to be tested was assembled using the wooden and aluminum inserts, and proper size flange. (There are eight different wooden inserts to adjust the height, two pairs of aluminum inserts to adjust the width, and three different flanges for three different values of hood model width. For the largest height and width case, no insert is used).

- The five total pressure probes were put into position on the traverse actuators. (For each probe the first position is at the shroud wall. Marked on every probe is the relative position of each probe with respect to the actuators, at which the probe tip is just entering the flow annulus (at shroud wall)).

- The necessary tygon tubing connections were prepared.

- The pressure measuring devices (gages and the manometer) were checked and zeroed if necessary.

- The compressor was started and set to a speed corresponding to the annulus Mach number that was to be tested (A waiting period of about half an hour was allowed

to achieve a steady temperature in the flow after the aftercooler).

- The values of the atmospheric pressure, atmospheric temperature, wet bulb temperature, pressure at the inlet to the venturi meter, pressure difference accross the venturi meter, total temperature at the venturi meter, and the total temperature at the model inlet were recorded (The values for these parameters are recorded several times during the test).

- The passage hole in the hub was set to *closed* position to prevent air flow through the hub (This passage hole is closed for traverses 1 to 5, and while taking the static pressure readings at the hub and shroud. For traverses 6 and 7, the passage hole is set to proper position which allows the probe pass through the hub).

- The static pressure values at the hub, shroud, and the exit flange were recorded.

- The electrical connection for the proper traverse actuator was made for the pressure probe to be used.(The order followed for the traverses is 1, 2, 3, 4, 5, 6 and 7. Note that the probes 4 and 3 are also used for the traverses 6 and 7, respectively).

- For traverses 1 through 5, the controller was turned on and set to *Datum*, with the total pressure probes tips located at the shroud diameter. Subsequently, the probe used was moved 0.025 inches inward in the radial direction to bring the holes on the probe to the shroud wall, and the first total pressure data was recorded.

- Increment radial was chosen using the function switch on the controller (The increment indicator is set to 0.050 inches and the total pressure values are recordeed for every 0.050 inches increments (see figure 12)).

- For traverses 6 and 7, first the controller was set to 2 inches, without tightening

the probe used to the actuator; that is, the actuator probe holder was allowed to move 2 inches inward in the radial direction. The probe was then pushed all the way into a 0.100 inches deep recess in the shroud, and tightened to the actuator probe holder. For traverses 6 and 7, since the traverse actuator is located on the opposite side of the annulus and hub, the actuator probe holder moves in radially outward direction. Subsequently, each probe used was moved inward by 0.075 inches to bring the holes on the probe to the shroud wall.

- When the traversing was completed, the actuator was set to *Datum,* and the probe was taken out of the flow passage on both sides of the hub, according to the mark made on the probe.

- When the total pressure traverses were completed, the static pressures at the hub, shroud and the exit flange were recorded once again.

- Subsequently, the compressor speed was adjusted to another value of the annulus Mach number , or was shut down.

7. ANALYSIS OF THE DATA

Nine different configurations of the generic model were tested. The results for the configurations 1 and 9 will be discussed in detail. The results of these tests indicate the range of the hood loss coefficient of the generic model, because configuration 1 corresponds to the largest and configuration 9 to the smallest internal hood in size. These configurations were tested for four different cases:

- with the screen, with the guide vane (referred as configuration 1 or 9).
- without the screen, with the guide vane (referred as configuration 1B or 9B).
- without the screen, without the guide vane(referred as configuration 1C or 9C).
- with the screen, without the guide vane (referred as configuration 1D or 9D).

The results of the tests are shown on the plots in appendix.

The effect of the screen can be seen on the total pressure variations across the annulus, shown on the plots on pages 74 to 101, in appendix B. Without the screen, the total pressure is uniform across the annulus, whereas with the screen, there are wakes created by the screen wire. The total pressure values drop to the static pressure values at the hub and the shroud.

The circumferential variation of the local hub and shroud pressure coefficient, C_P, for different annulus Mach number tests, is shown on pages 58 to 73 in appendix B. When the configurations 1 and 9 are compared in general (that is for all of the four cases), it is observed that, as expected, in configuration 9 (small hood) higher pressure level exits in the hood than in configuration 1 (large hood). It can also be observed that

in configuration 9 the flow is more blocked at the front of the hood (at about 180°).

The variation of the hood loss coefficient with the annulus Mach number is shown on pages 53 to 57 in appendix B. Six different performance coefficients (discussed in chapter 3, pages 15 to 18) are plotted. For most of the tests, a good agreement between these values are obtained. For the highest Mach number tests of configurations 1B, 1D and 9D, the Mach number obtained using the annulus average static and total pressures is somewhat different than the Mach number obtained using the mass flow rate measured by the venturi meter, and the average annulus total pressure. For configurations 1D and 9D, which are tests with the screen, the annulus Mach number is already above 0.7, which is about the choking limit for the annulus with a screen having a solidity of 10%. Therefore, it appears that these points are not reliable. For configuration 1B, the Mach number obtained using the mass flow rate measured by the venturi meter and the average total pressure is more reliable than the Mach number obtained using the average annulus static and total pressure, because there is no screen, and the flow is uniform in the annulus.

For configuration 1, the hood loss coefficient curves for the "with" and "without" the screen cases (both with guide vane) intersect at around annulus Mach number of 0.71 (page 53 in appendix B). Since with the screen the flow is already beginning to choke around 0.7, after the intersection point, the hood loss coefficient curve for the case without the screen should be considered as valid.

The results show that at high Mach numbers the use of a guide vane increases the hood loss. However, more tests should be performed using intermediate sized guide

vanes in order to understand better the effect of the guide vane on the hood loss.

8. CONCLUSIONS

Dependency of the hood loss coefficient on the annulus Mach number was experimentally determined for the generic model. The results from the tests can be used as a guide for turbine exhaust hoods having different geometries. The large differences between the values of the hood loss coefficients for the configurations 1 and 9 indicate that it is possible to significantly affect the hood loss by changes in geometry. Configuration 1 represents the largest exhaust hood model, and configuration 9 the smallest. For the tests with a guide vane and screen, in the annulus Mach number range of 0.5 to 0.7, the hood loss coefficient of configuration 1 was found to be between 0.2 and 0.4 smaller than that of configuration 9.

The tests on the effect of the guide vane are not sufficient to draw any conclusions. Without the guide vane similar hood loss coefficient values were obtained for both configurations 1 and 9 tested with the screen. The results show that at high Mach numbers, the use of a guide vane tested increases the hood loss. However, in order to understand the effect of the guide vane on the hood loss more tests should be performed using different guide vane shapes.

As a final remark, it should be remembered that the improvement on the flow in the hood should result in an improvement of the last stage efficiency and condenser effectiveness, which will increase the overall turbine efficiency over the values predicted by improvements of the exhaust hood.

APPENDIX A - TABLES AND FIGURES

R_H/L	1.0								
B/L	4.4								
A/B	0.5								
L_v/L	0.75								
CONFIGURATION NO	1	2	3	4	5	6	7	8	9
H/L	3.8	3.4	3.0	3.8	3.4	3.0	3.8	3.4	3.0
D/L	8.15			7.5			7.0		
$\frac{A_{CF}}{\frac{1}{2}A_{AN}} = \frac{(D-2(L+R_H))B}{\frac{1}{2}\pi(2R_H+L)L}$	3.87			3.27			2.8		
$\frac{A_{FL}}{A_{AN}} = \frac{D\ B}{\pi(2R_H+L)L}$	3.81			3.5			3.27		
$\frac{A_{FL,EFF}}{A_{AN}} = \frac{D\ B\ -\ 2(R_H+L}{\pi(2R_H+L)}$	2.66			2.36			2.12		

Table 1
Characteristic Dimensionless Lengths and Areas for Generic Model

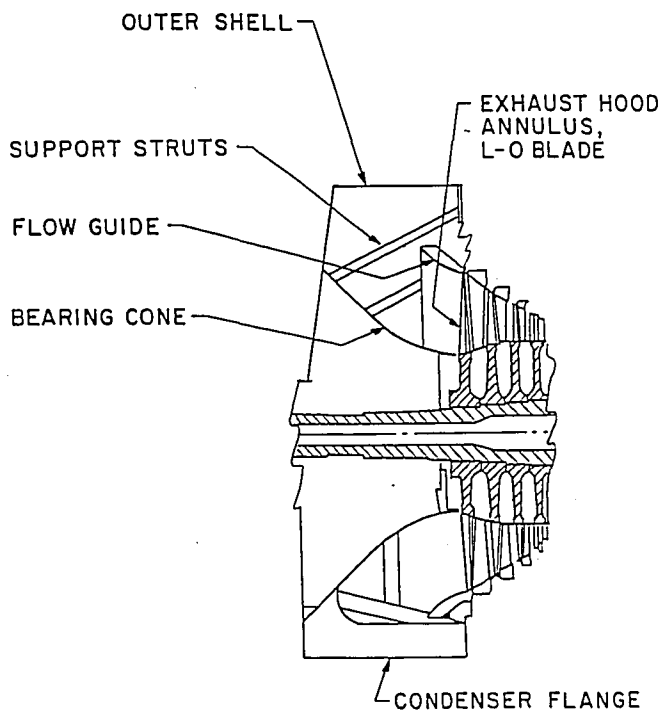

Figure 1
Schematic of a Typical Steam Turbine Exhaust Hood

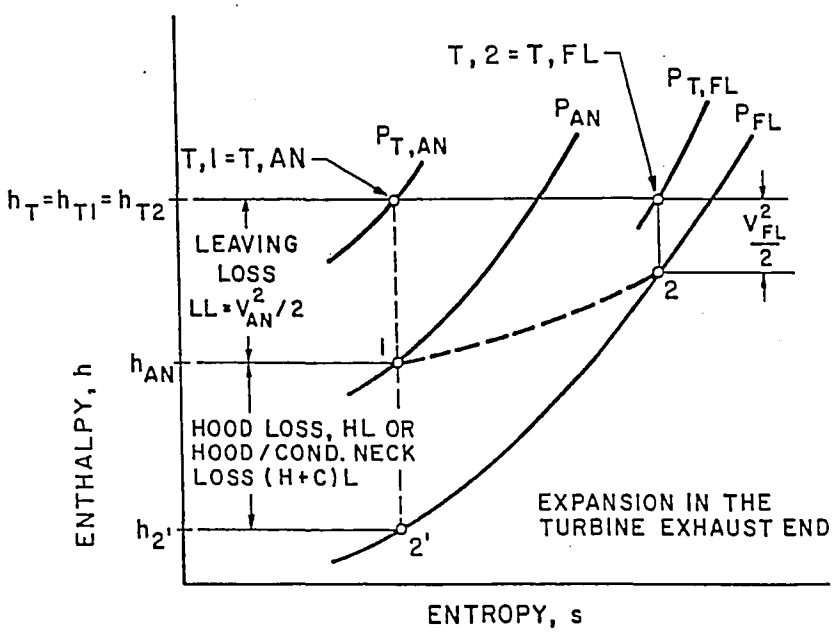

Figure 2
h-s Diagram of an Expanding Exhaust Hood ($P_{AN} > P_{FL}$) [1]

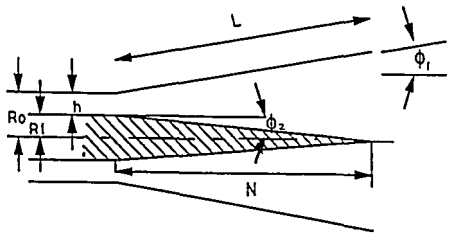

a) Equi-Angular Annular Diffuser

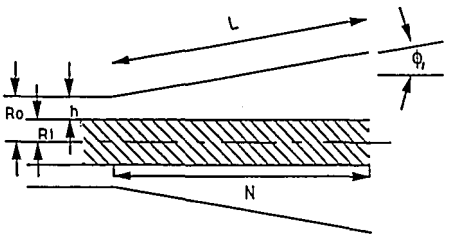

b) Straight Cone Annular Diffuser

Figure 3
Diffuser Geometries [2]

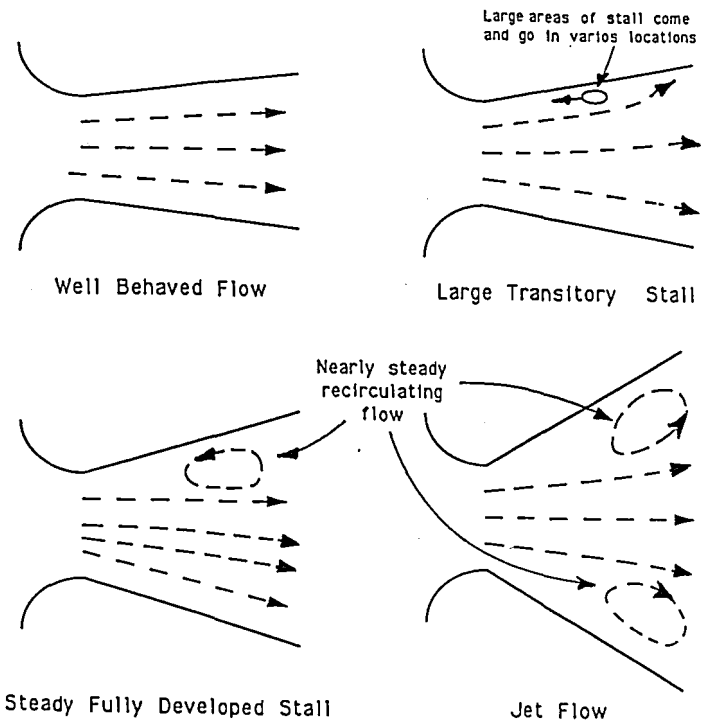

Figure 4
Schematic Diagram of Diffuser Flow Regimes [3]

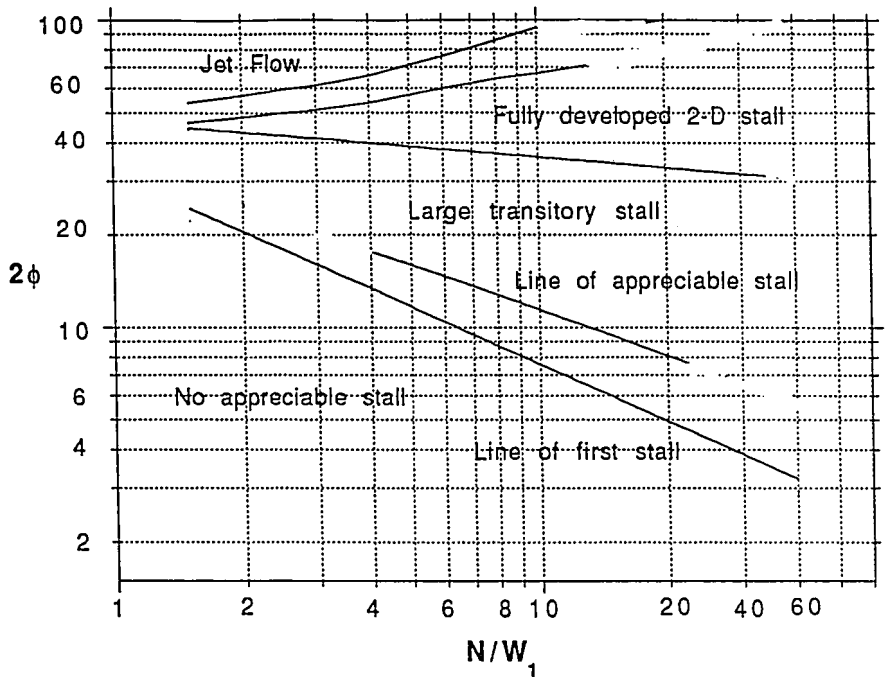

Figure 5
Flow Regime Chart for 2-D Diffusers [4]

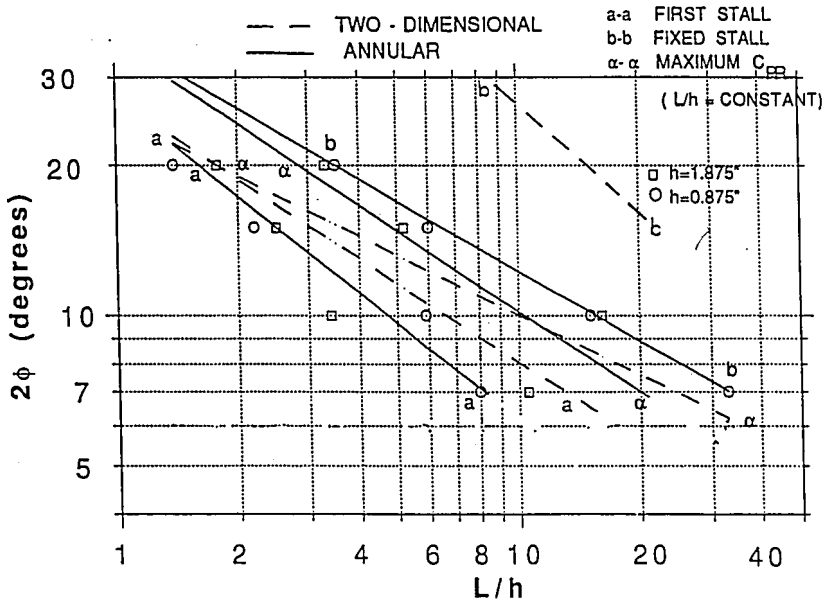

Figure 6
First Stall and Optimum Performance for
Equiangular Annular Diffusers [2]

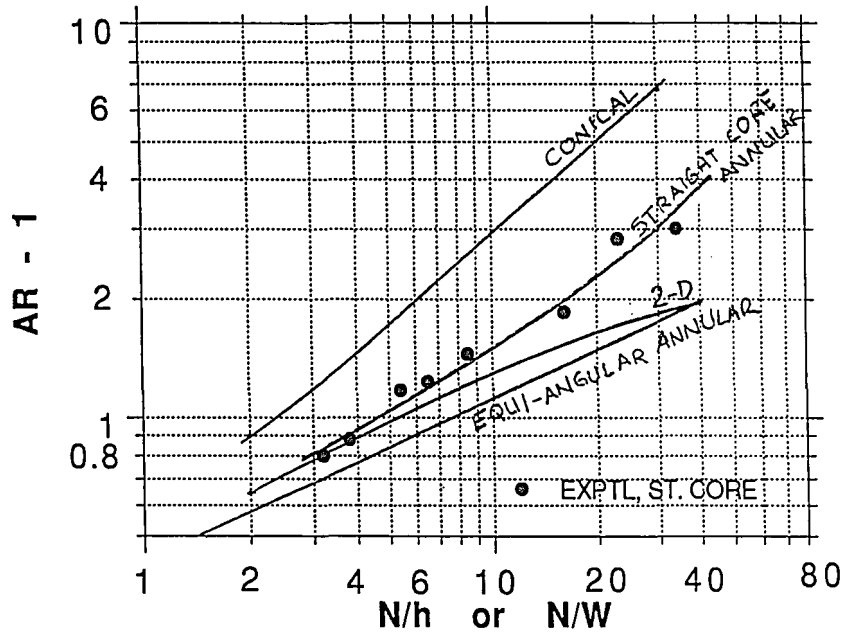

Figure 7
Comparison of First Stall Lines [2]

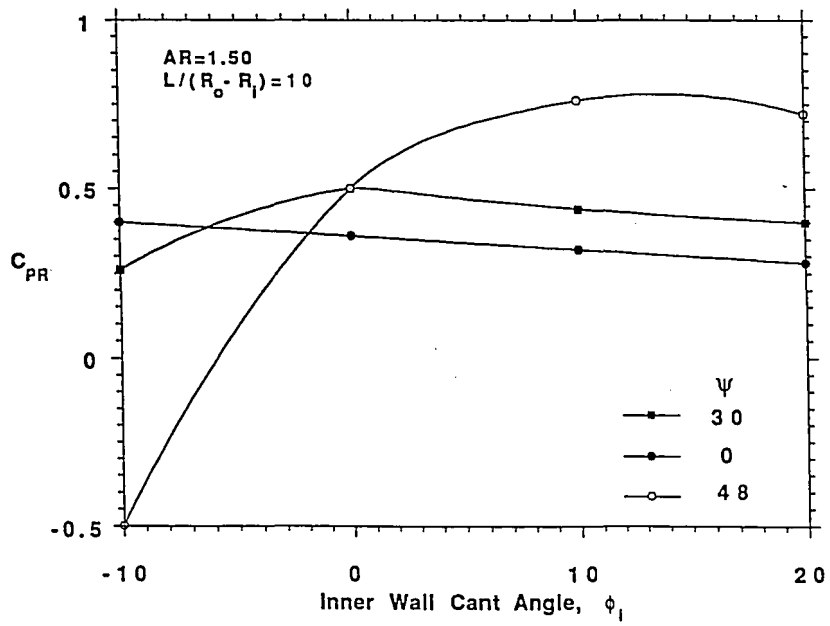

Figure 8
Effect of Cant Angle (ϕ_i) and Inlet Swirl Angle (Ψ)
on Pressure Recovery of Annular Diffusers

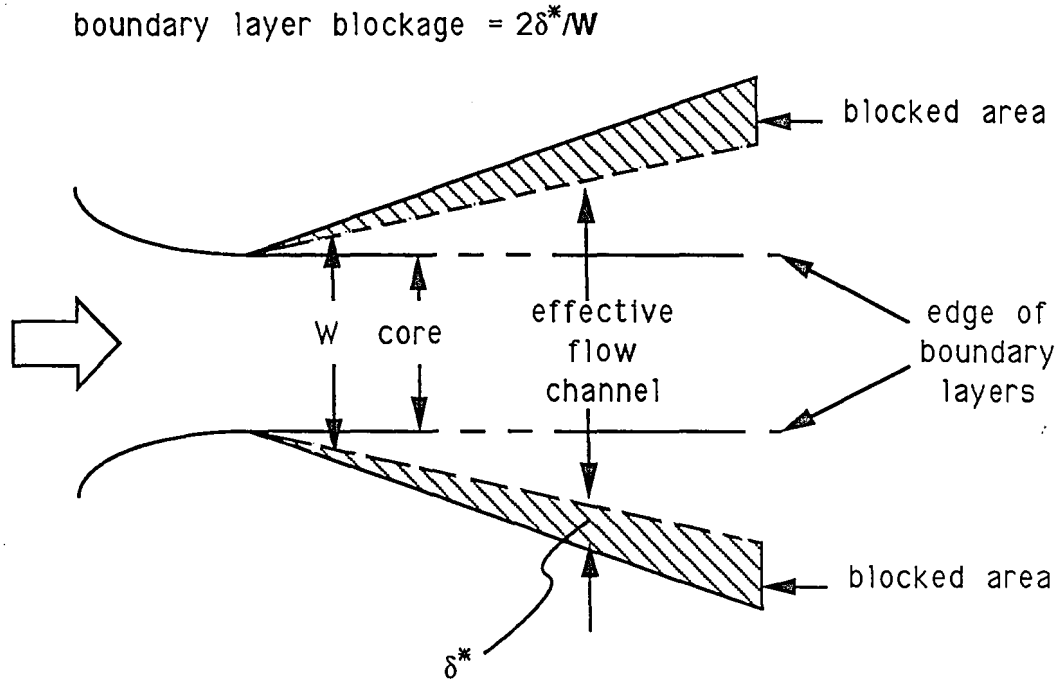

Figure 9
Boundary Layer Blockage

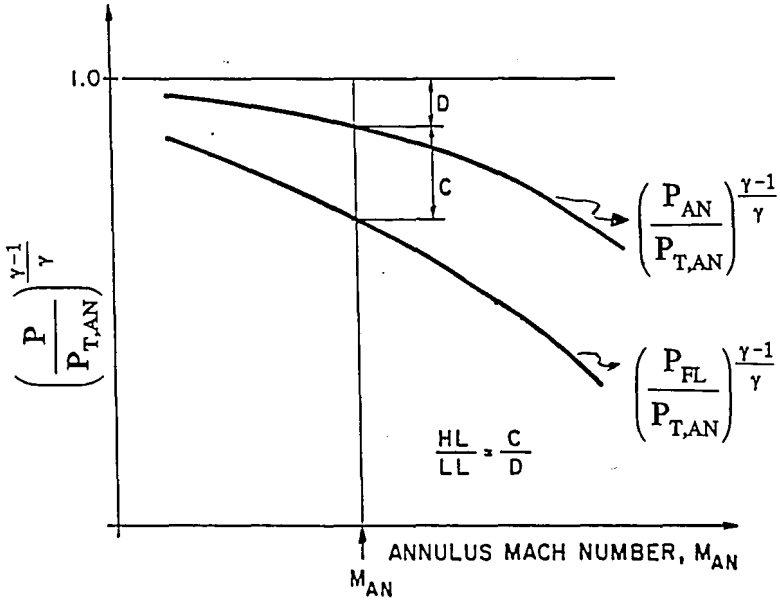

Figure 10
Graphical Determination of Hood Loss Coefficient, HL/LL [1]

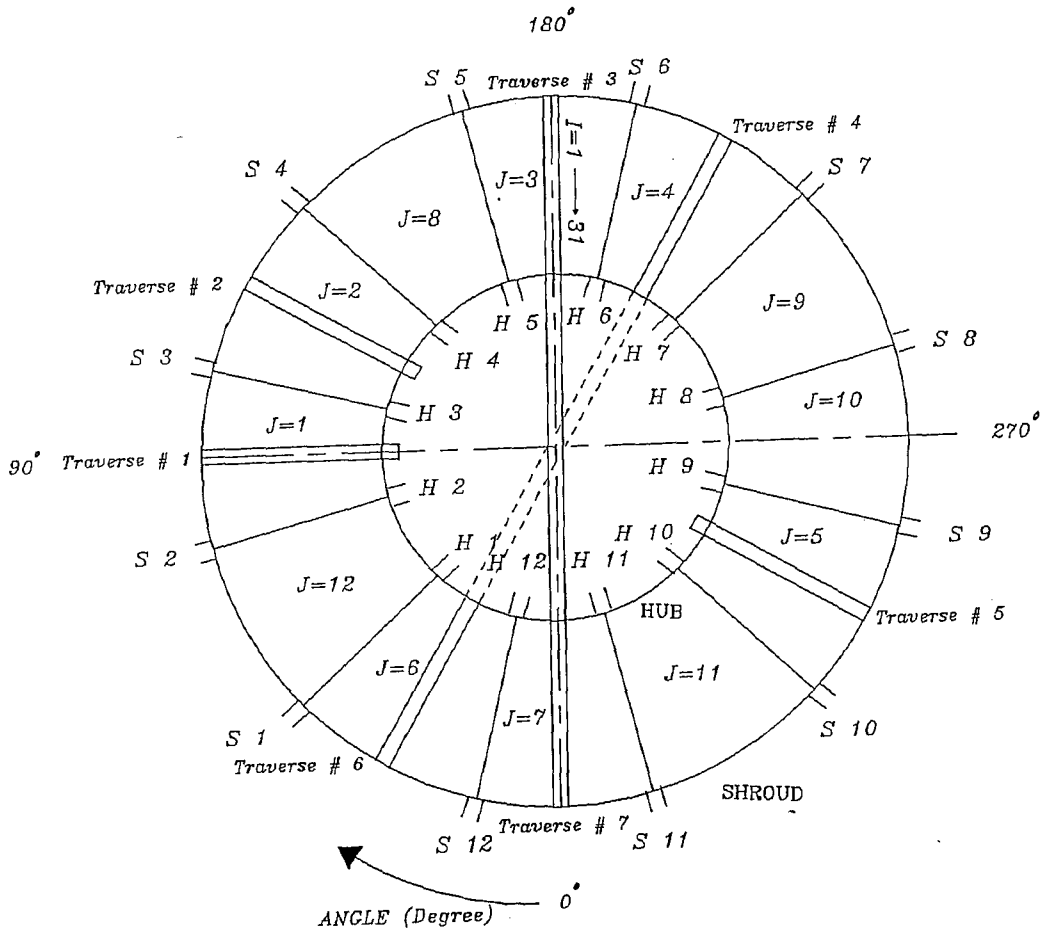

Figure 11
Flow Annulus

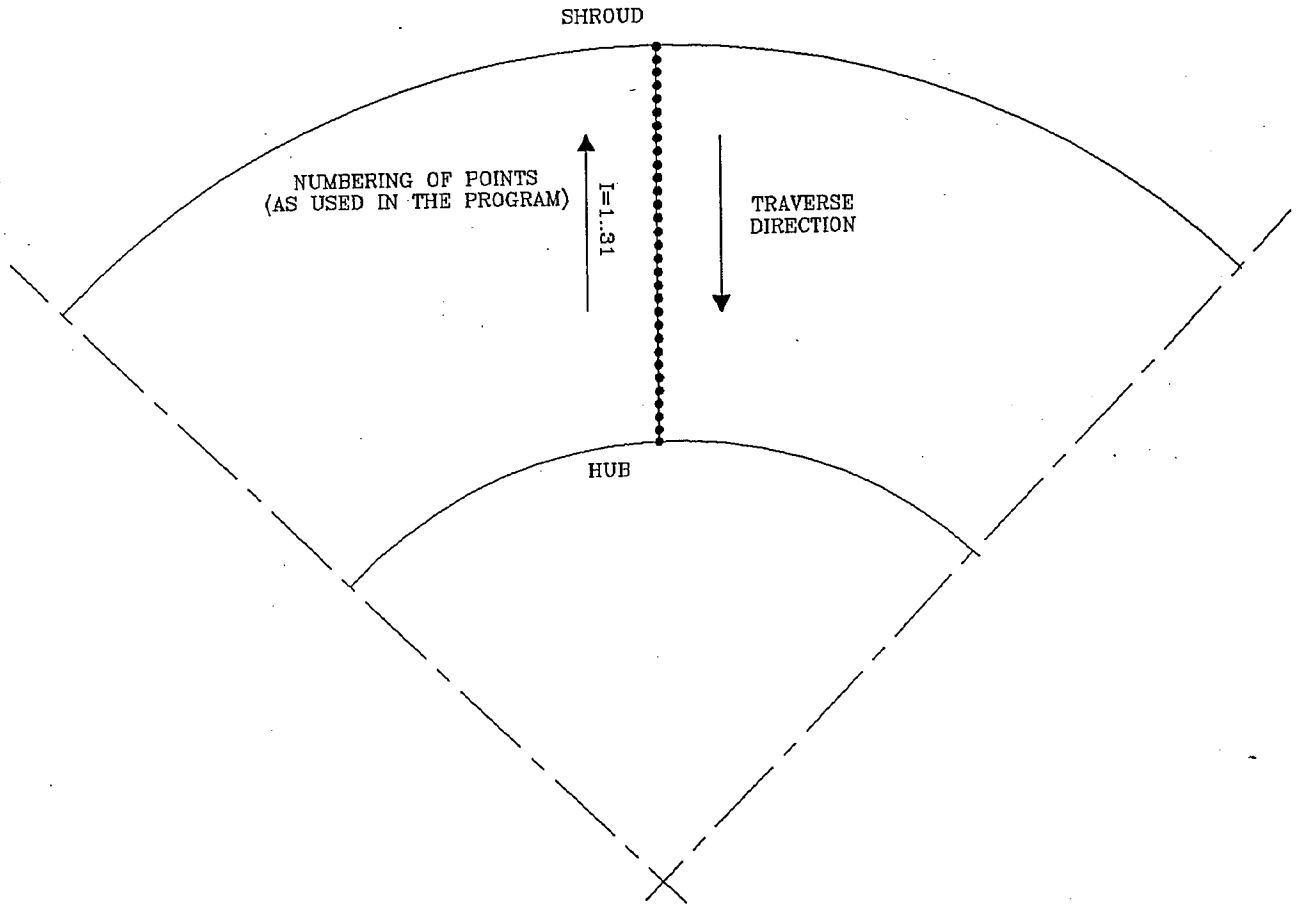

Figure 12
Traverse Points in Radial Direction

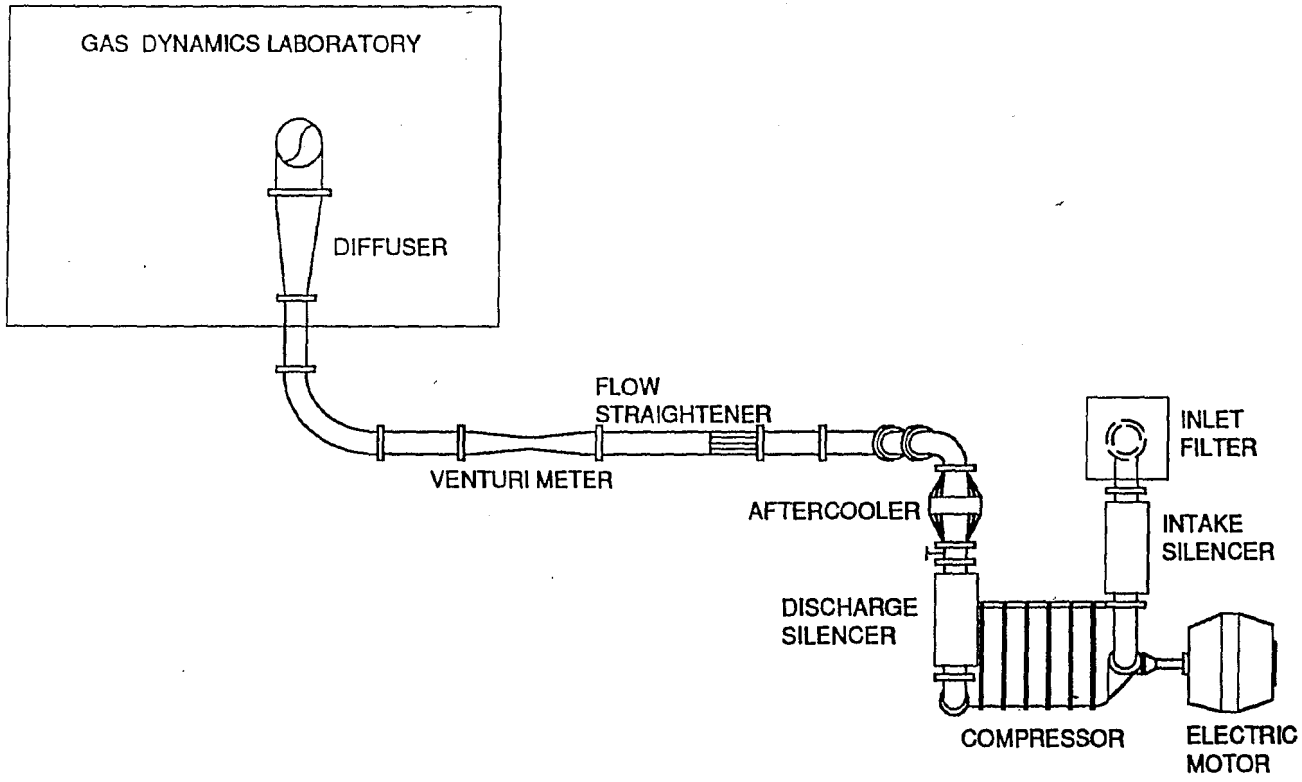

Figure 13
Schematic Diagram of Air Test Loop

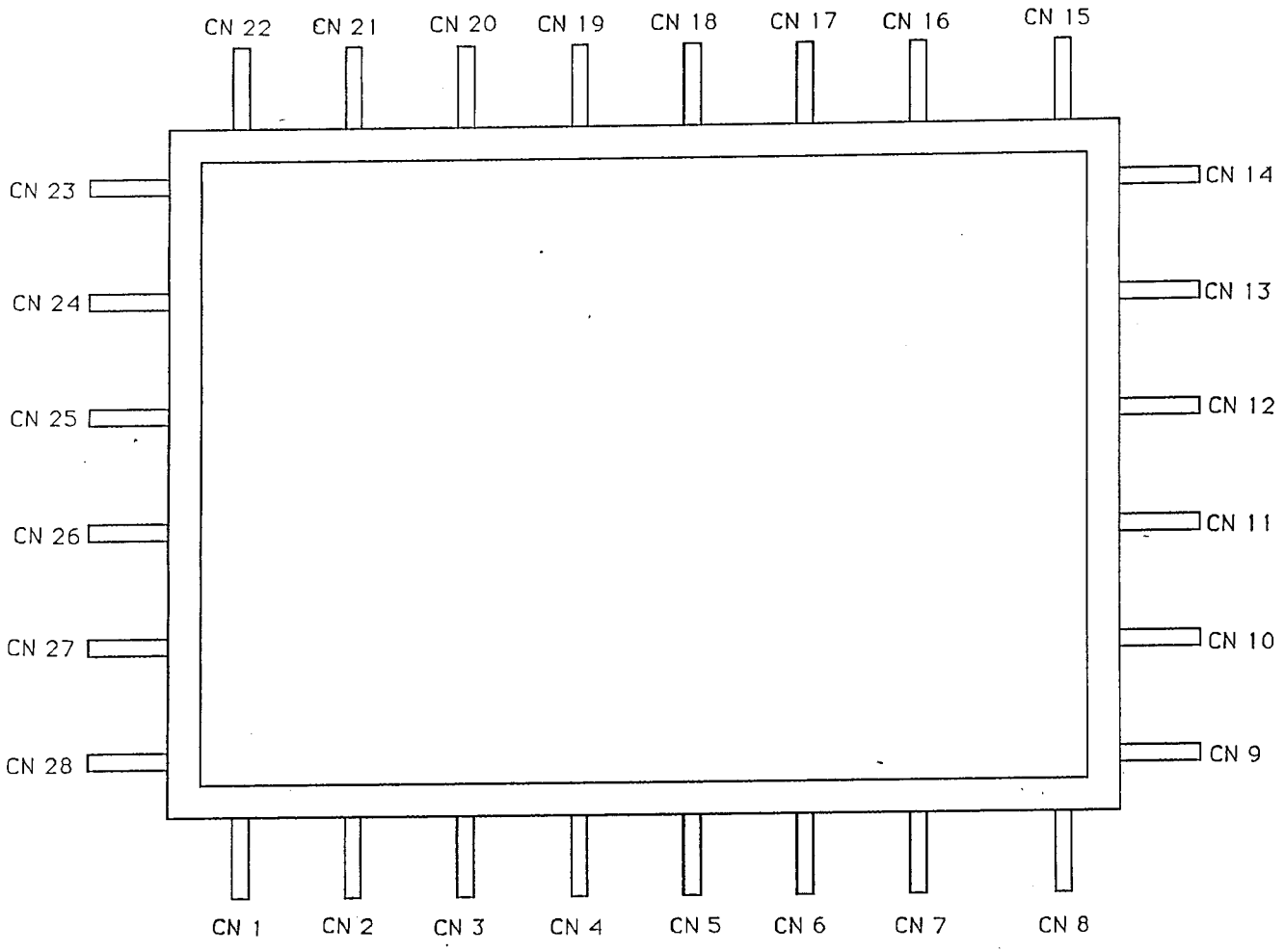

Figure 14
Exit Flange

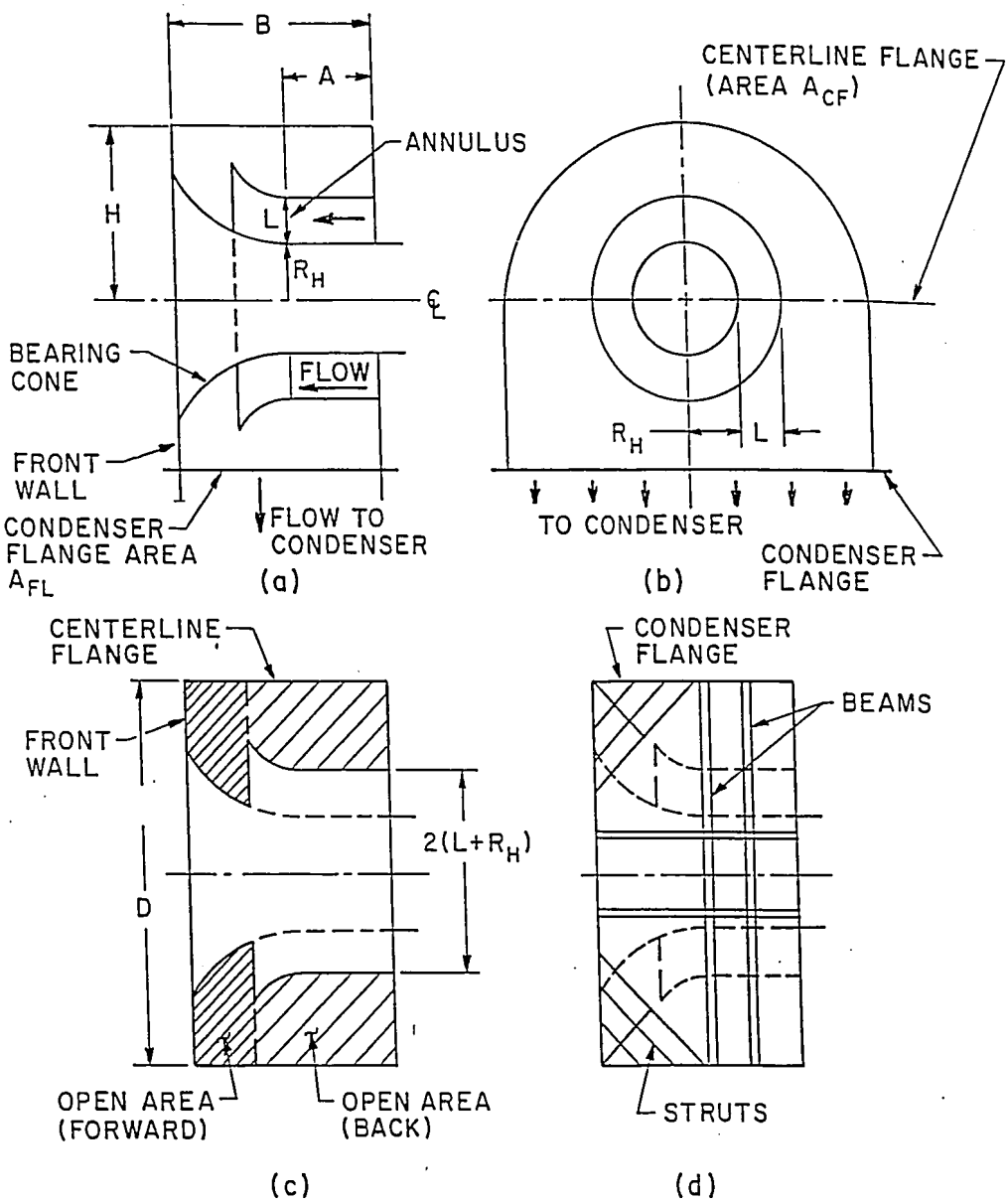

Figure 15
Variables Used to Describe
Geometry of an Exhaust Hood [9]

APPENDIX B - RESULTS FOR GENERIC MODEL CONFIGURATIONS 1 AND 9

- Drawings of configurations 1 and 9
- HL/LL versus annulus Mach number curves
- Circumferential Variation of C_P on hub and shroud
- Total pressure variations across the annulus

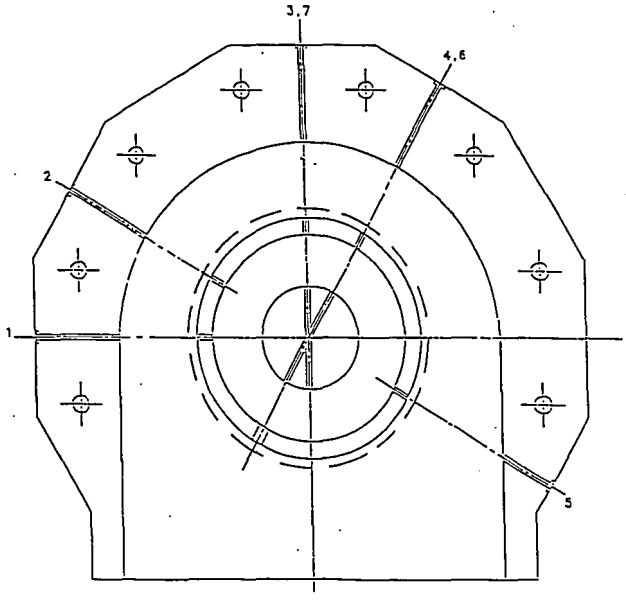

CONFIGURATION 1
(NO INSERTS)
D/L=8.15
H/L=3.8

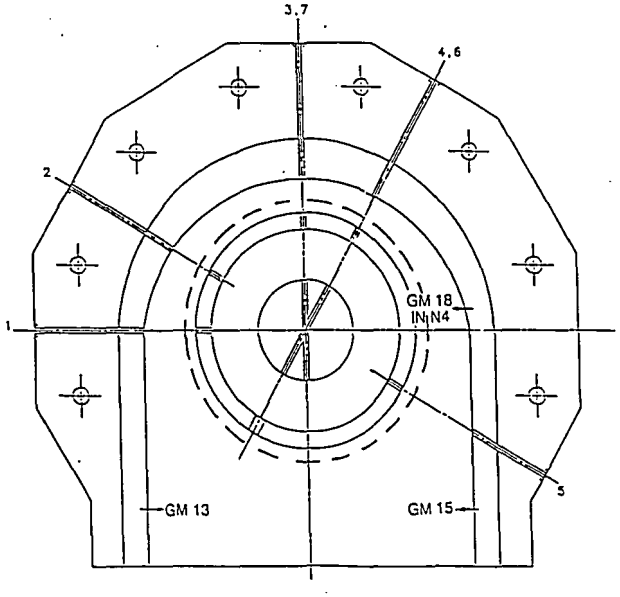

CONFIGURATION 9
WITH INSERTS GM 18 IN N4 , GM 13 & GM 15
D/L=7
H/L=3

GENERIC MODEL
CONFIGURATION 1
HL/LL vs ANNULUS MACH NUMBER

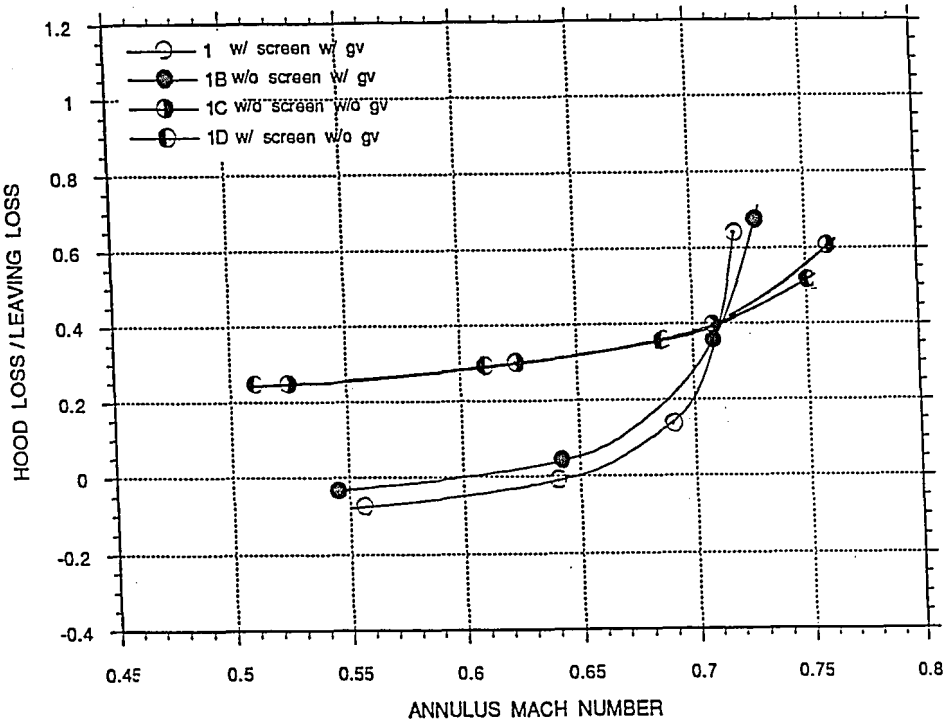

GENERIC MODEL
CONFIGURATION 9
HL/LL vs MACH NUMBER

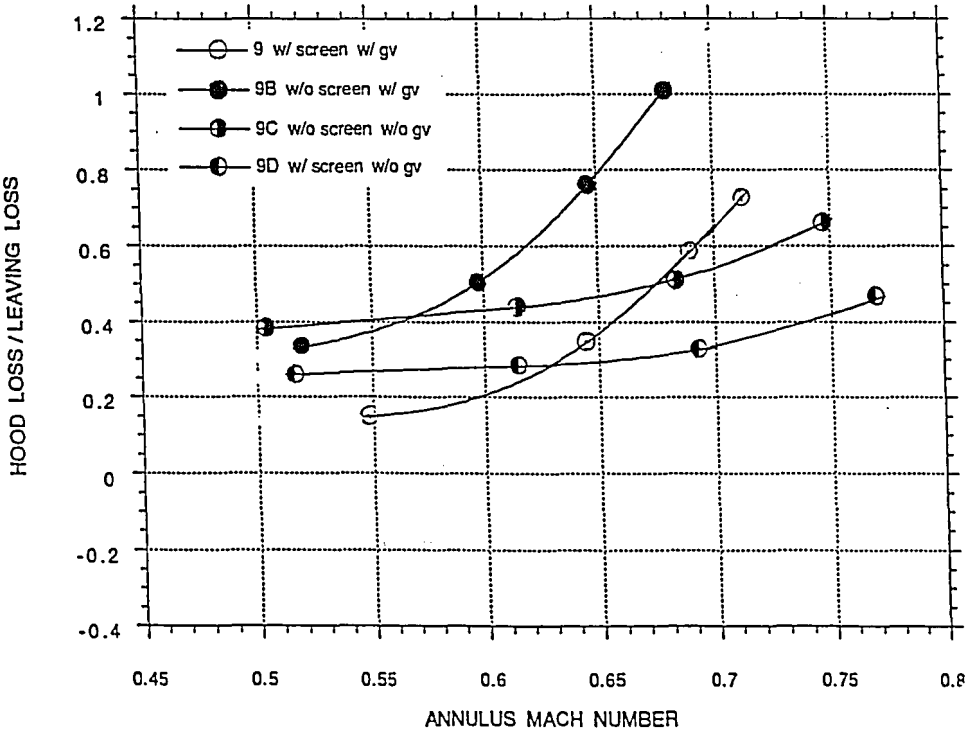

GENERIC MODEL
CONFIGURATION 1
W/ SCREEN W/ GUIDE VANE

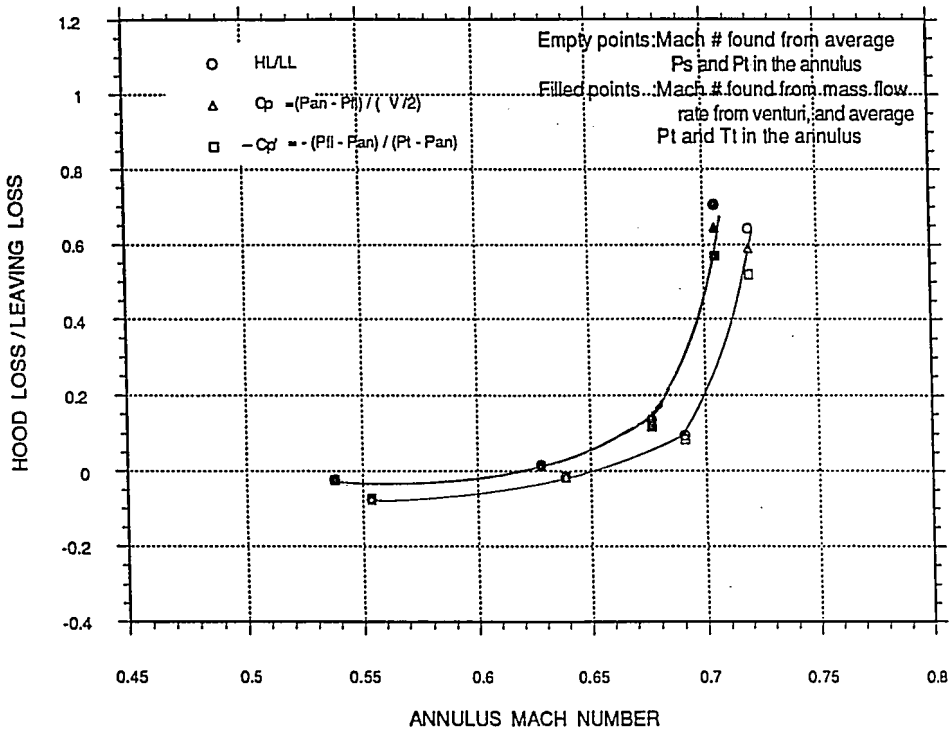

GENERIC MODEL
CONFIGURATION 1B
W/O SCREEN W/ GUIDE VANE

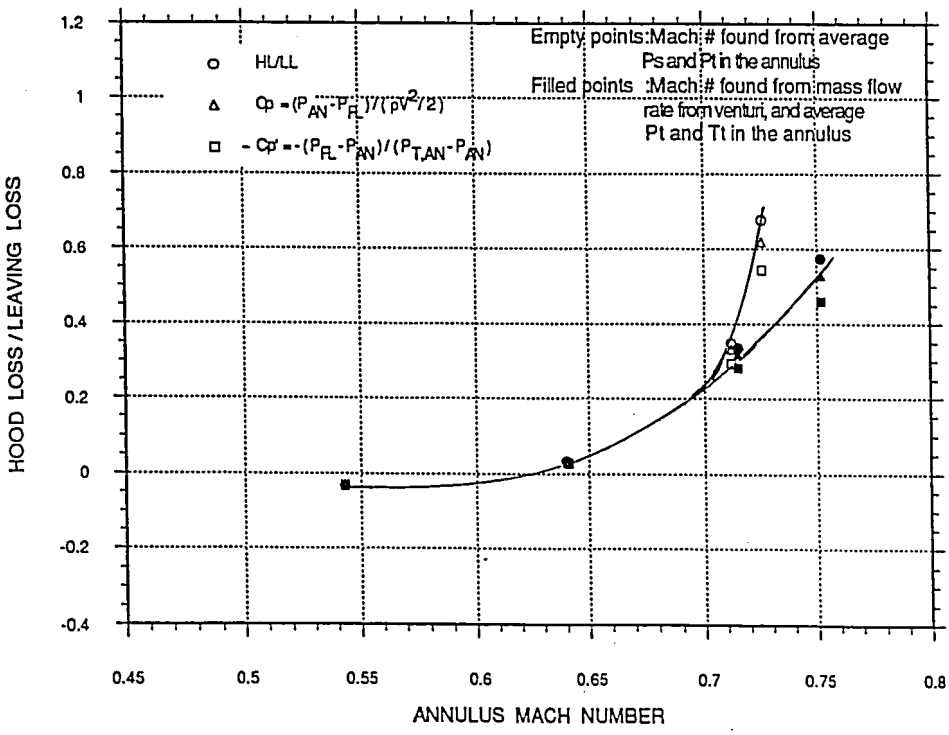

GENERIC MODEL
CONFIGURATION 1C
W/O SCREEN W/O GUIDE VANE

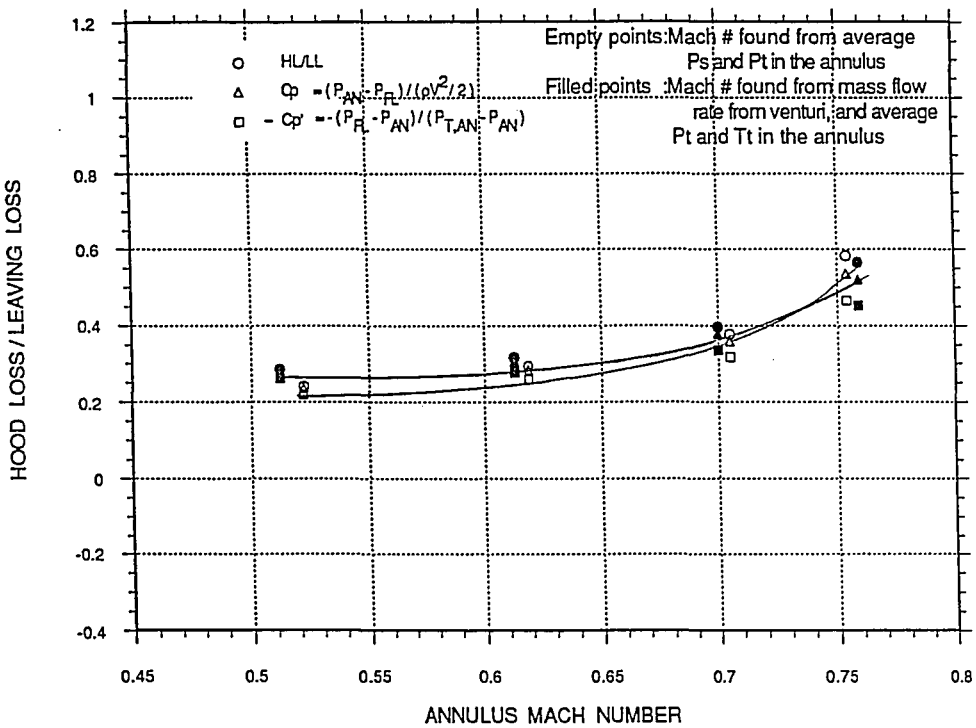

GENERIC MODEL
CONFIGURATION 1D
W/ SCREEN W/O GUIDE VANE

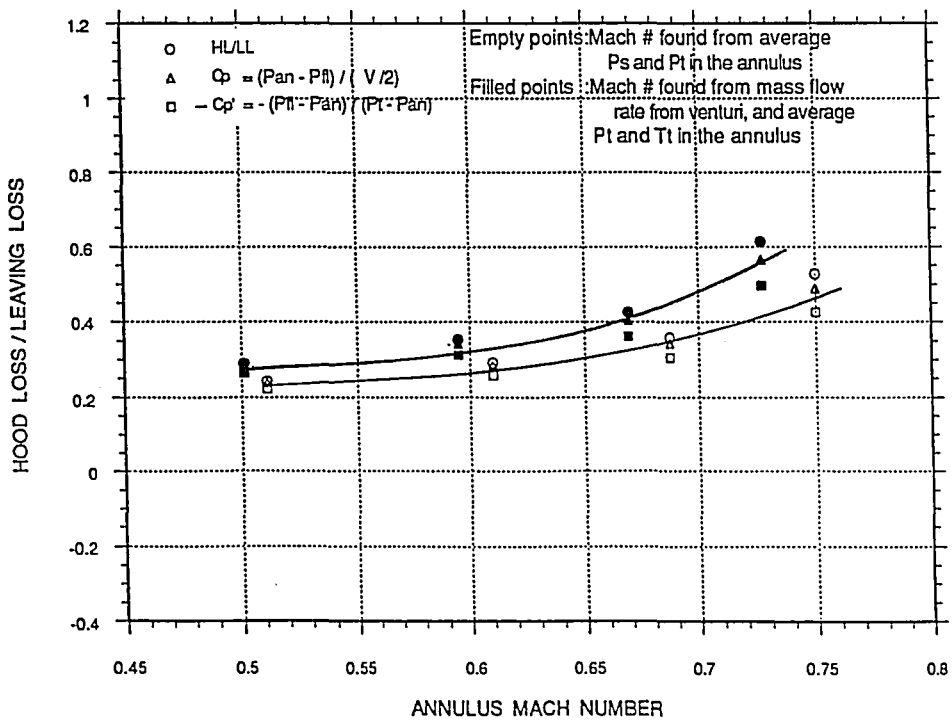

GENERIC MODEL
CONFIGURATION 9
W/ SCREEN W/ GUIDE VANE

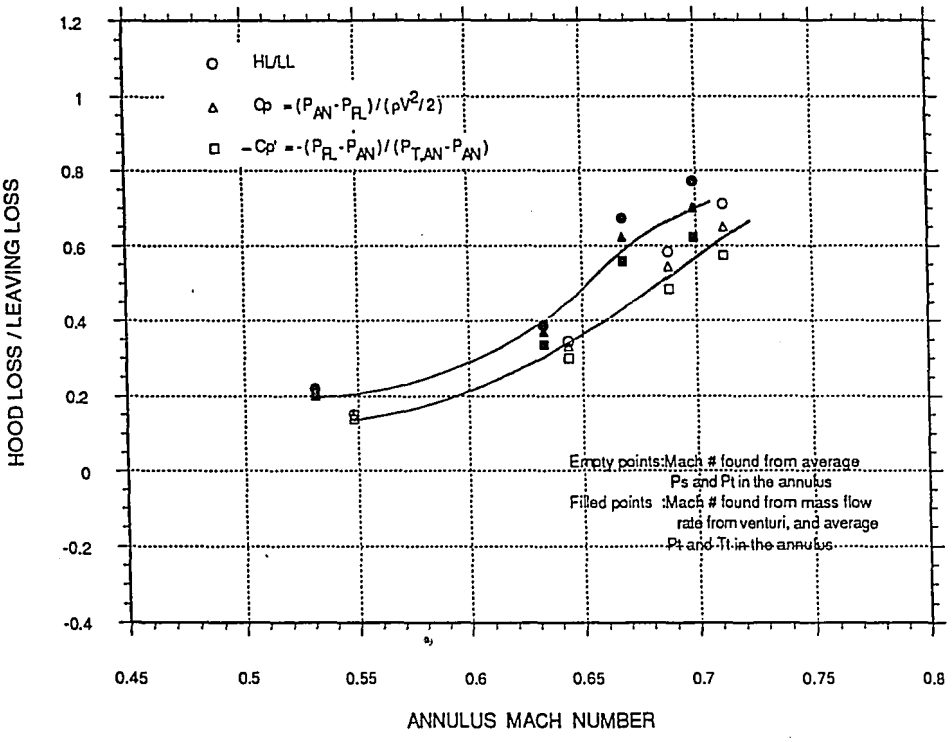

GENERIC MODEL
CONFIGURATION 9B
W/O SCREEN W/ GUIDE VANE

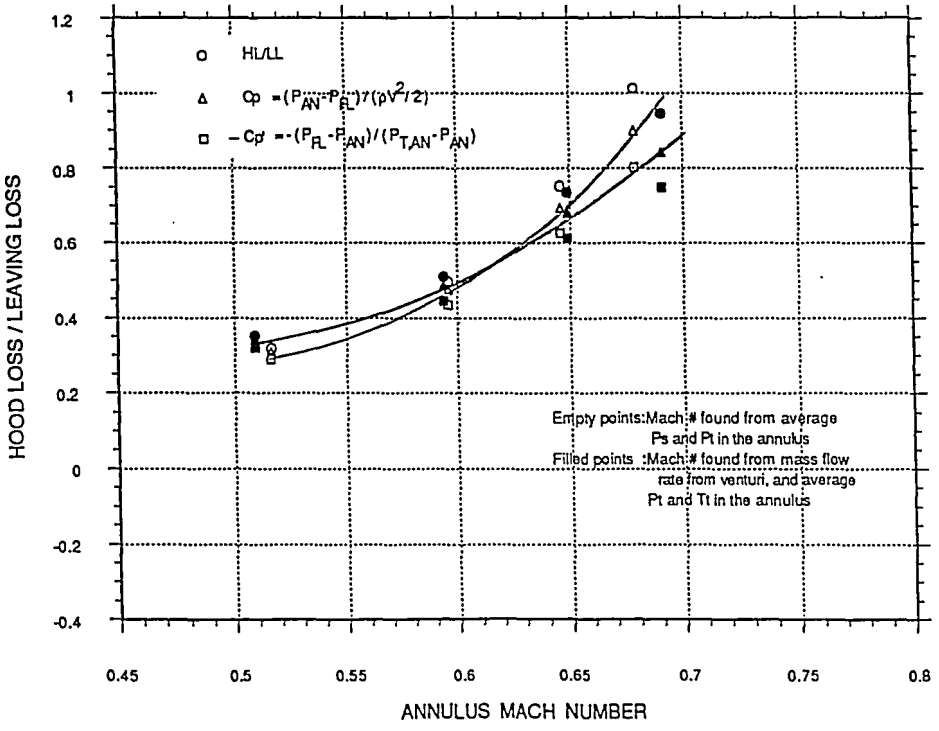

GENERIC MODEL
CONFIGURATION 9C
W/O SCREEN W/O GUIDE VANE

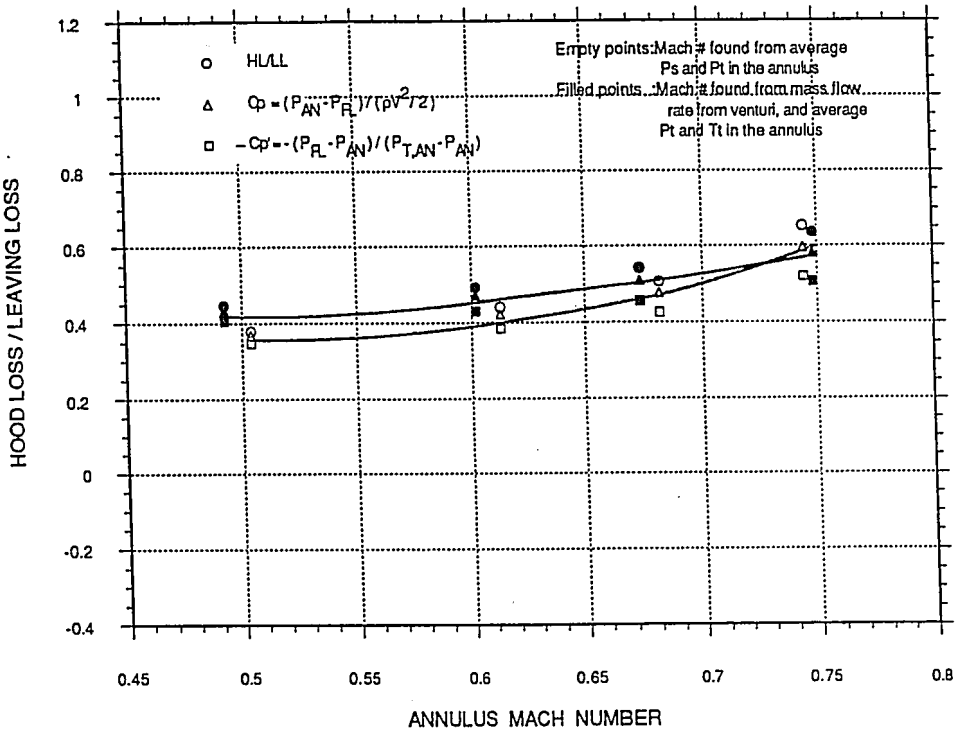

GENERIC MODEL
CONFIGURATION 9D
W/ SCREEN W/O GUIDE VANE

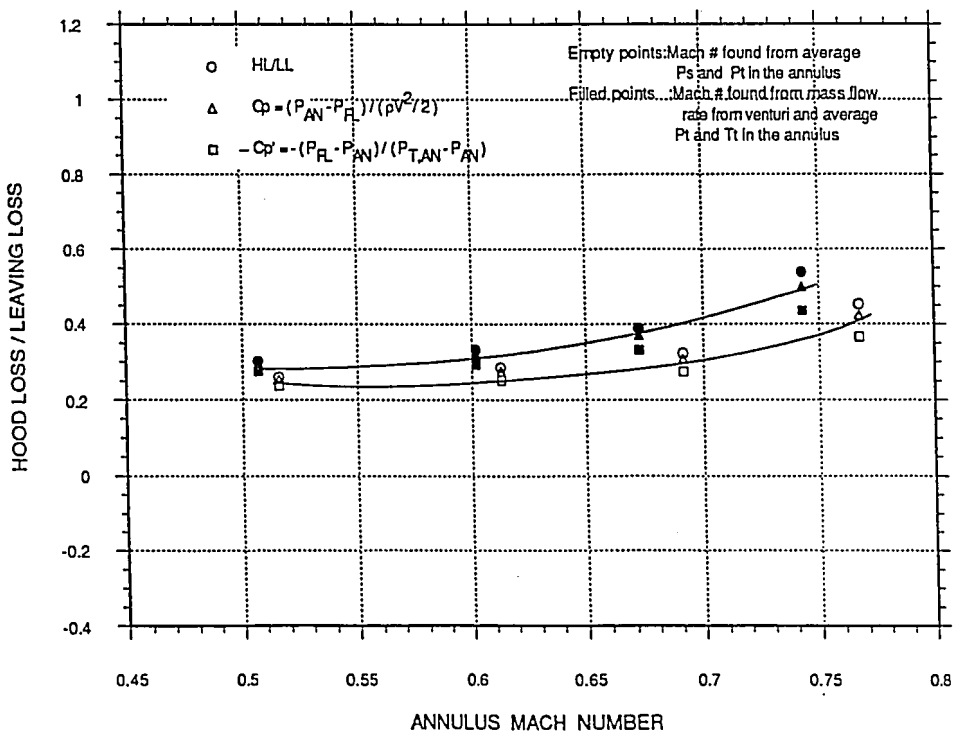

CIRCUMFERENTIAL VARIATION OF Cp
TEST 49 OF CONFIGURATION 1
W/ SCREEN W/ GUIDE VANE

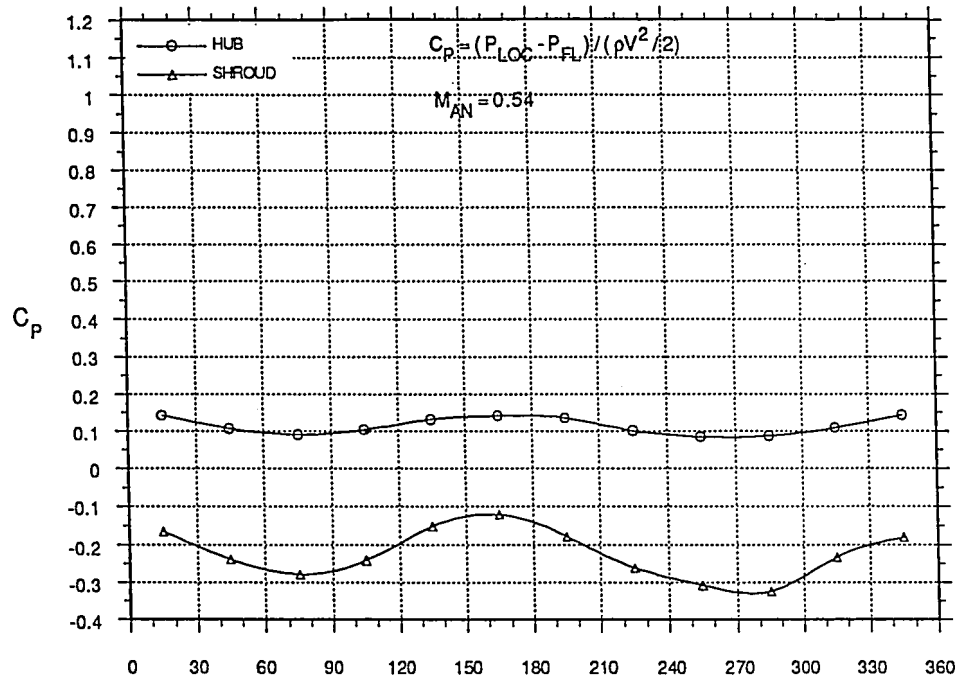

CIRCUMFERENTIAL VARIATION OF Cp
TEST 50 OF CONFIGURATION 1
W/ SCREEN W/ GUIDE VANE

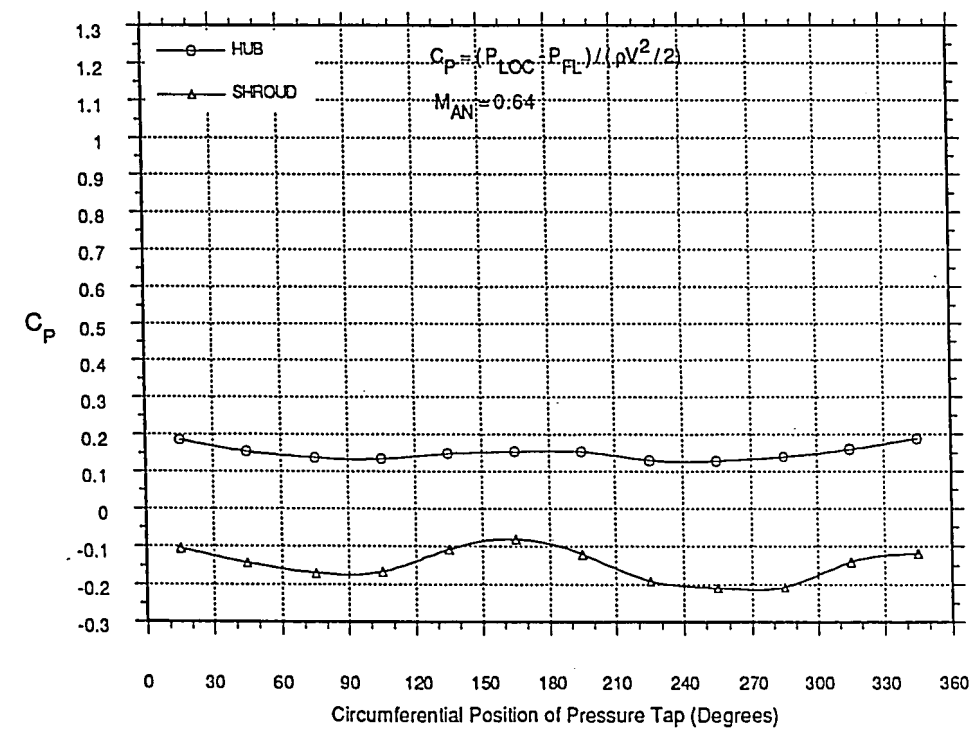

CIRCUMFERENTIAL VARIATION OF Cp
TEST 51 OF CONFIGURATION 1
W/ SCREEN W/ GUIDE VANE

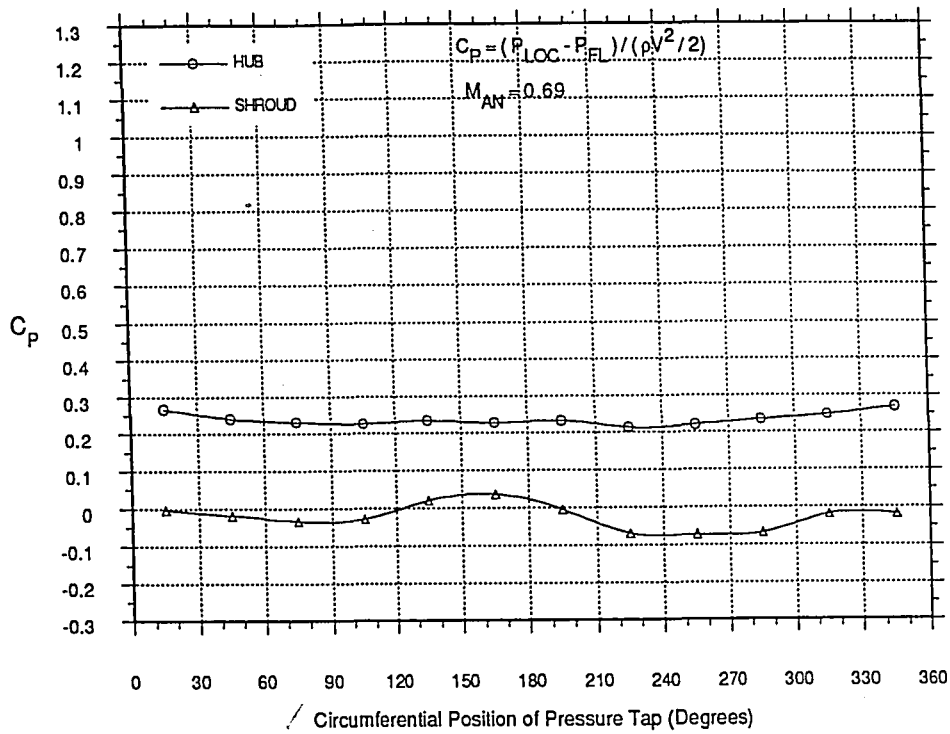

CIRCUMFERENTIAL VARIATION OF Cp
TEST 52 OF CONFIGURATION 1
W/ SCREEN W/ GUIDE VANE

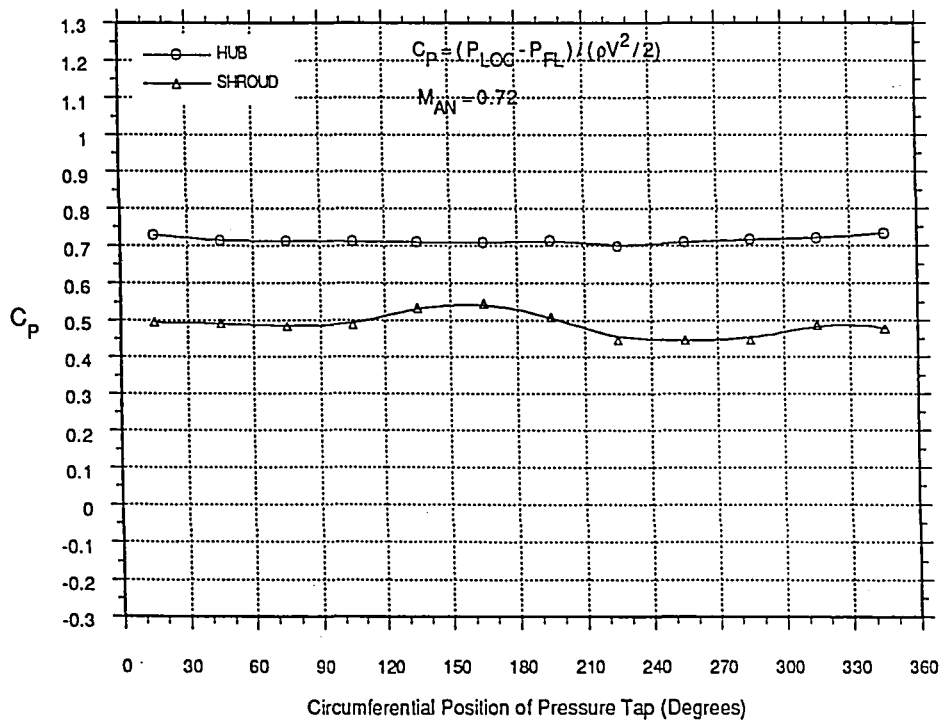

CIRCUMFERENTIAL VARIATION OF Cp
TEST 61 OF CONFIGURATION 1B
W/O SCREEN W/ GUIDE VANE

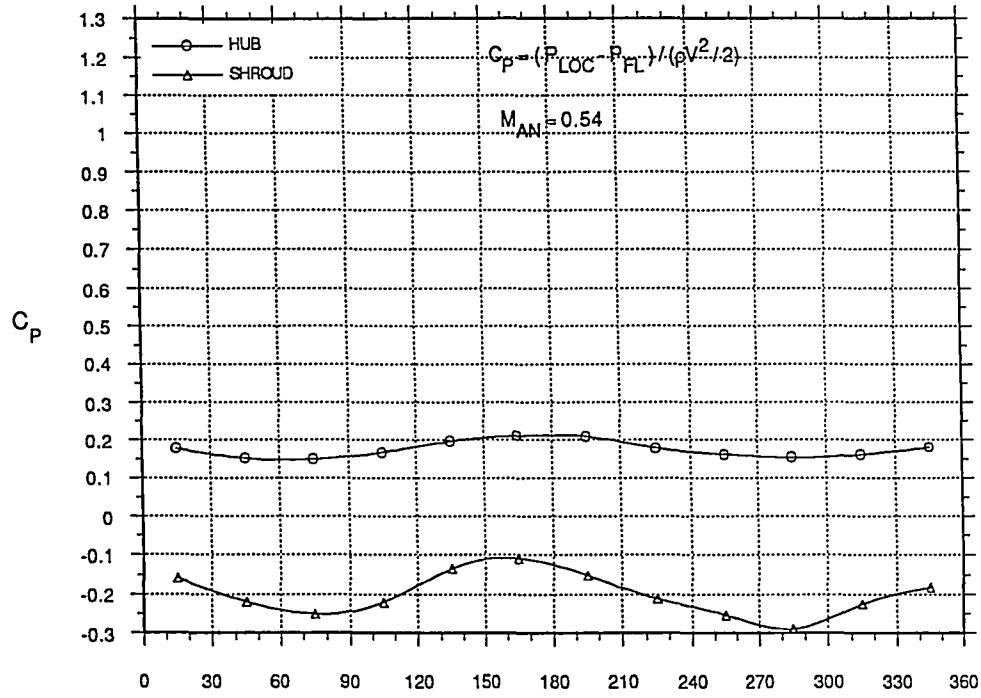

CIRCUMFERENTIAL VARIATION OF Cp
TEST 62 OF CONFIGURATION 1B
W/O SCREEN W/ GUIDE VANE

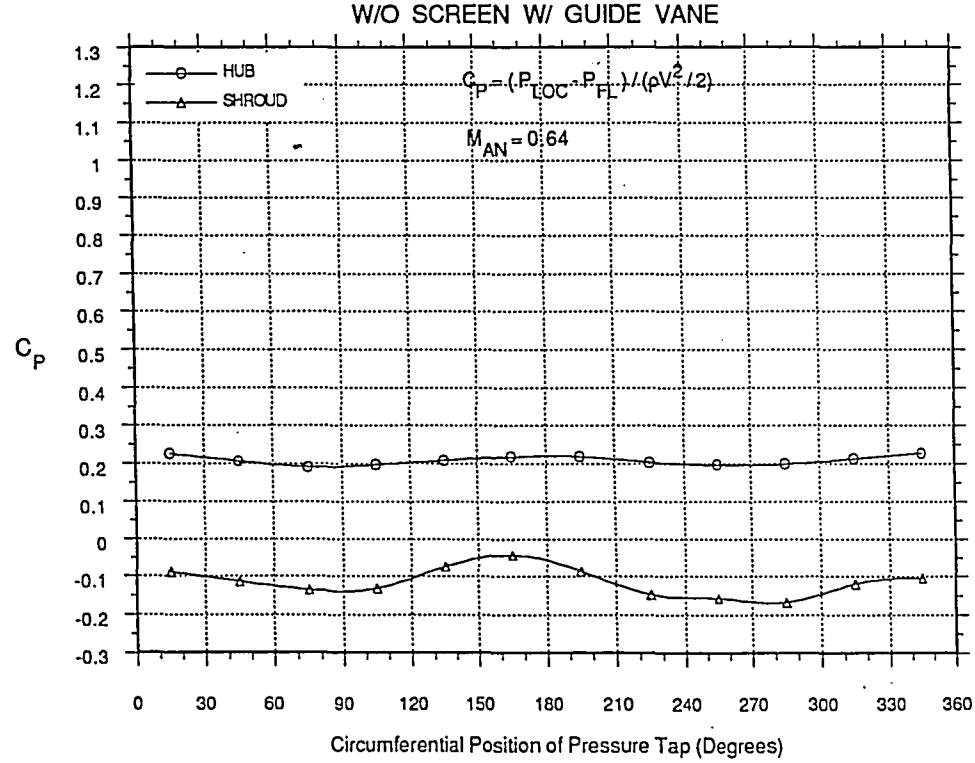

CIRCUMFERENTIAL VARIATION OF Cp
TEST 63 OF CONFIGURATION 1B
W/O SCREEN W/ GUIDE VANE

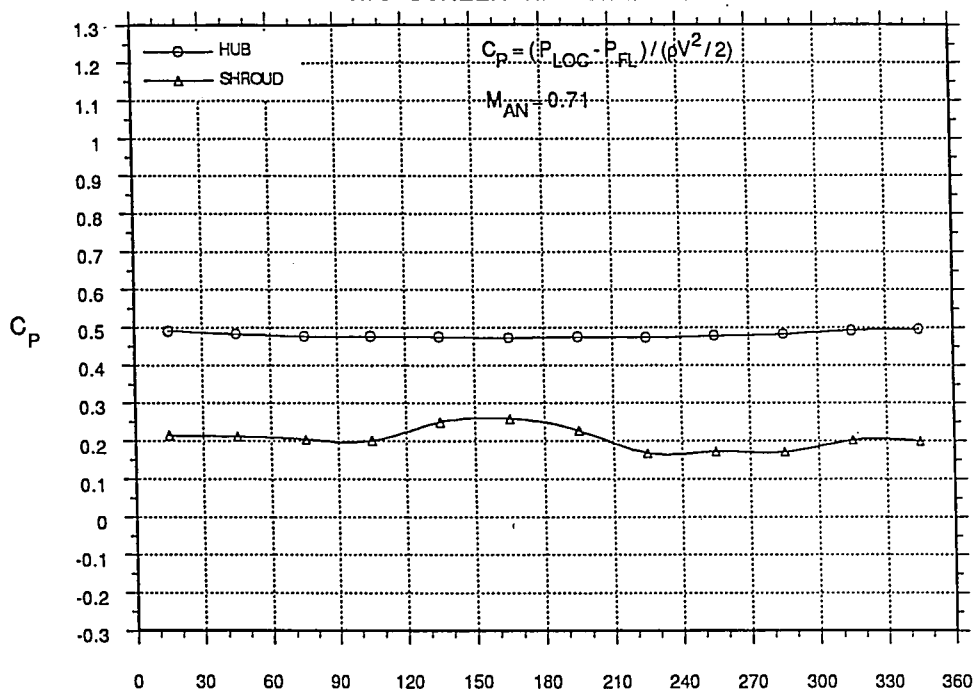

CIRCUMFERENTIAL VARIATION OF Cp
TEST 64 OF CONFIGURATION 1B
W/O SCREEN W/ GUIDE VANE

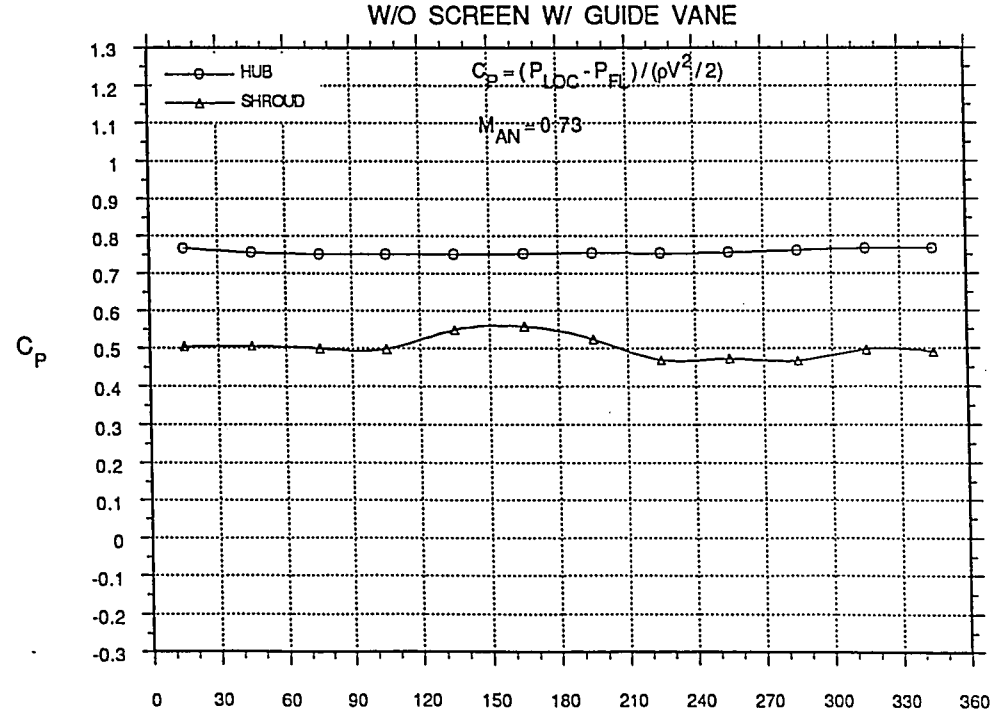

CIRCUMFERENTIAL VARIATION OF Cp
TEST 101 OF CONFIGURATION 1C
W/O SCREEN W/O GUIDE VANE

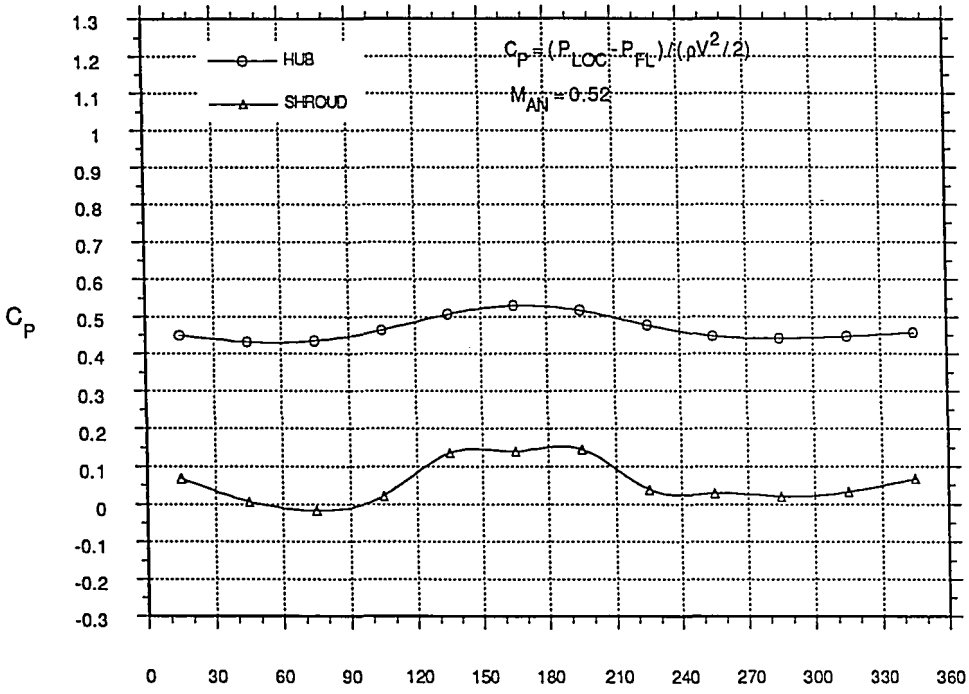

CIRCUMFERENTIAL VARIATION OF Cp
TEST 102 OF CONFIGURATION 1C
W/O SCREEN W/O GUIDE VANE

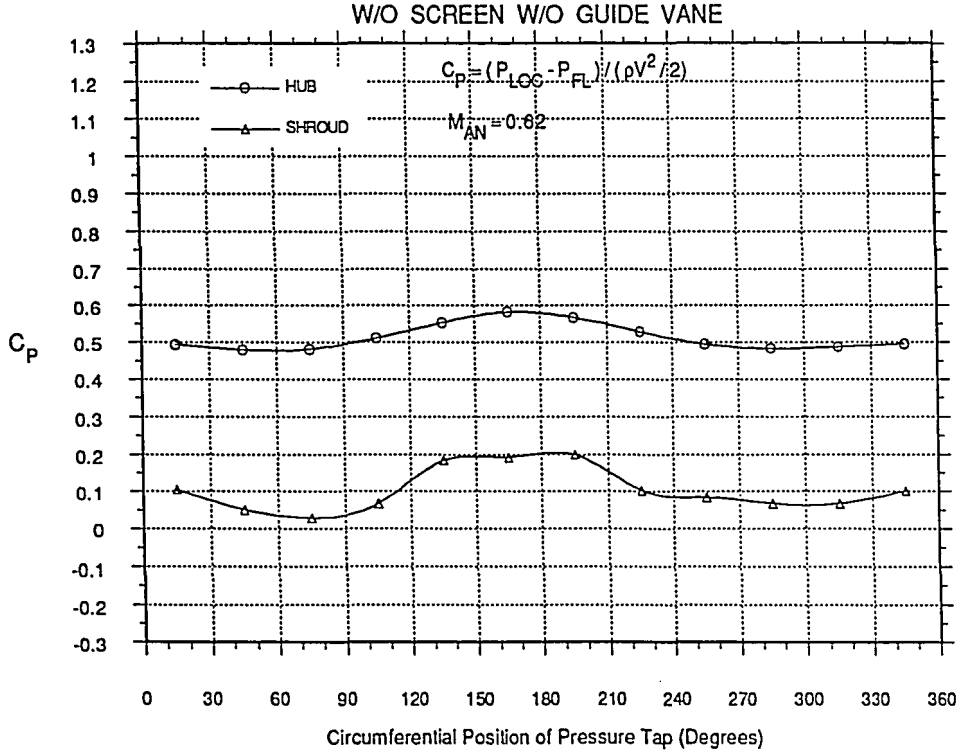

CIRCUMFERENTIAL VARTIATION OF Cp
TEST 103 OF CONFIGURATION 1C
W/O SCREEN W/O GUIDE VANE

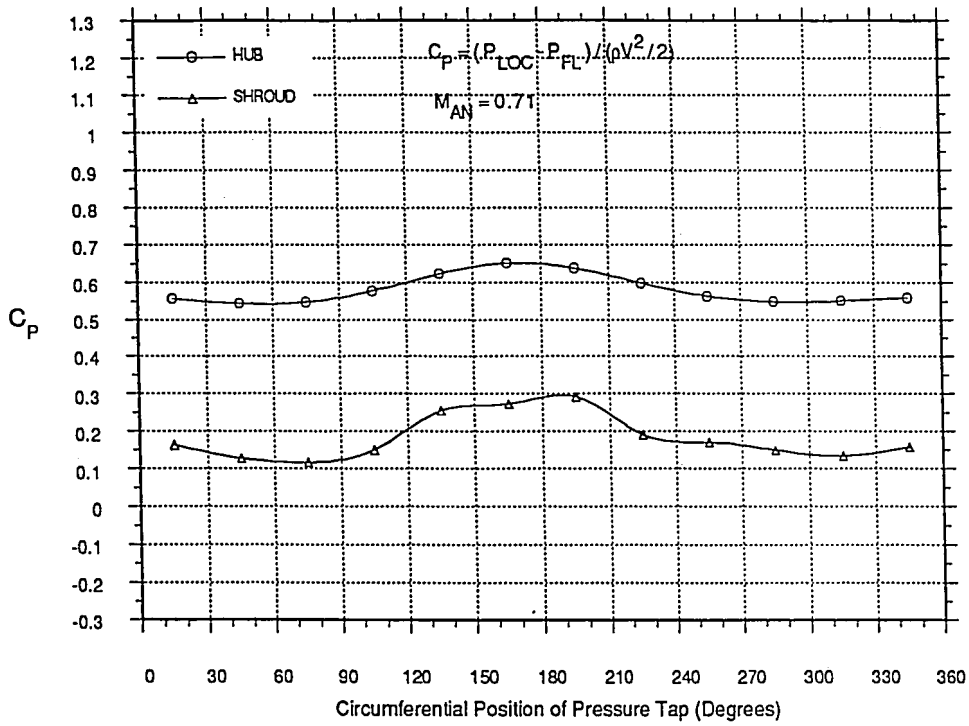

CIRCUMFERENTIAL VARIATION OF Cp
TEST 104 OF CONFIGURATION 1C
W/O SCREEN W/O GUIDE VANE

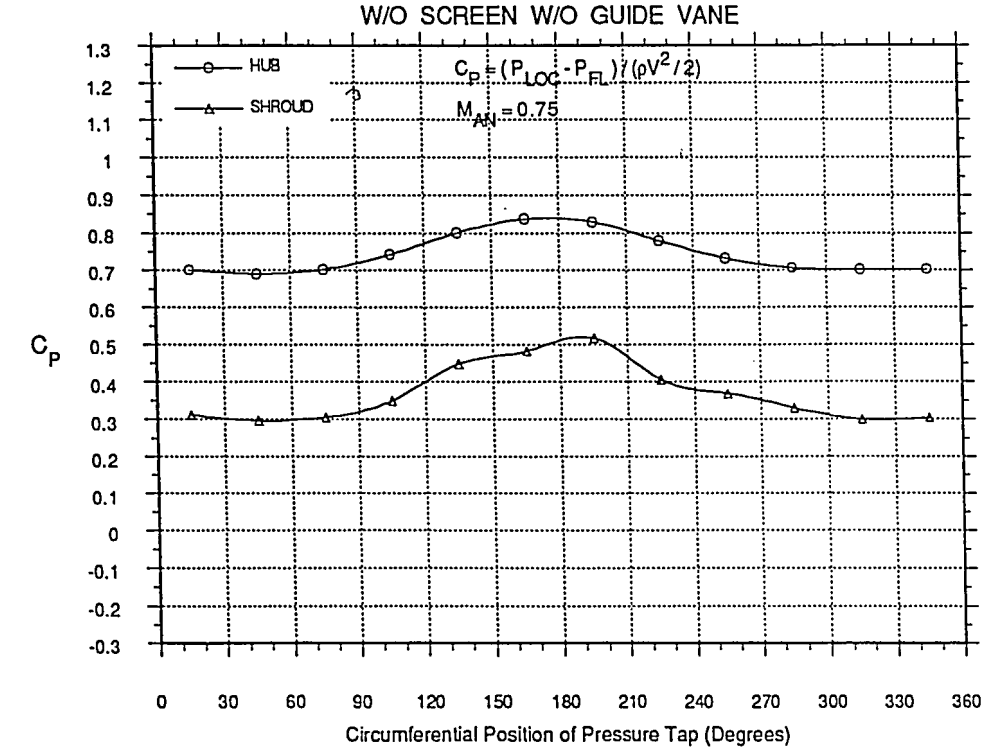

CIRCUMFERENTIAL VARIATION OF Cp
TEST 105 OF CONFIGURATION 1D
W/ SCREEN W/O GUIDE VANE

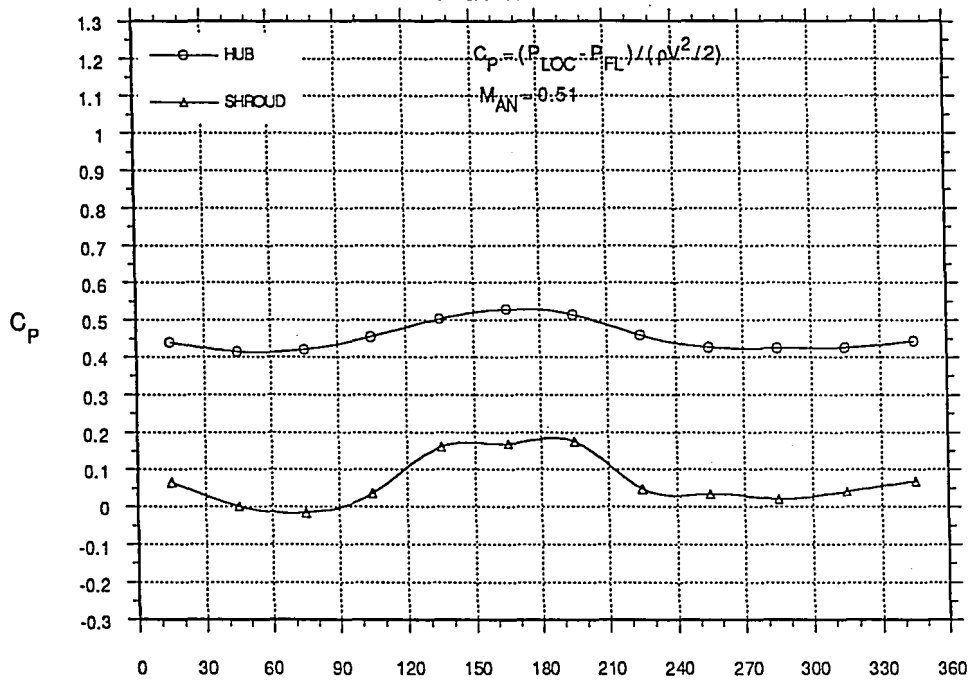

CIRCUMFERENTIAL VARIATION OF Cp
TEST 106 OF CONFIGURATION 1D
W/ SCREEN W/O GUIDE VANE

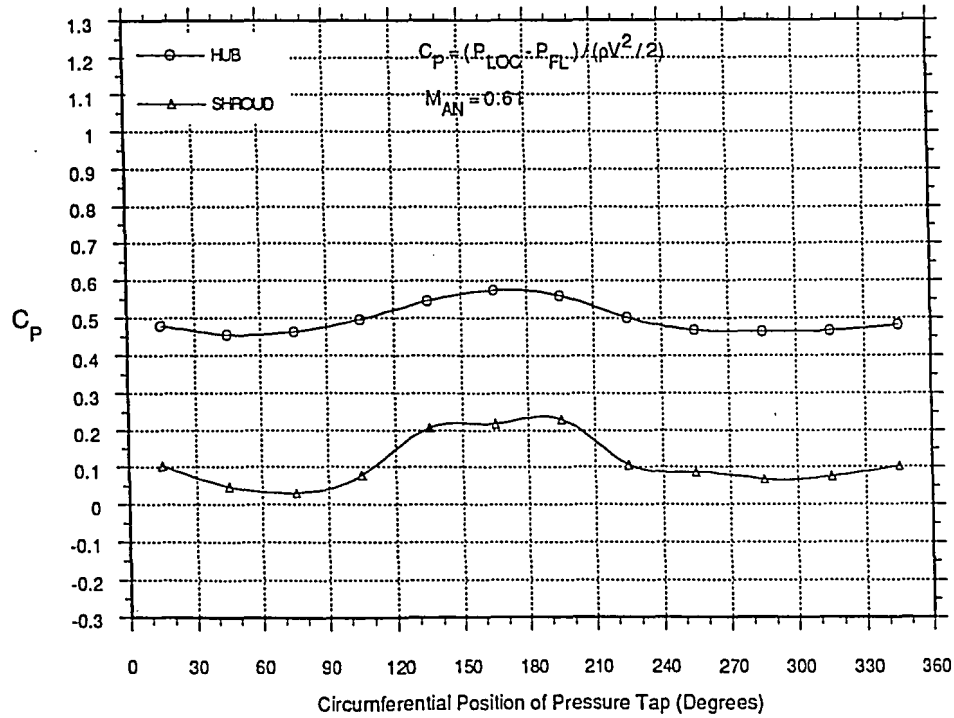

CIRCUMFERENTIAL VARIATION OF Cp
TEST 107 OF CONFIGURATION 1D
W/ SCREEN W/O GUIDE VANE

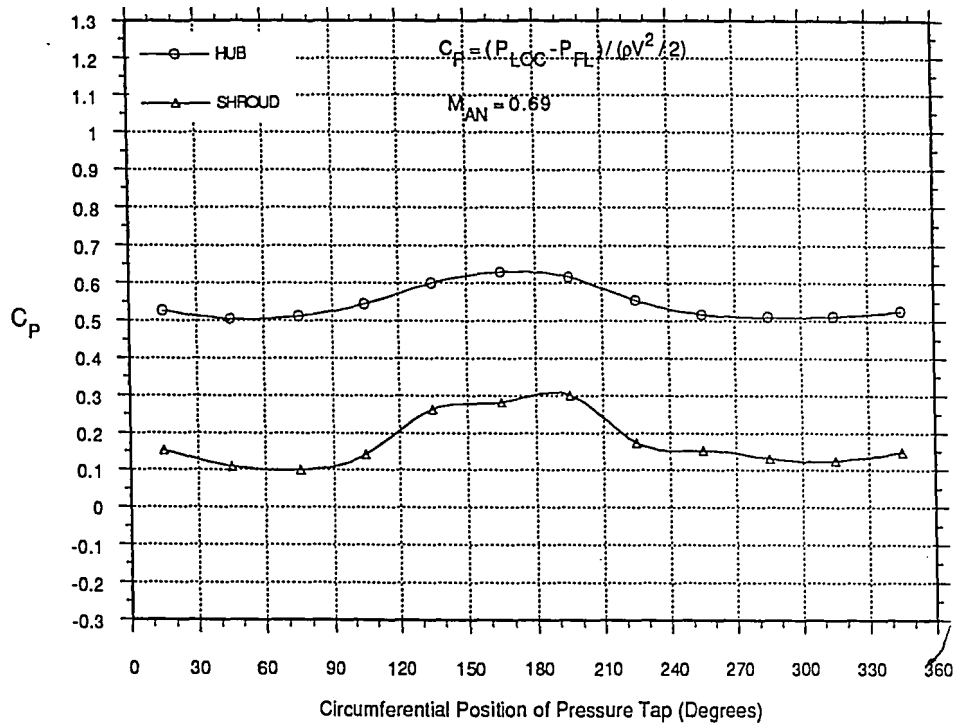

CIRCUMFERENTIAL VARIATION OF Cp
TEST 108 OF CONFIGURATION 1D
W/ SCREEN W/O GUIDE VANE

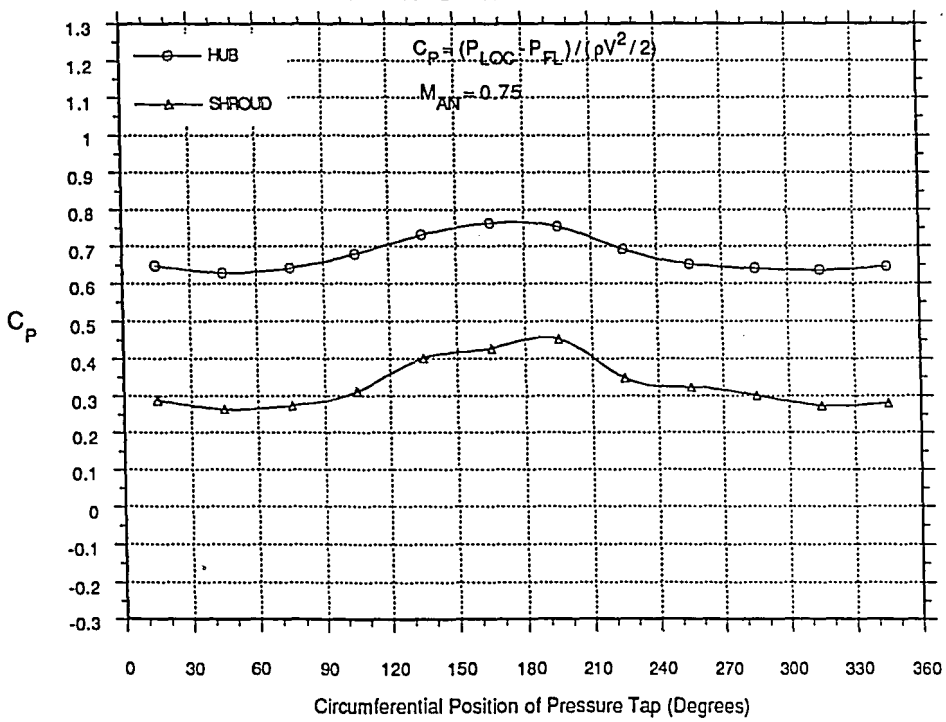

CIRCUMFERENTIAL VARIATION OF Cp
TEST 9 OF CONFIGURATION 9
W/ SCREEN W/ GUIDE VANE

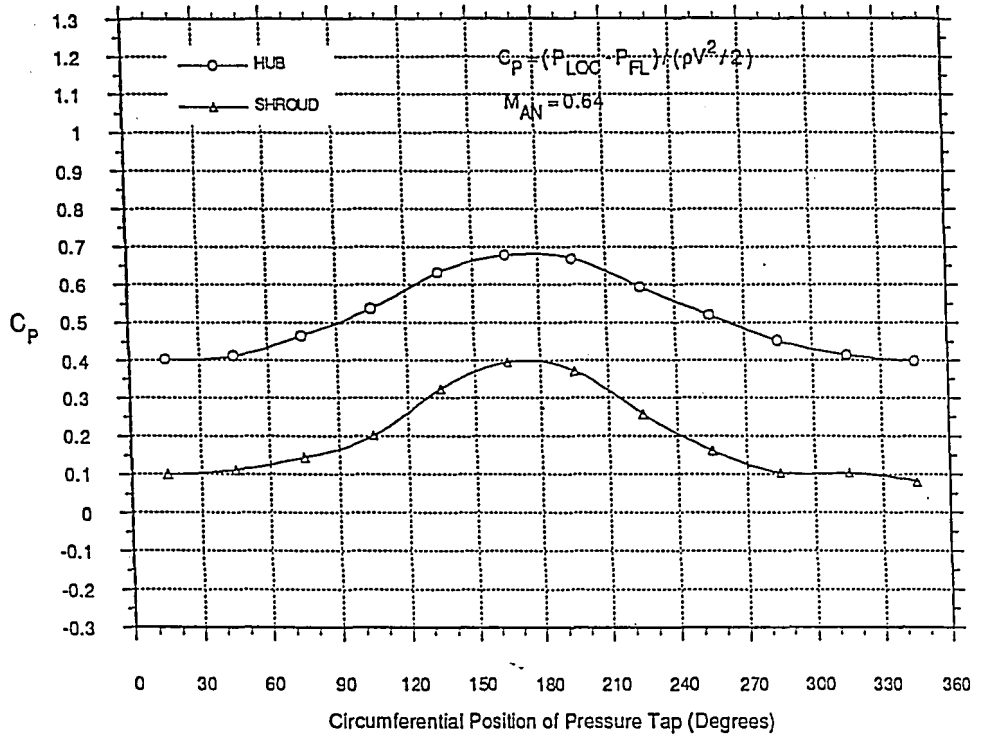

CIRCUMFERENTIAL VARIATION OF Cp
TEST 10 OF CONFIGURATION 9
W/ SCREEN W/ GUIDE VANE

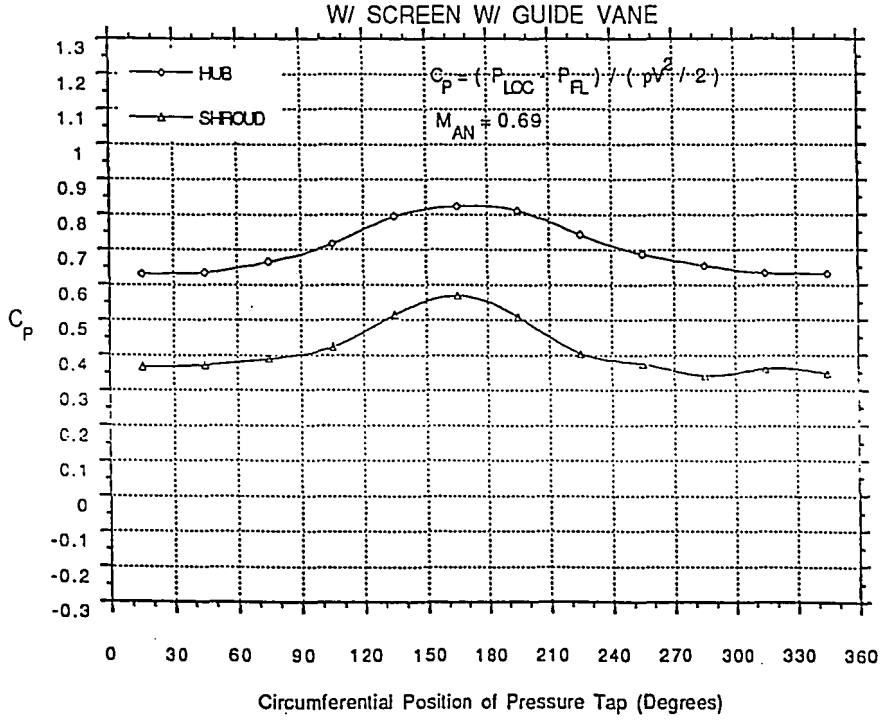

CIRCUMFERENTIAL VARIATION OF Cp
TEST 11 OF CONFIGURATION 9
W/ SCREEN W/ GUIDE VANE

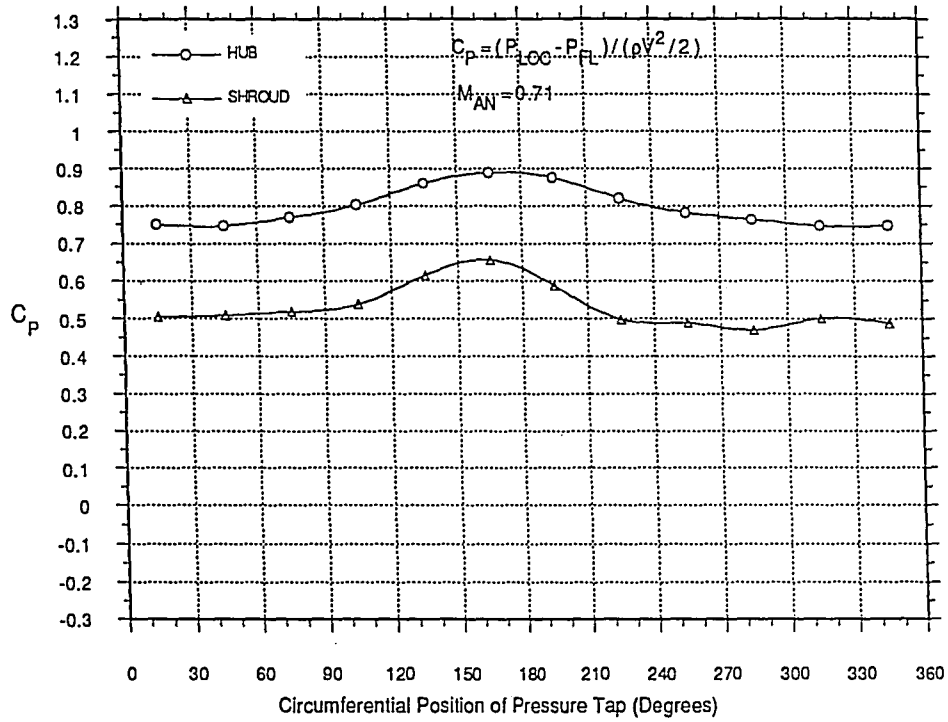

CIRCUMFERENTIAL VARIATION OF Cp
TEST 12 OF CONFIGURATION 9
W/ SCREEN W/ GUIDE VANE

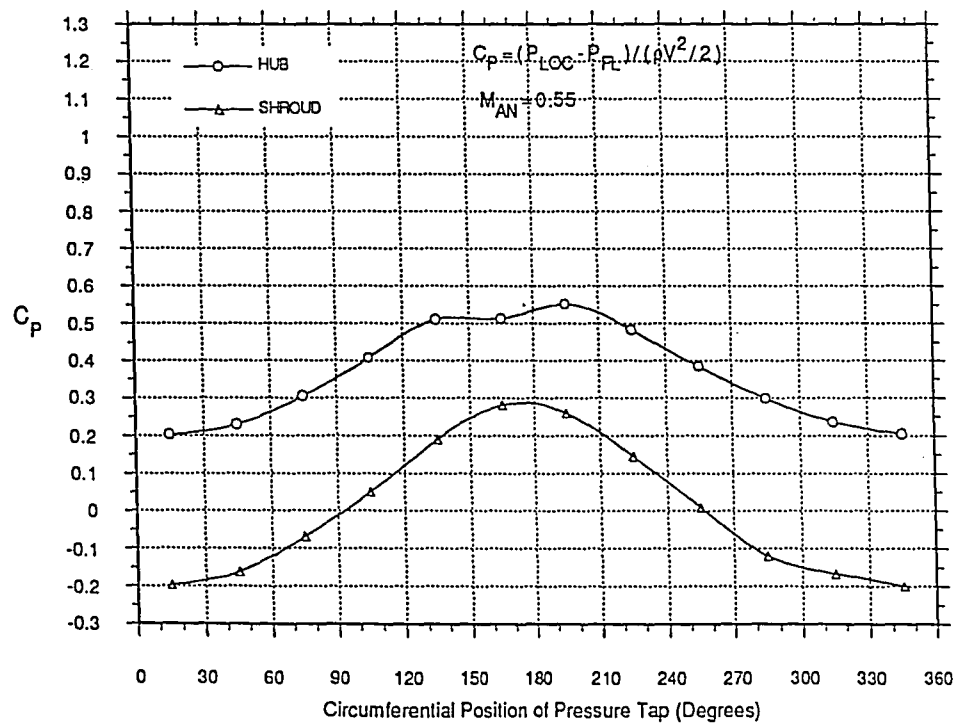

CIRCUMFERENTIAL VARIATION OF Cp
TEST 89 OF CONFIGURATION 9B
W/O SCREEN W/ GUIDE VANE

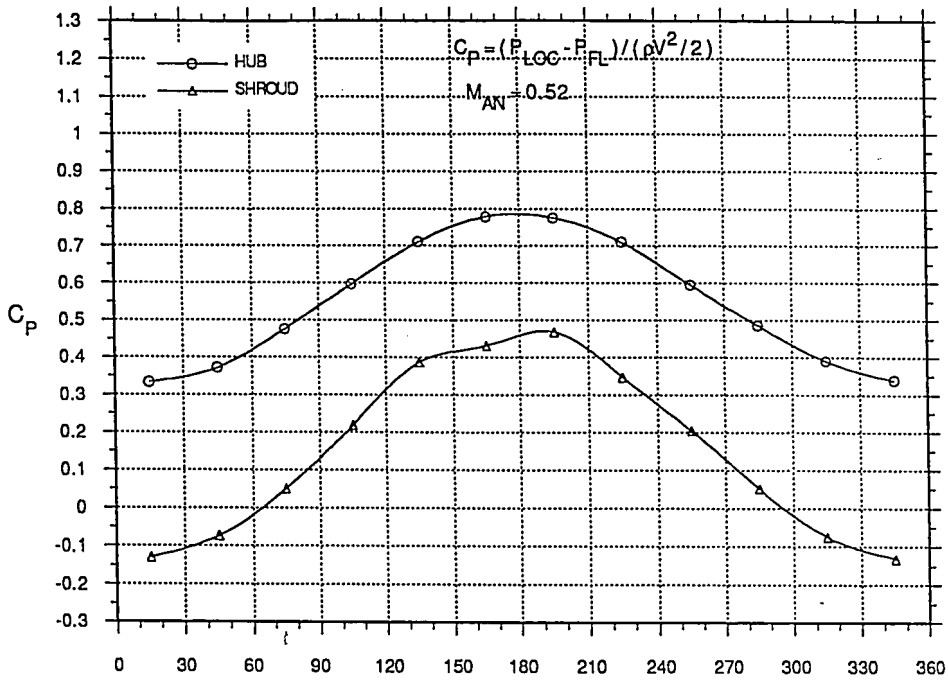

CIRCUMFERENTIAL VARIATION OF Cp
TEST 90 OF CONFIGURATION 9B
W/O SCREEN W/ GUIDE VANE

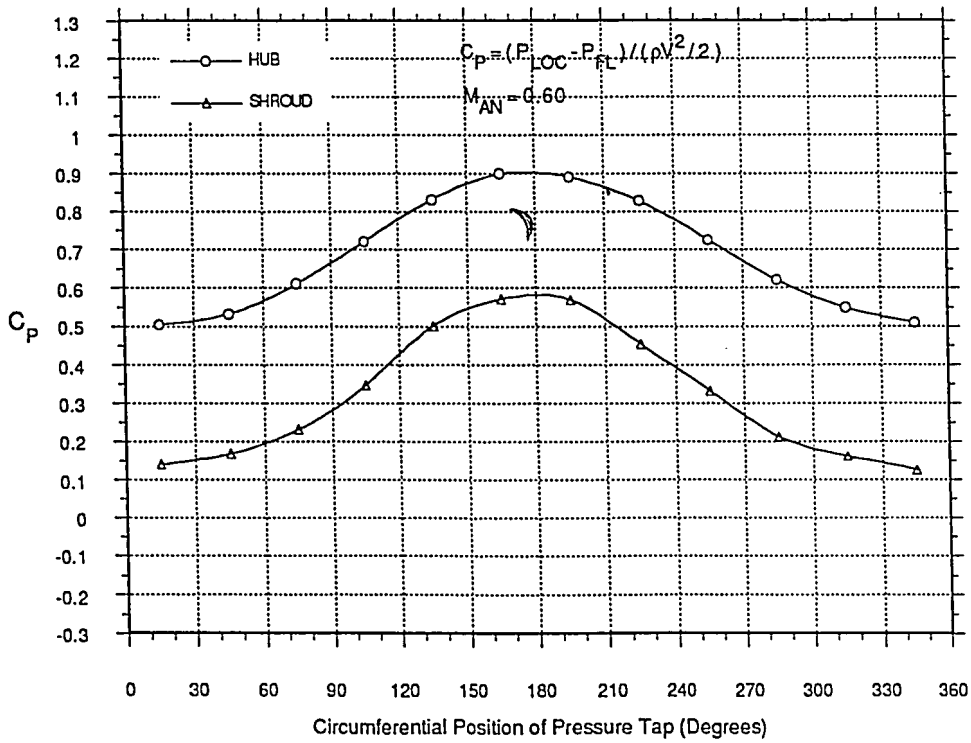

CIRCUMFERENTIAL VARIATION OF Cp
TEST 91 OF CONFIGURATION 9B
W/O SCREEN W/ GUIDE VANE

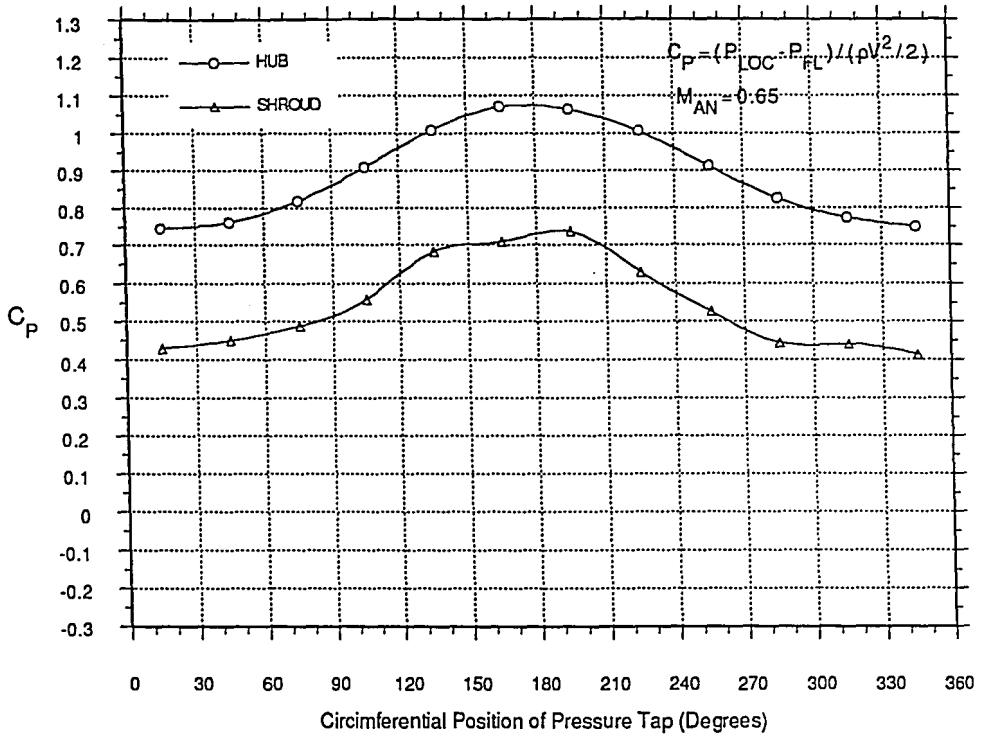

CIRCUMFERENTIAL VARIATION OF Cp
TEST 92 OF CONFIGURATION 9B
W/O SCREEN W/ GUIDE VANE

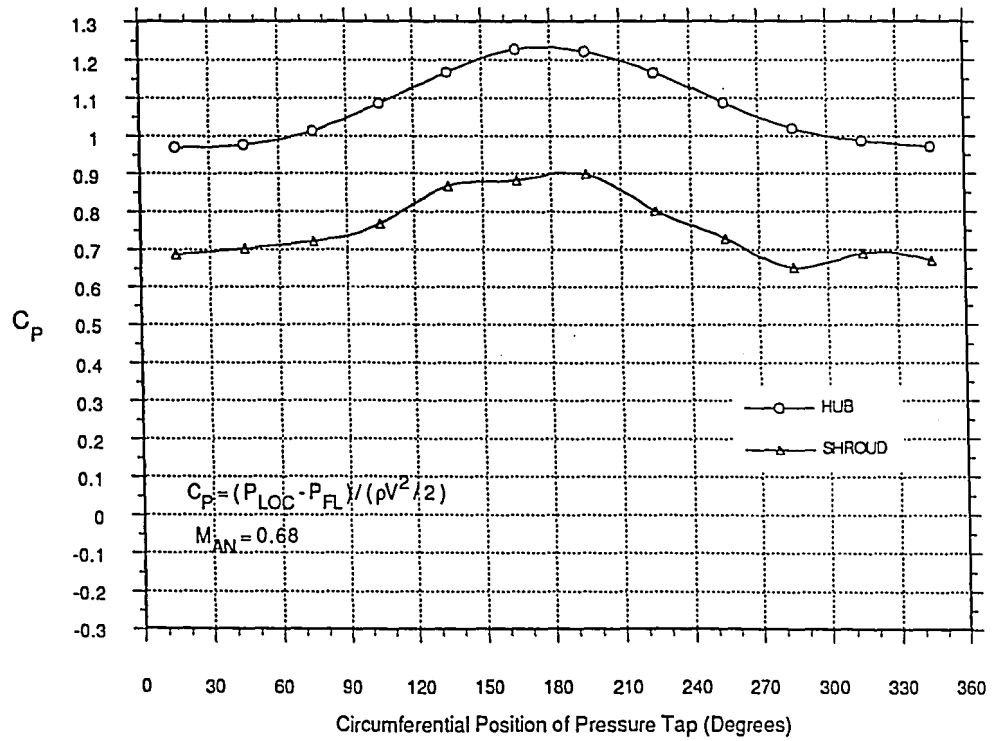

CIRCUMFERENTIAL VARIATION OF Cp
TEST 93 OF CONFIGURATION 9C
W/O SCREEN W/O GUIDE VANE

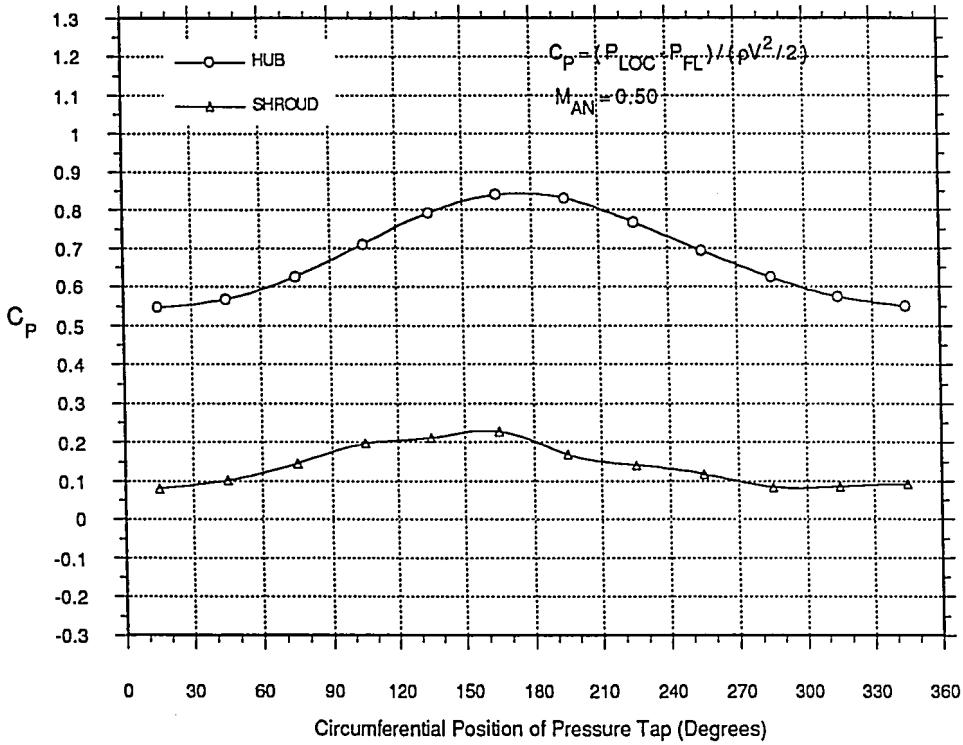

CIRCUMFERENTIAL VARIATION OF Cp
TEST 94 OF CONFIGURATION 9C
W/O SCREEN W/O GIDE VANE

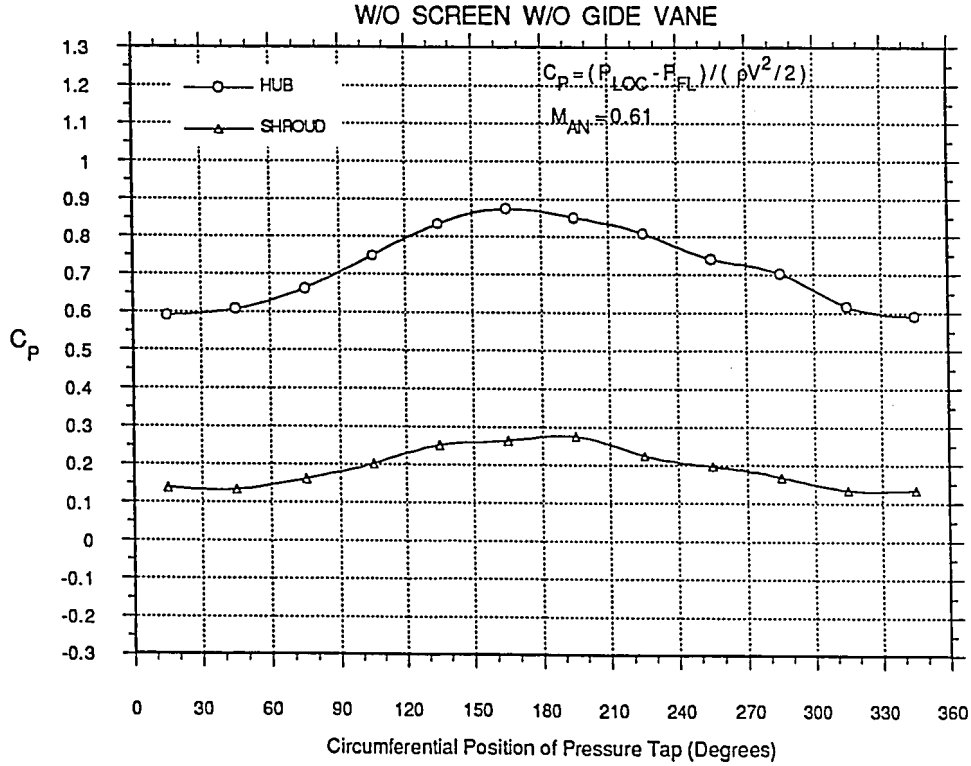

CIRCUMFERENTIAL VARIATION OF Cp
TEST 95 OF CONFIGURATION 9C
W/O SCREEN W/O GUIDE VANE

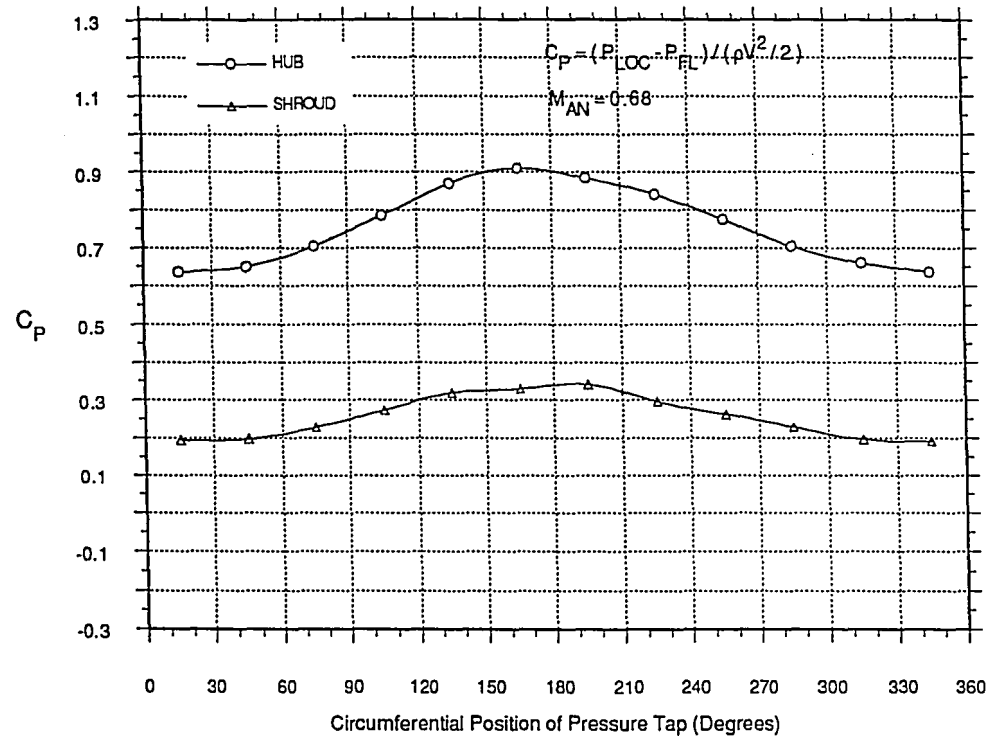

CIRCUMFERENTIAL VARIATION OF Cp
TEST 96 OF CONFIGURATION 9C
W/O SCREEN W/O GUIDE VANE

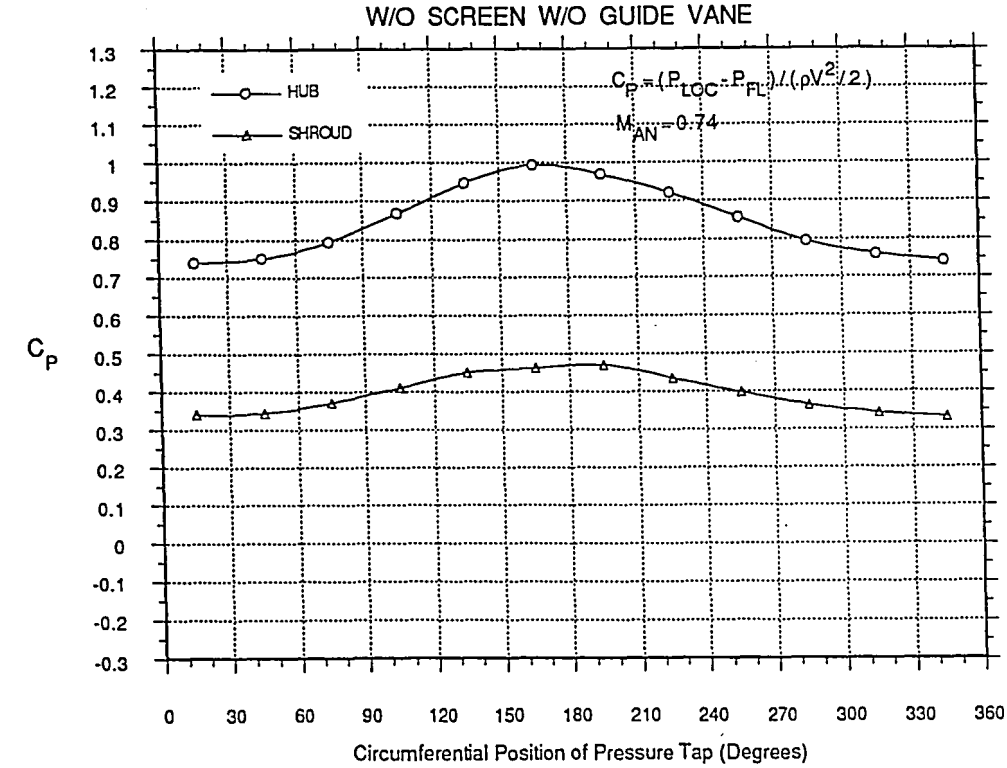

CIRCUMFERENTIAL VARIATION OF Cp
TEST 109 OF CONFIGURATION 9D
W/ SCREEN W/O GUIDE VANE

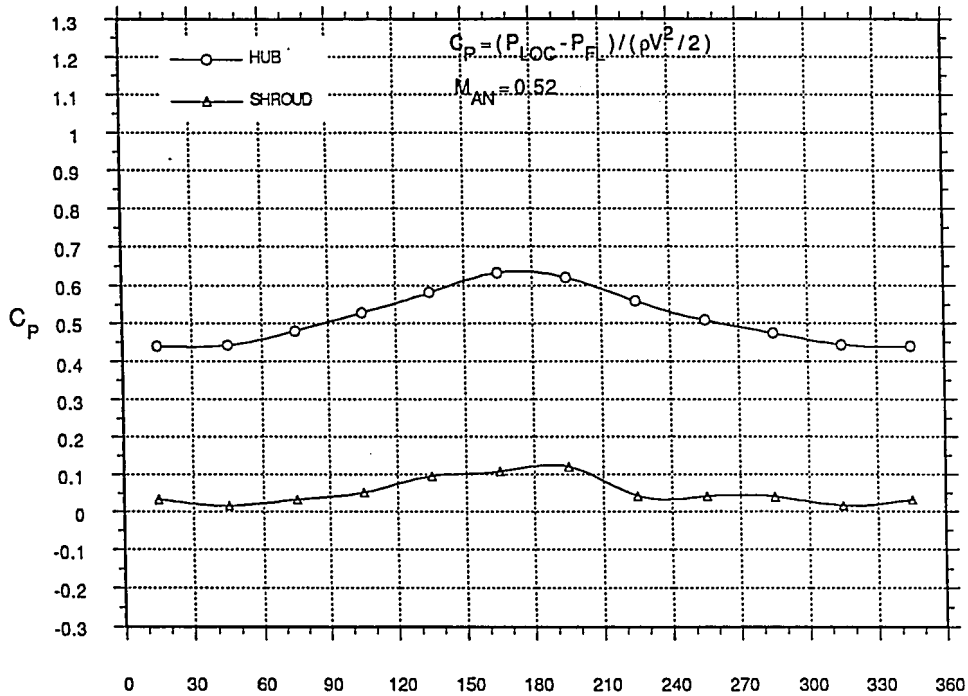

CIRCUMFERENTIAL VARIATION OF Cp
TEST 110 OF CONFIGURATION 9D
W/ SCREEN W/O GUIDE VANE

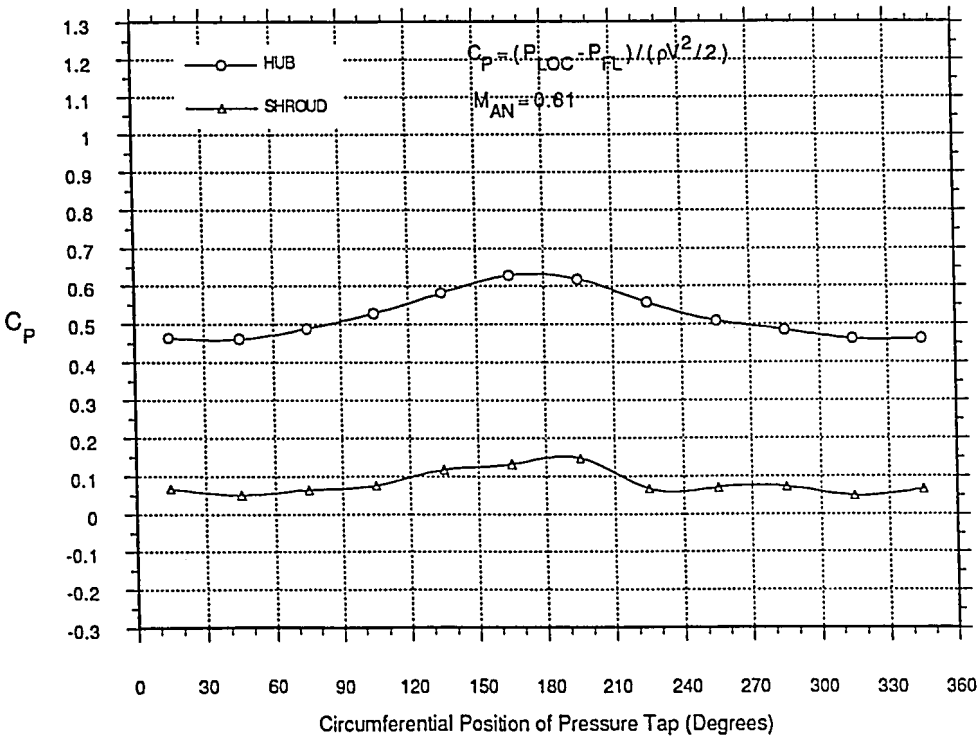

CIRCUMFERENTIAL VARIATION OF Cp
TEST 111 OF CONFIGURATION 9D
W/ SCREEN W/O GUIDE VANE

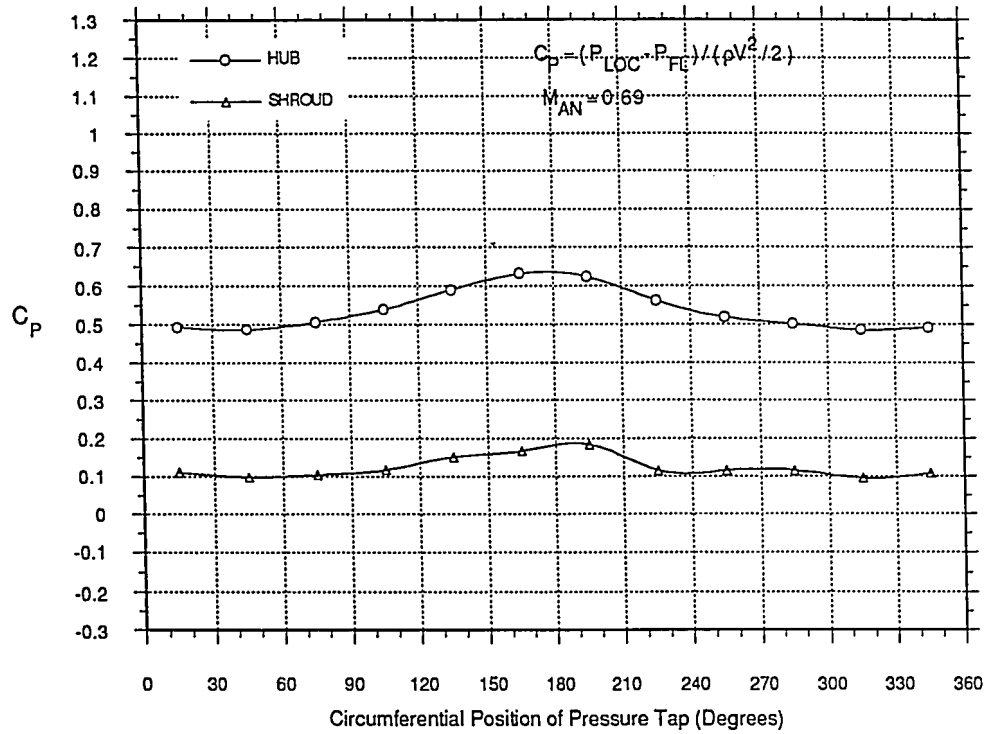

CIRCUMFERENTIAL VARIATION OF Cp
TEST 112 OF CONFIGURATION 9D
W/ SCREEN W/O GUIDE VANE

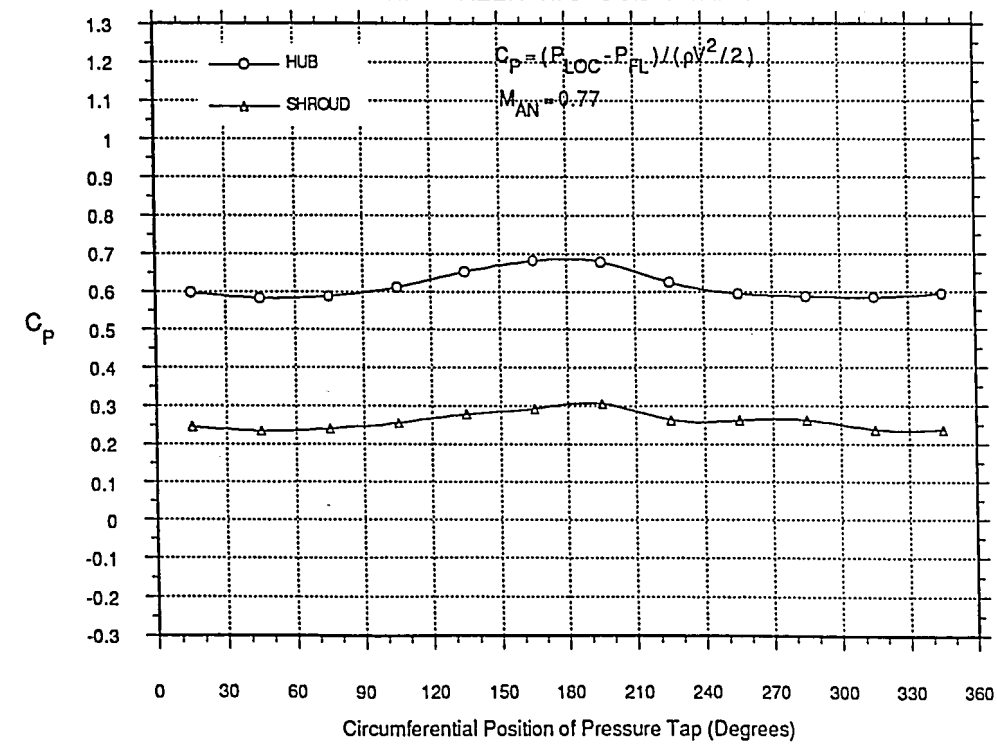

TRAVERSE NO 1
GENERIC MODEL CONFIGURATION 1
W/ SCREEN W/ GUIDE VANE

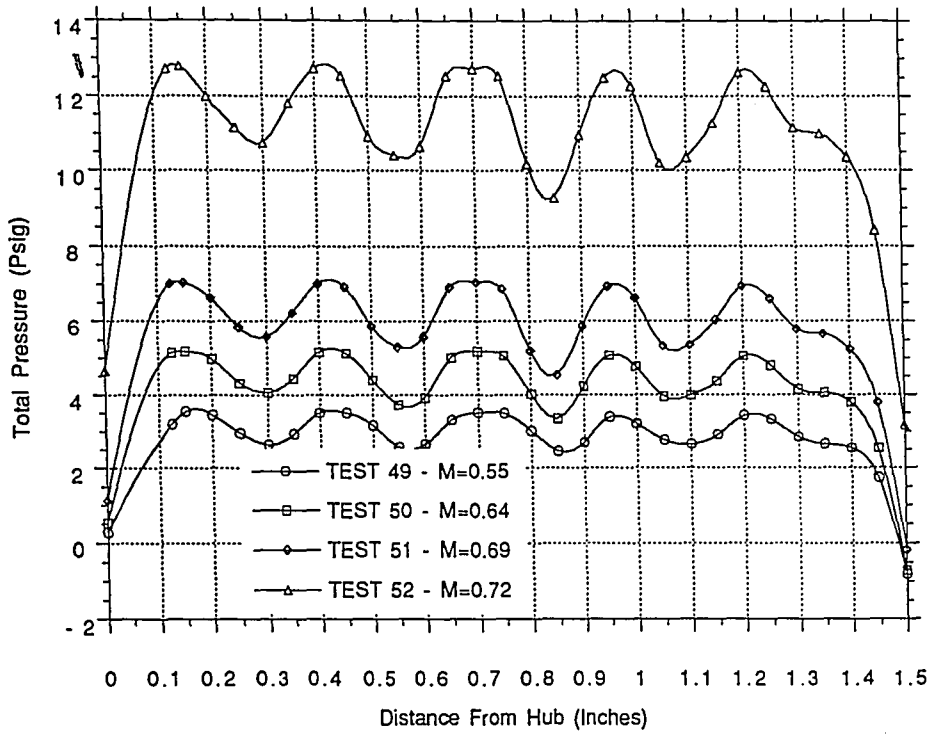

TRAVERSE NO 2
GENERIC MODEL CONFIGURATION 1
W/ SCREEN W/ GUIDE VANE

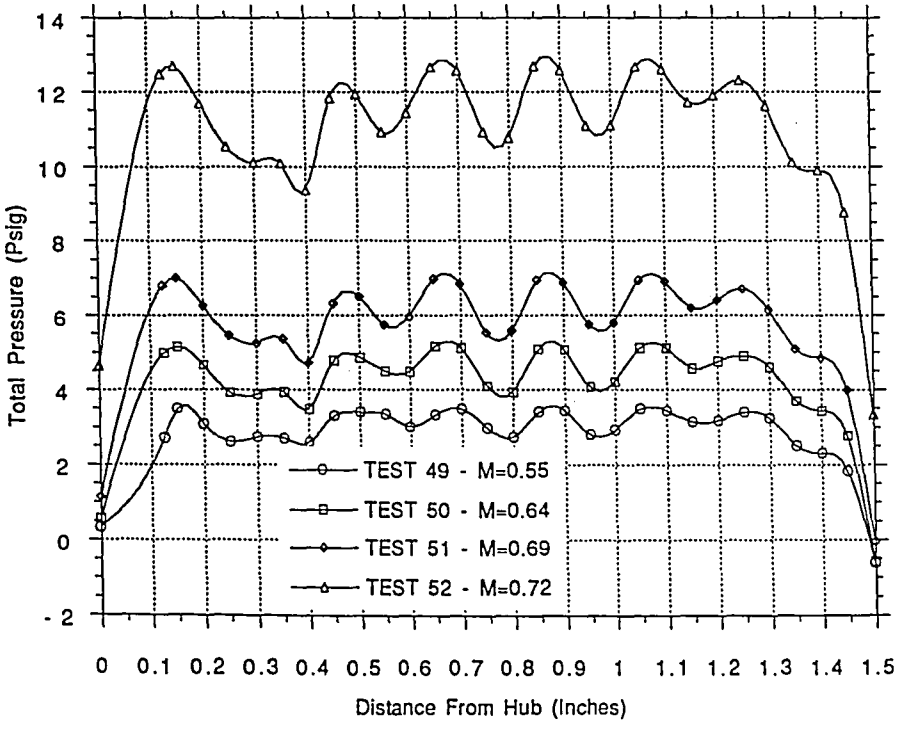

TRAVERSE NO 3
GENERIC MODEL CONFIGURATION 1
W/ SCREEN W/ GUIDE VANE

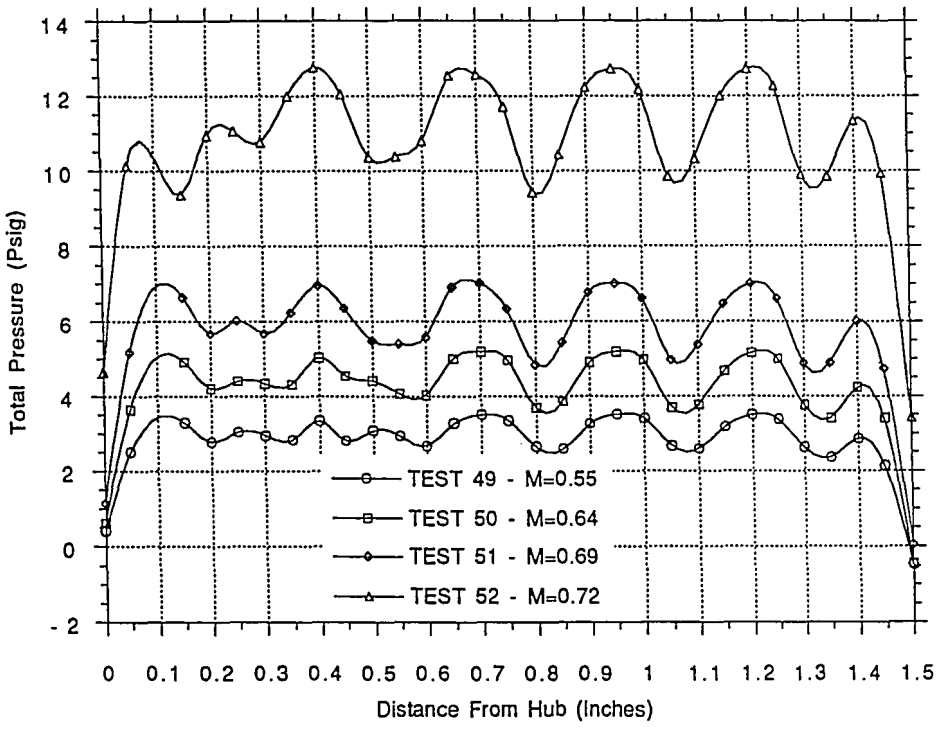

TRAVERSE NO 4
GENERIC MODEL CONFIGURATION 1
W/ SCREEN W/ GUIDE VANE

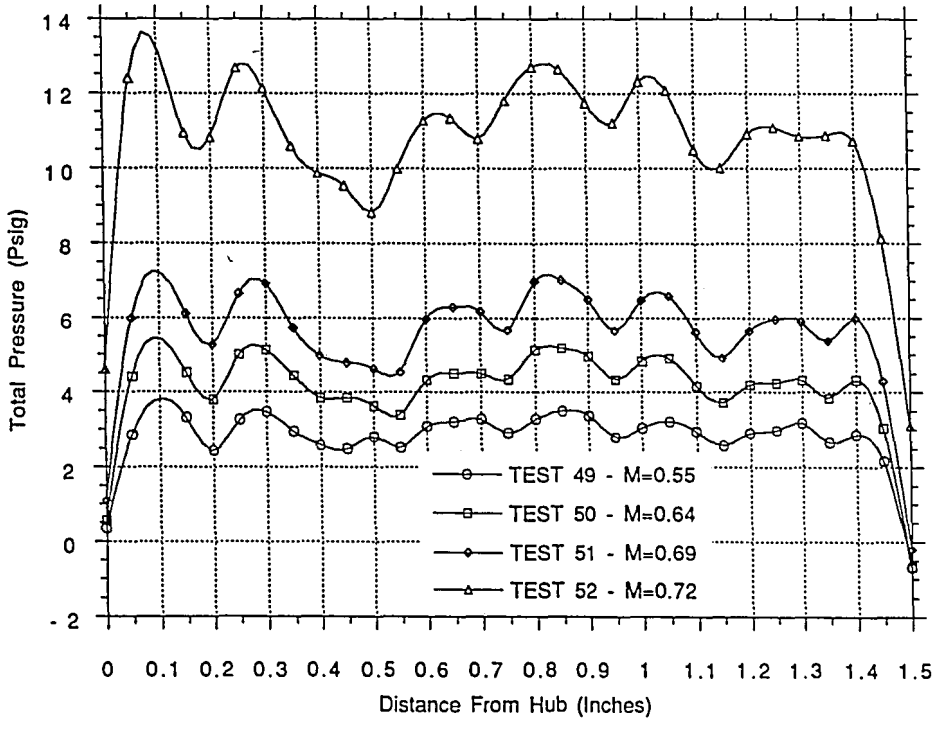

TRAVERSE NO 5
GENERIC MODEL CONFIGURATION 1
W/ SCREEN W/ GUIDE VANE

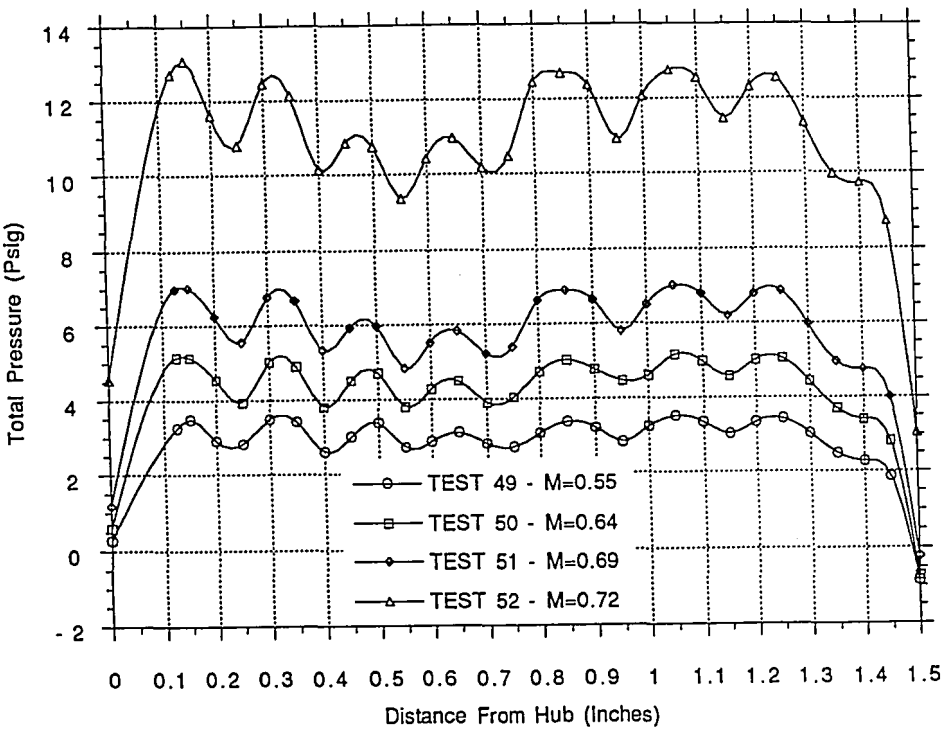

TRAVERSE NO 6
GENERIC MODEL CONFIGURATION 1
W/ SCREEN W/ GUIDE VANE

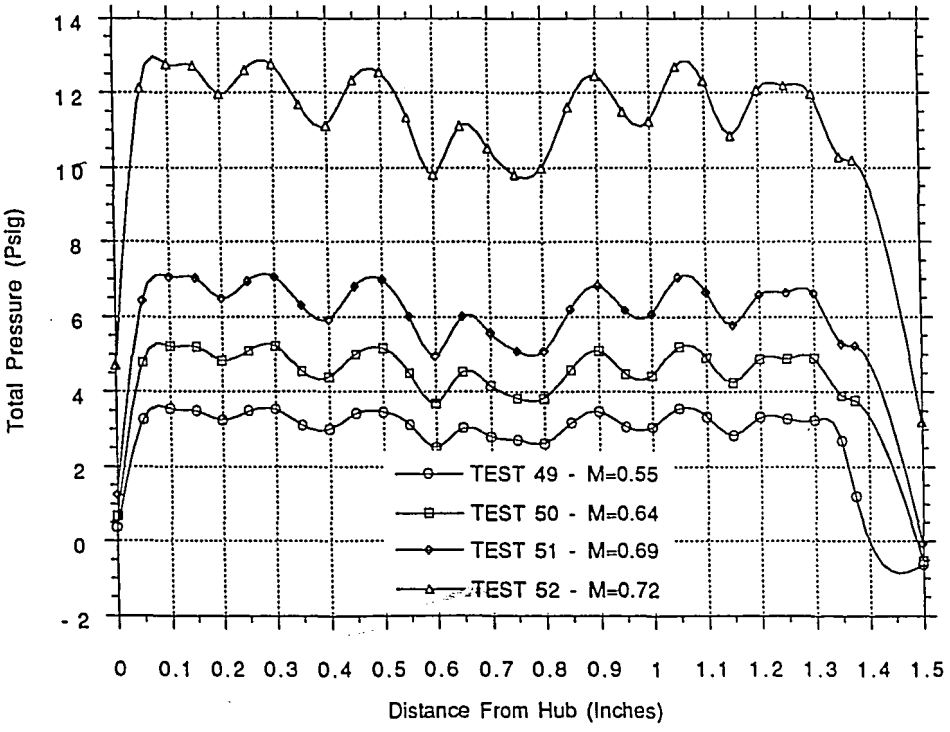

TRAVERSE NO 7
GENERIC MODEL CONFIGURATION 1
W/ SCREEN W/ GUIDE VANE

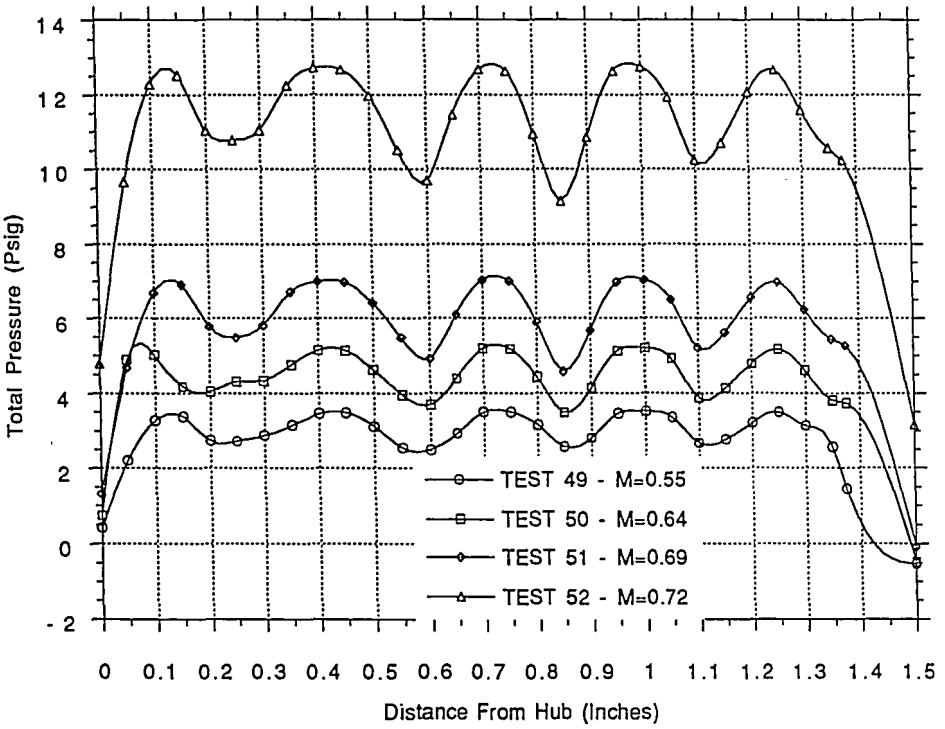

TRAVERSE NO 1
GENERIC MODEL CONFIGURATION 1B
W/O SCREEN W/ GUIDE VANE

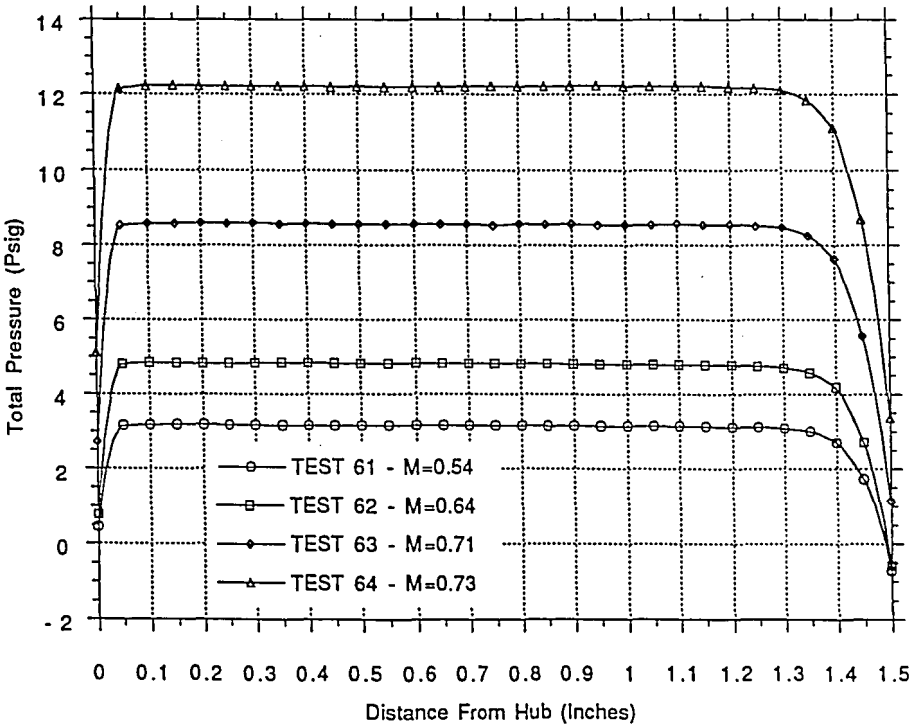

TRAVERSE NO 2
GENERIC MODEL CONFIGURATION 1B
W/O SCREEN W/ GUIDE VANE

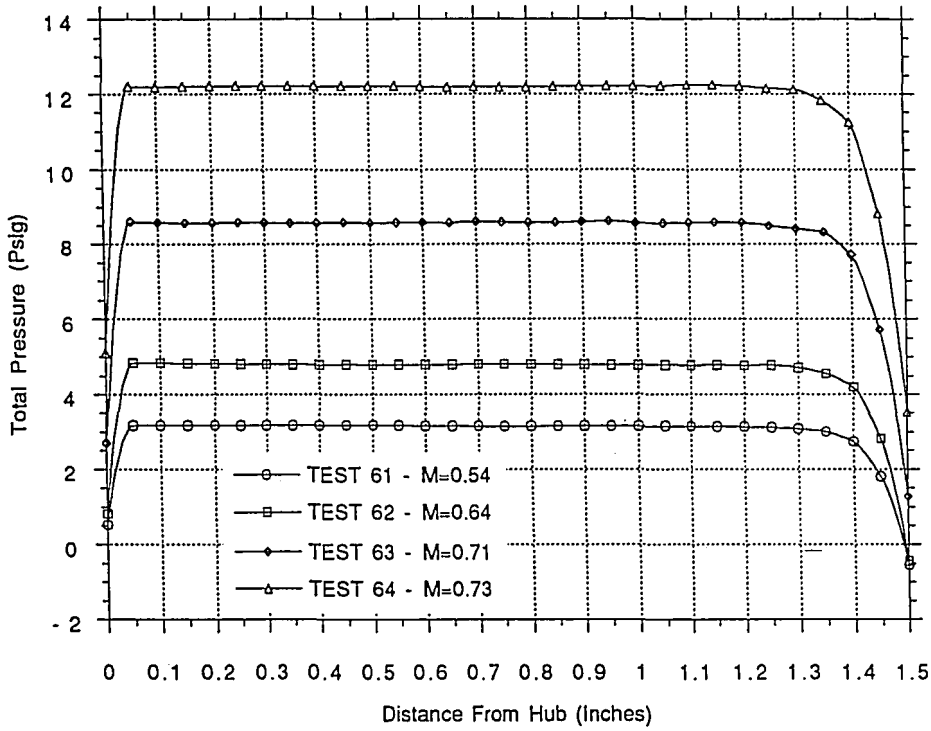

TRAVERSE NO 3
GENERIC MODEL CONFIGURATION 1B -
W/O SCREEN W/ GUIDE VANE

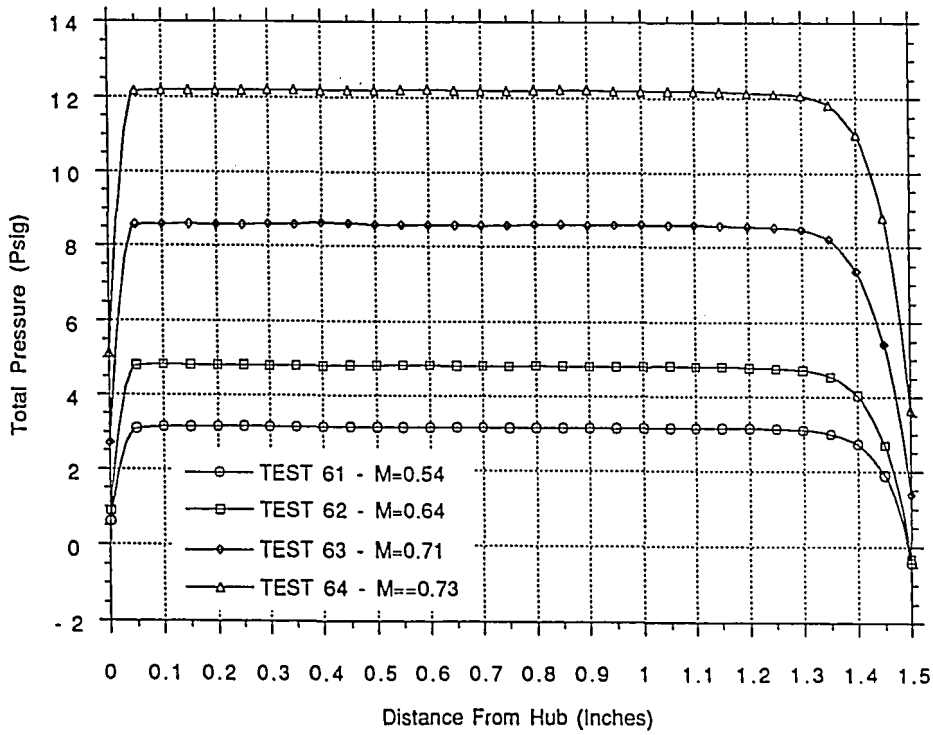

TRAVERSE NO 4
GENERIC MODEL CONFIGURATION 1B
W/O SCREEN W/ GUIDE VANE

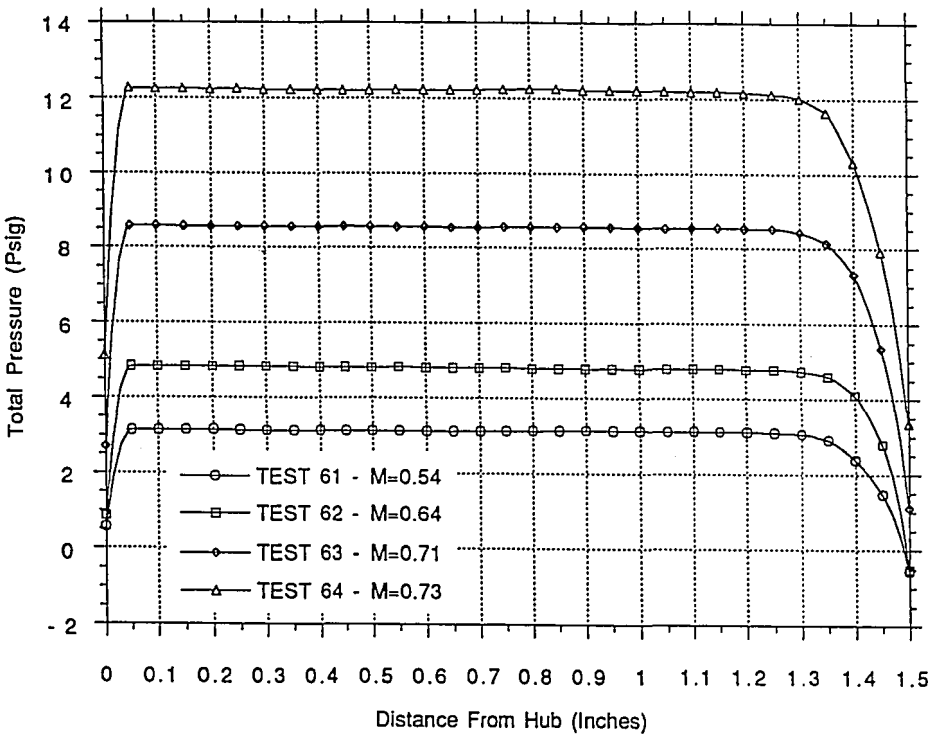

TRAVERSE NO 5
GENERIC MODEL CONFIGURATION 1B
W/O SCREEN W/ GUIDE VANE

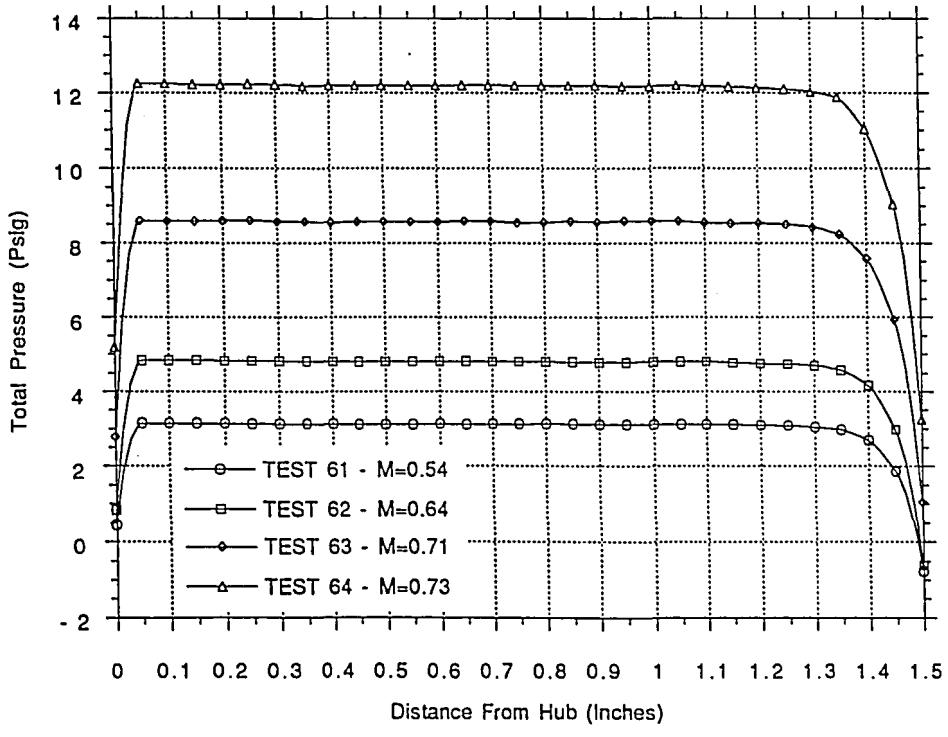

TRAVERSE NO 6
GENERIC MODEL CONFIGURATION 1B
W/O SCREEN W/ GUIDE VANE

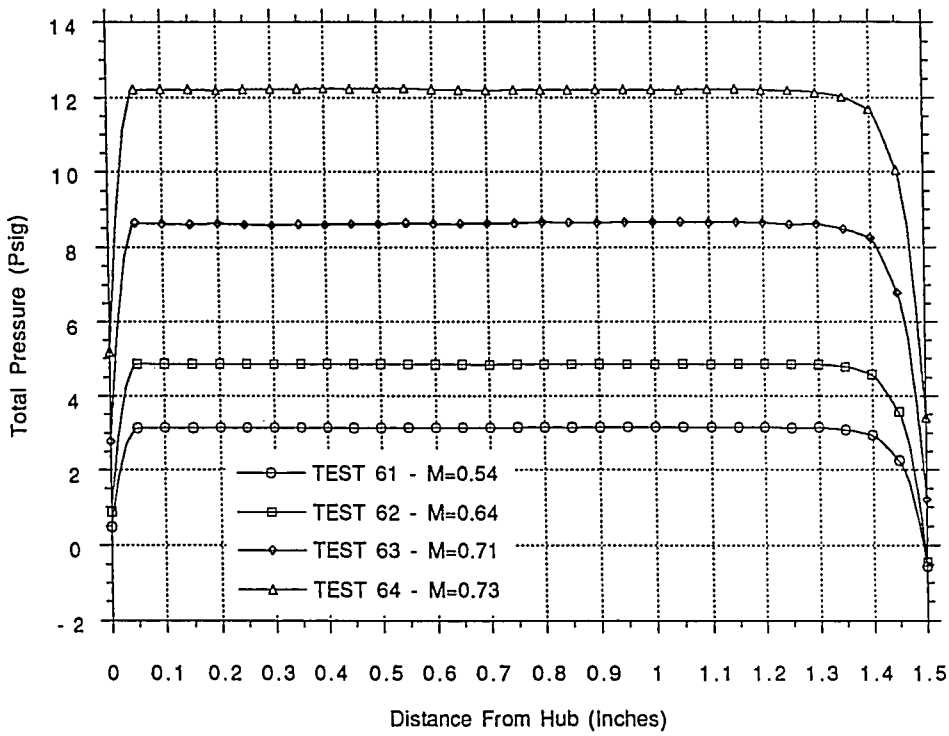

TRAVERSE NO 7
GENERIC MODEL CONFIGURATION 1B
W/O SCREEN W/ GUIDE VANE

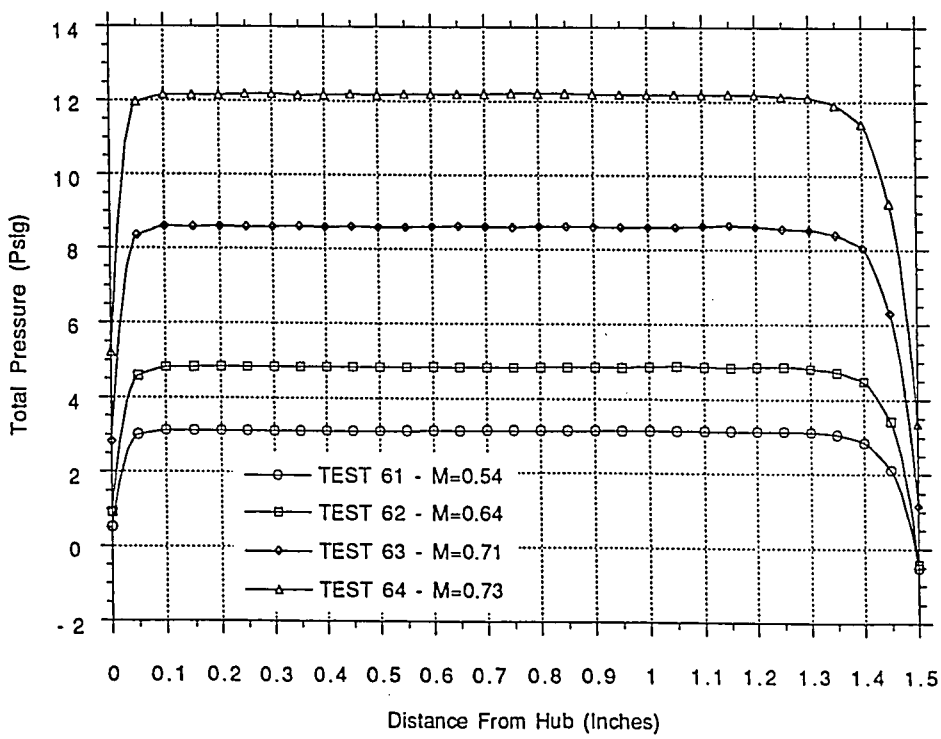

TRAVERSE NO 1
GENERIC MODEL CONFIGURATION 1C
W/O SCREEN W/O GUIDE VANE

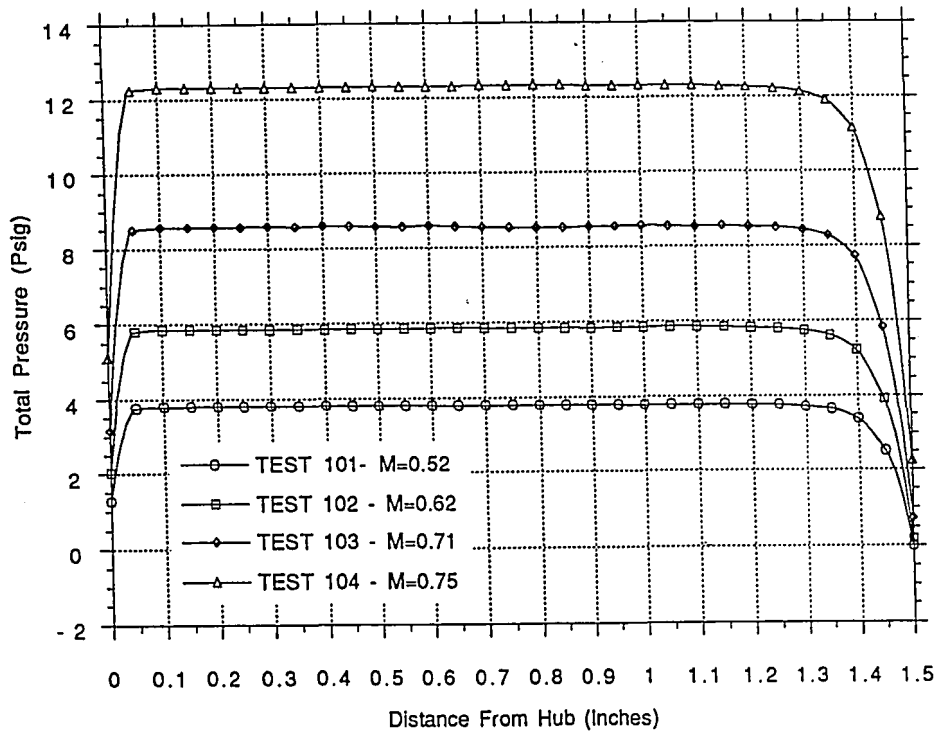

TRAVERSE NO 2
GENERIC MODEL CONFIGURATION 1C
W/O SCREEN W/O GUIDE VANE

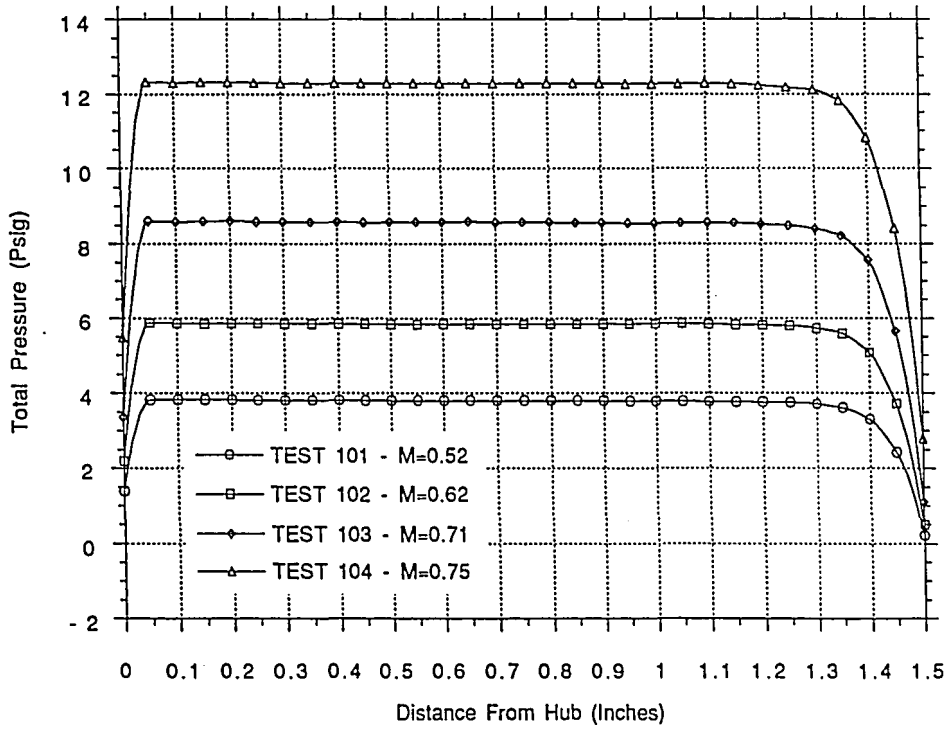

TRAVERSE NO 3
GENERIC MODEL CONFIGURATION 1C
W/O SCREEN W/O GUIDE VANE

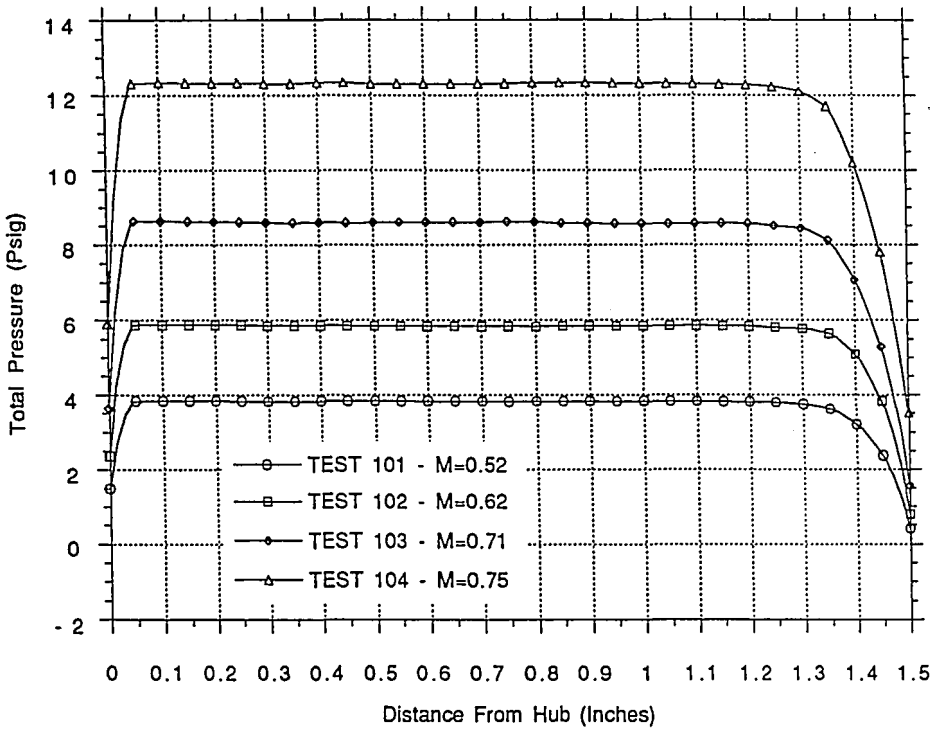

TRAVERSE NO 4
GENERIC MODEL CONFIGURATION 1C
W/O SCREEN W/O GUIDE VANE

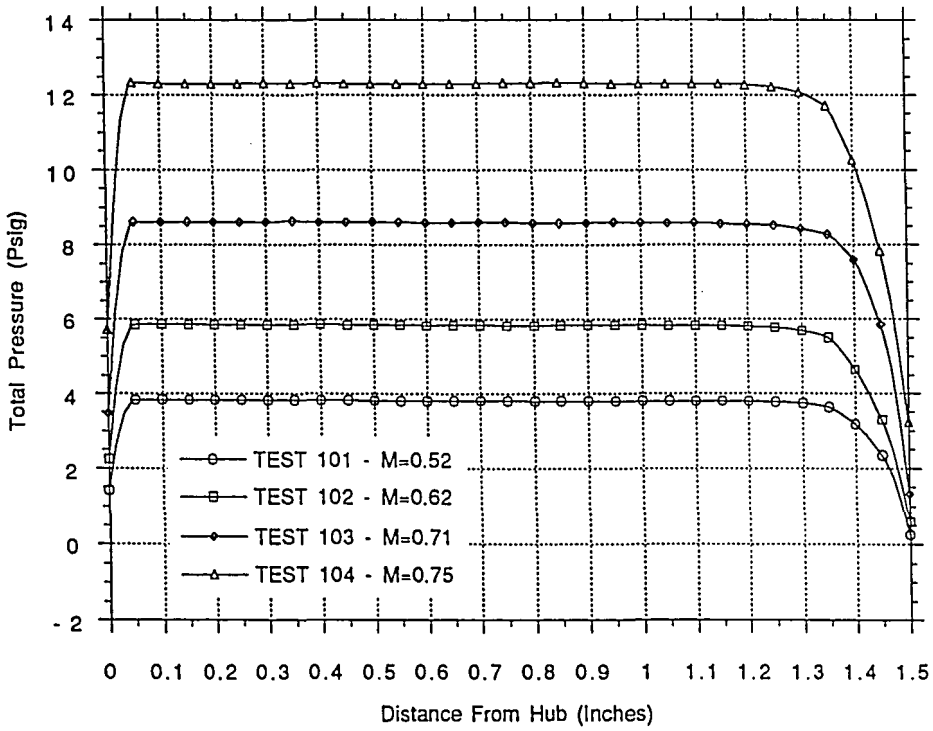

TRAVERSE NO 5
GENERIC MODEL CONFIGURATION 1C
W/O SCREEN W/O GUIDE VANE

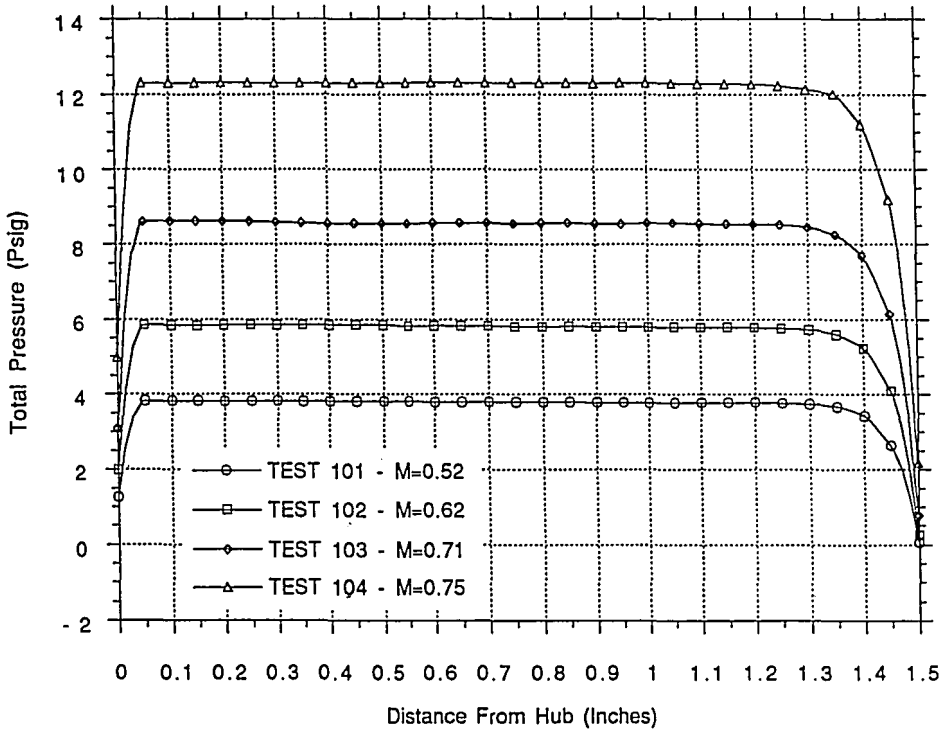

TRAVERSE NO 6
GENERIC MODEL CONFIGURATION 1C
W/O SCREEN W/O GUIDE VANE

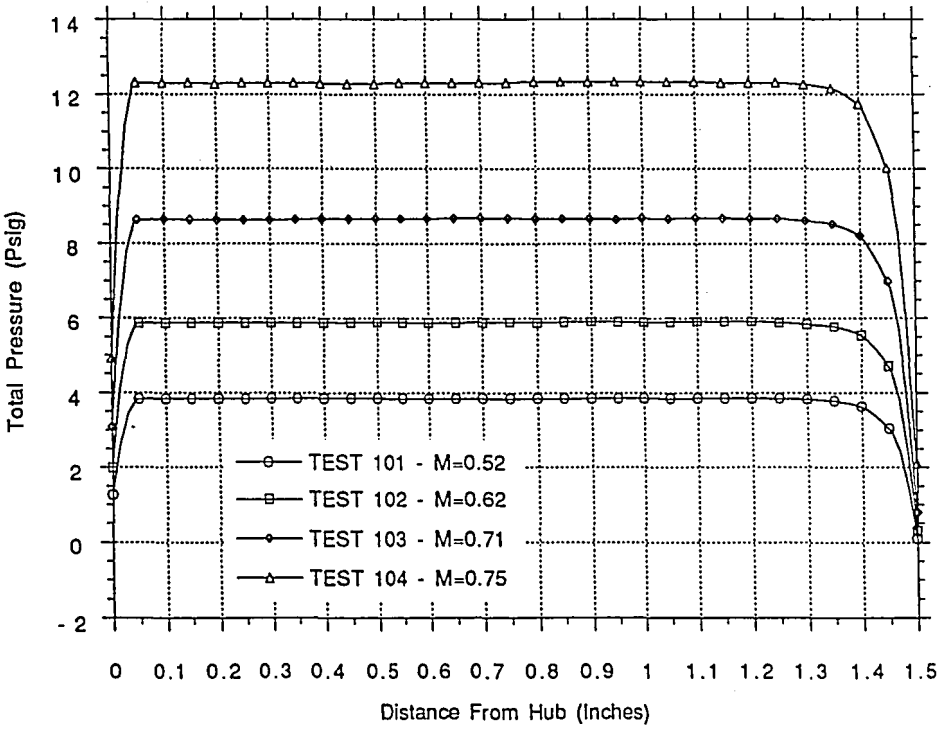

TRAVERSE NO 7
GENERIC MODEL CONFIGURATION 1C
W/O SCREEN W/O GUIDE VANE

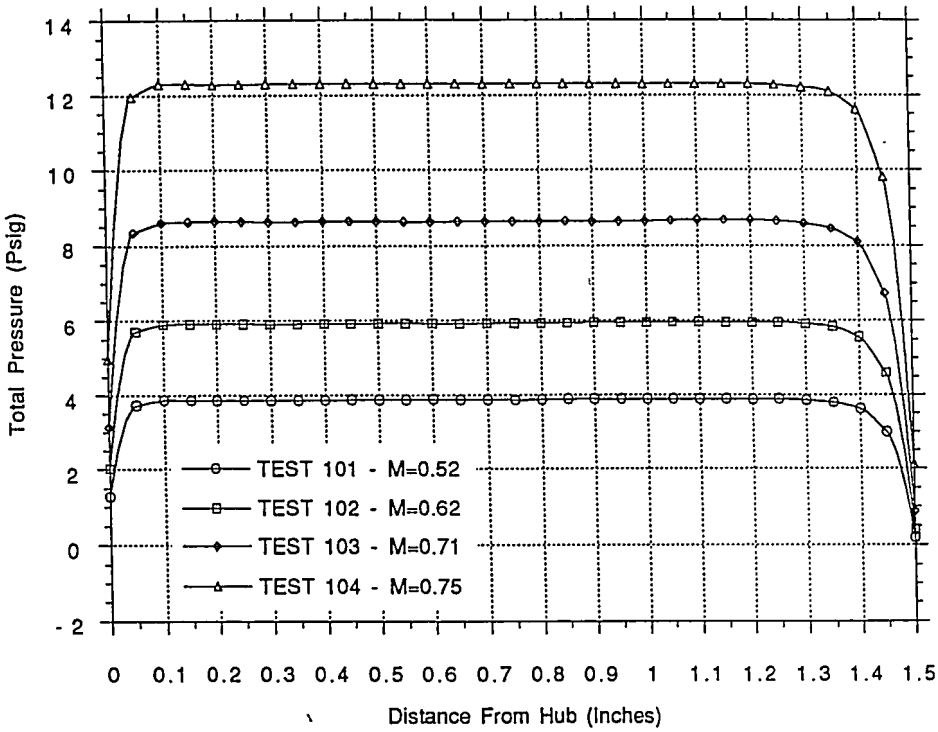

TRAVERSE NO 1
GENERIC MODEL CONFIGURATION 1D
W/ SCREEN W/O GUIDE VANE

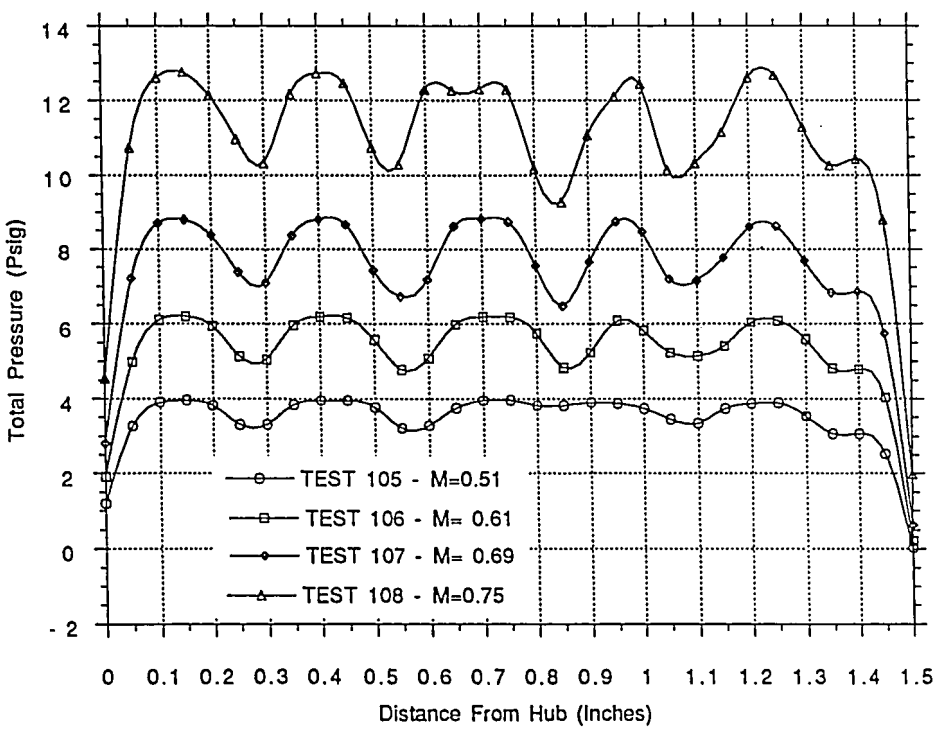

TRAVERSE NO 2
GENERIC MODEL CONFIGURATION 1D
W/ SCREEN W/O GUIDE VANE

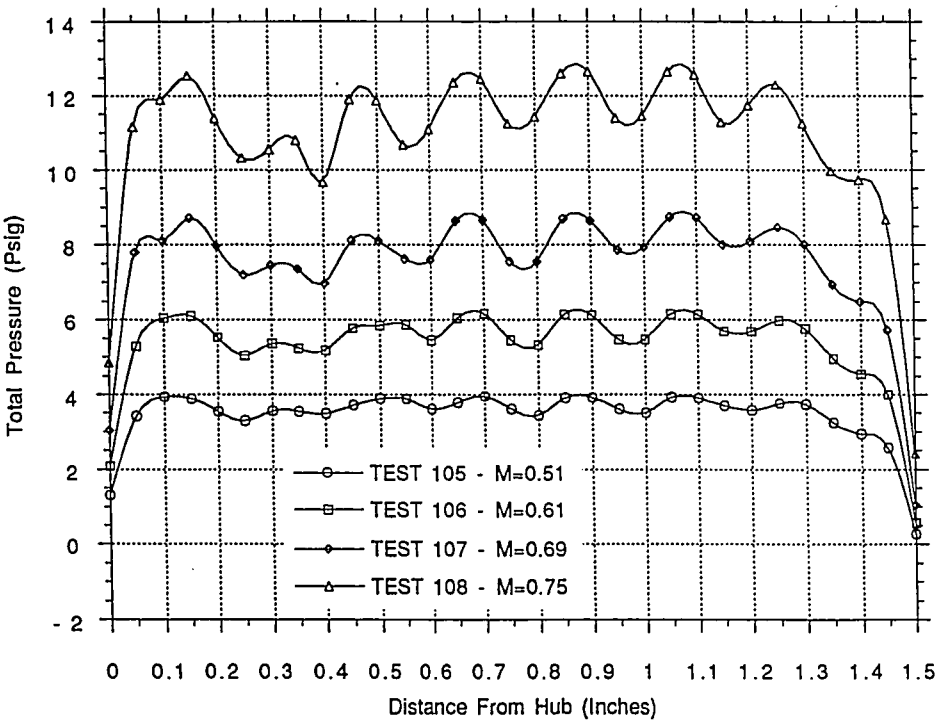

TRAVERSE NO 3
GENERIC MODEL CONFIGURATION 1D
W/ SCREEN W/O GUIDE VANE

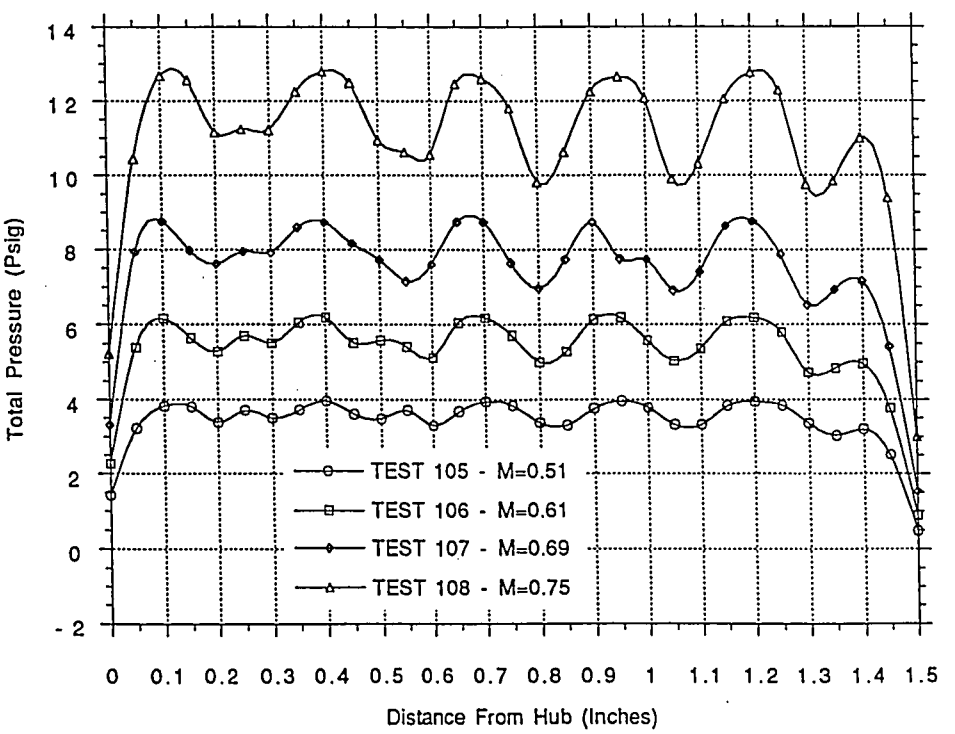

TRAVERSE NO 4
GENERIC MODEL CONFIGURATION 1D
W/ SCREEN W/O GUIDE VANE

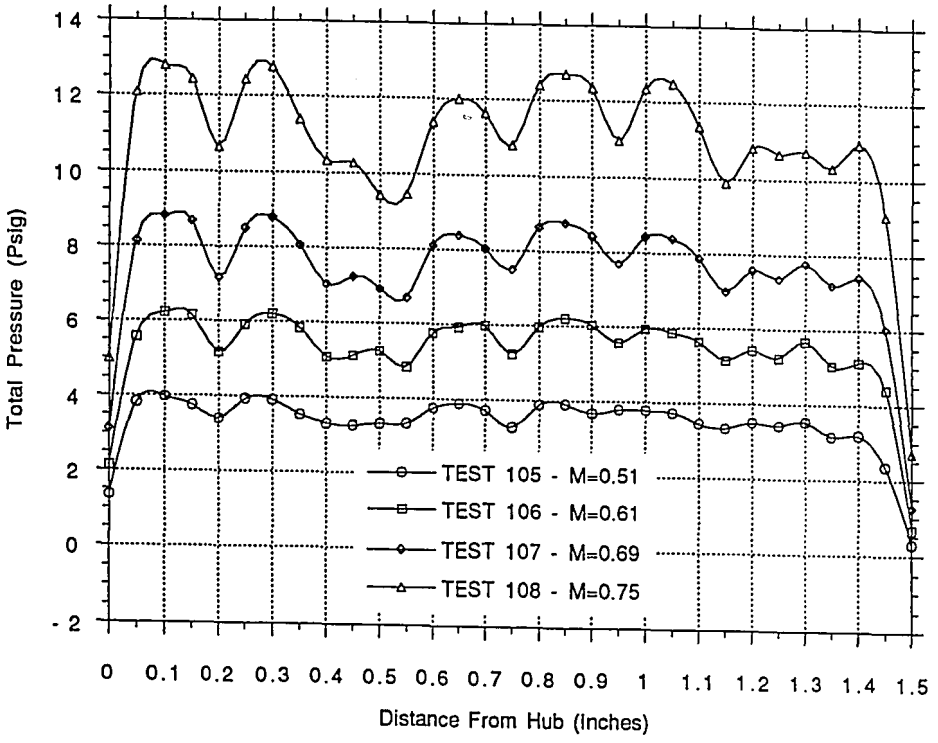

TRAVERSE NO 5
GENERIC MODEL CONFIGURATION 1D
W/ SCREEN W/O GUIDE VANE

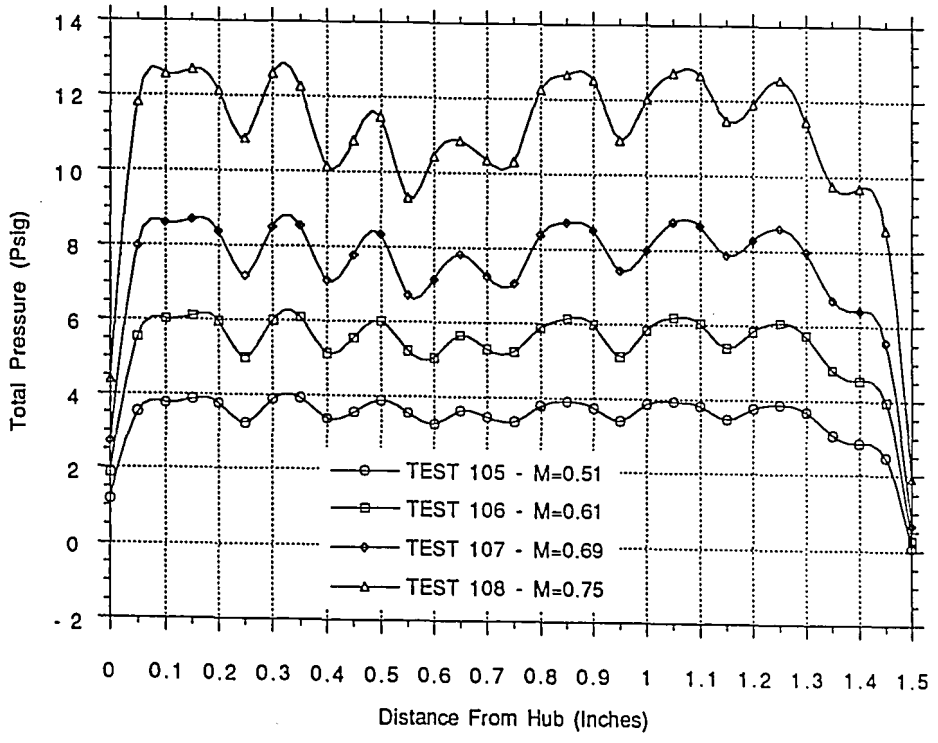

TRAVERSE NO 6
GENERIC MODEL CONFIGURATION 1D
W/ SCREEN W/O GUIDE VANE

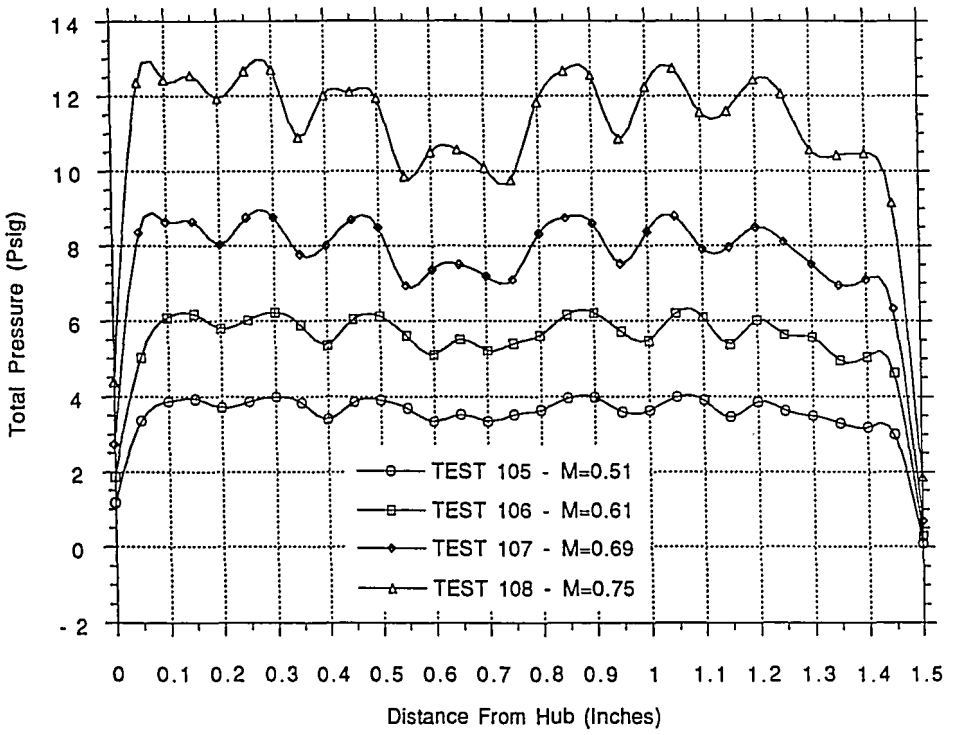

TRAVERSE NO 7
GENERIC MODEL CONFIGURATION 1D
W/ SCREEN W/O GUIDE VANE

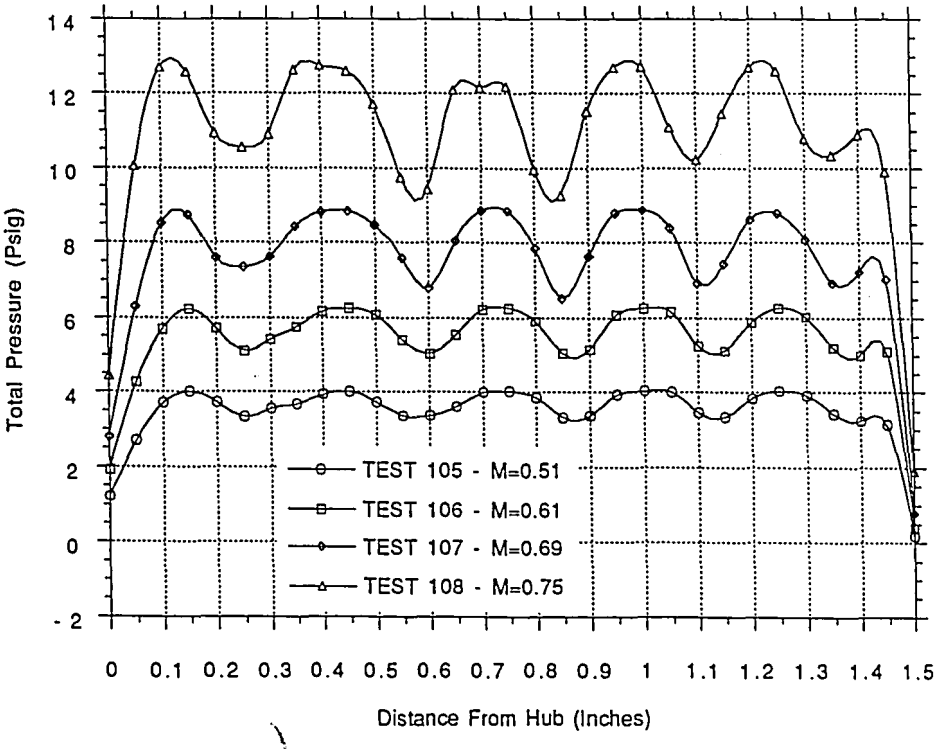

TRAVERSE NO 1
GENERIC MODEL CONFIGURATION 9
W/ SCREEN W/ GUIDE VANE

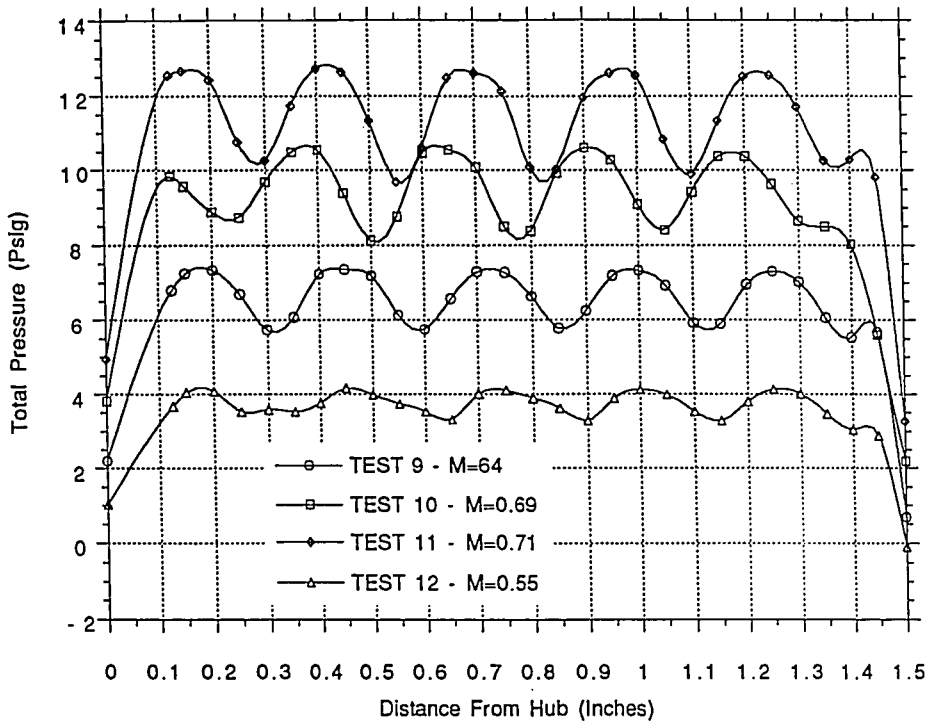

TRAVERSE NO 2
GENERIC MODEL CONFIGURATION 9
W/ SCREEN W/ GUIDE VANE

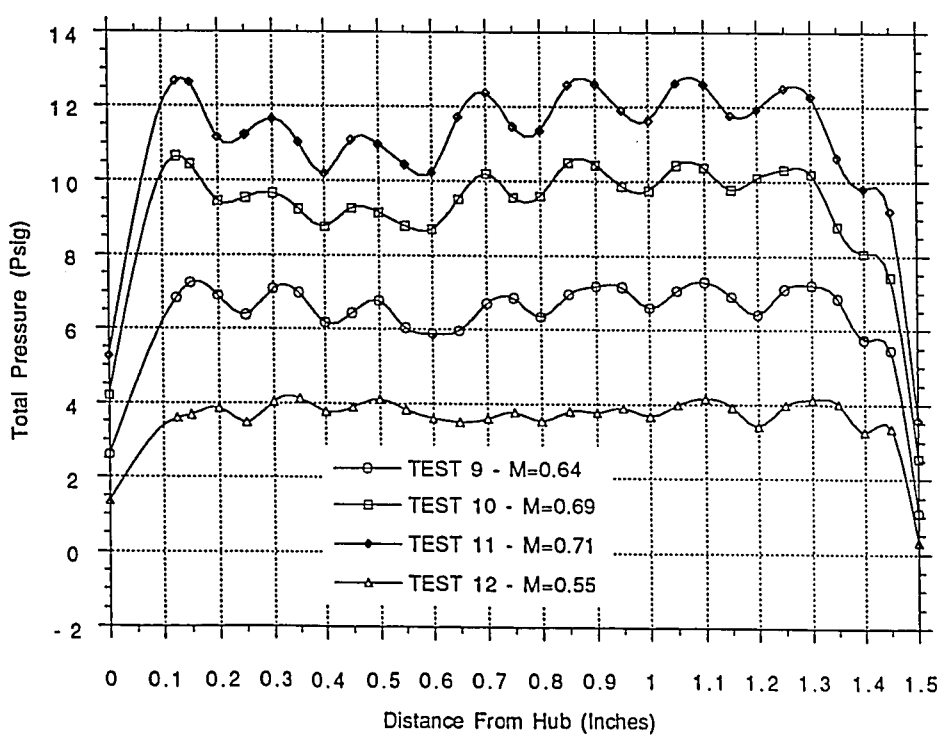

TRAVERSE NO 3
GENERIC MODEL CONFIGURATION 9
W/ SCREEN W/ GUIDE VANE

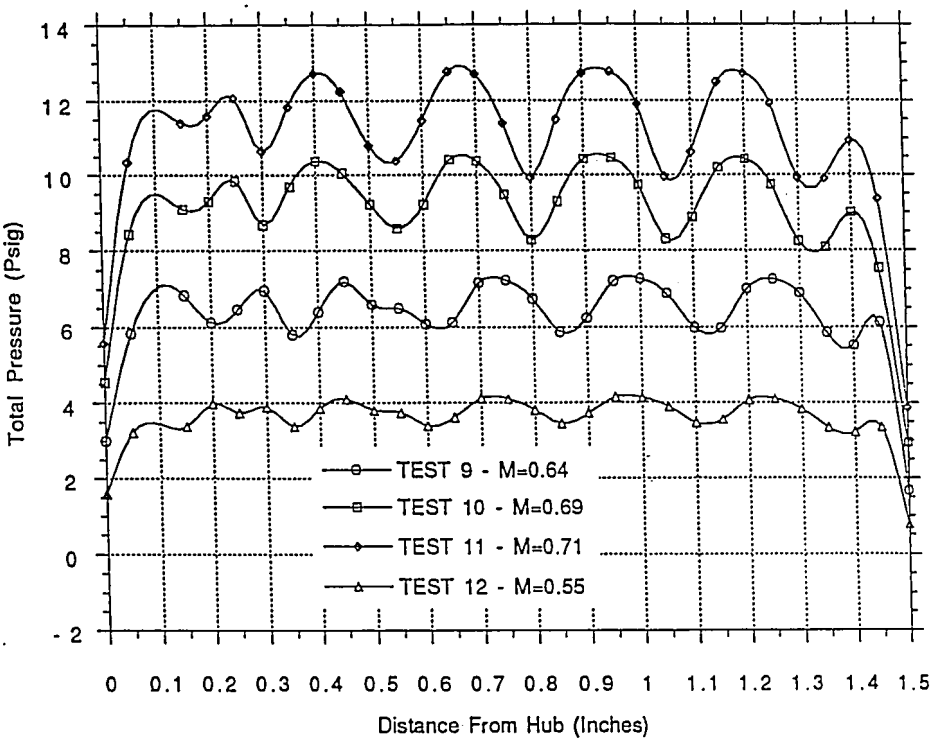

TRAVERSE NO 4
GENERIC MODEL CONFIGURATION 9
W/ SCREEN W/ GUIDE VANE

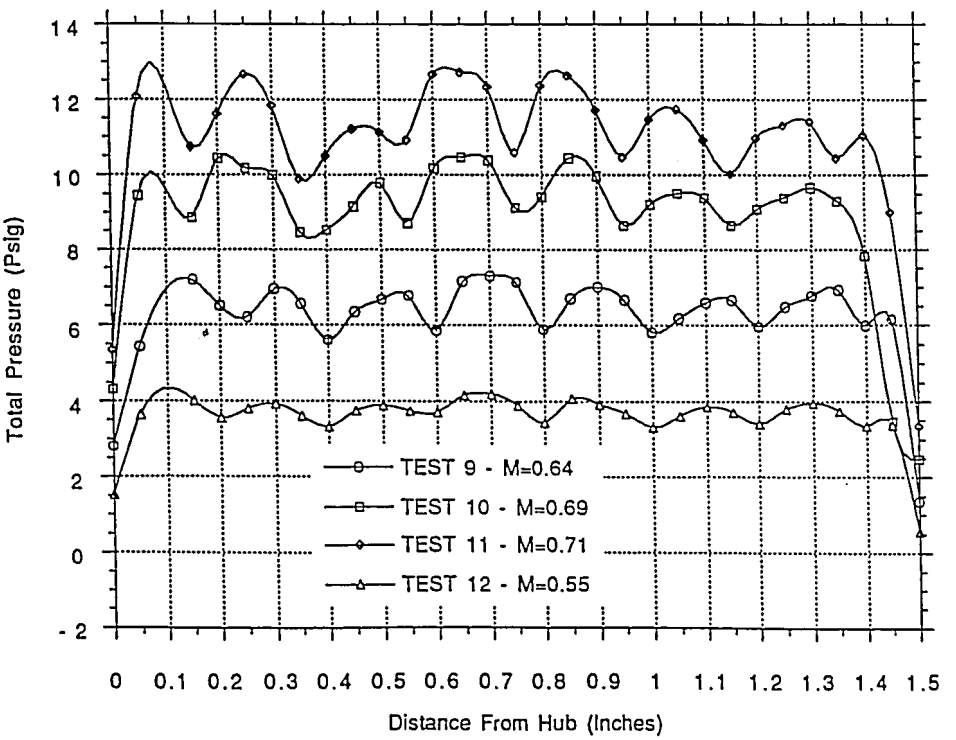

TRAVERSE NO 5
GENERIC MODEL CONFIGURATION 9
W/ SCREEN W/ GUIDE VANE

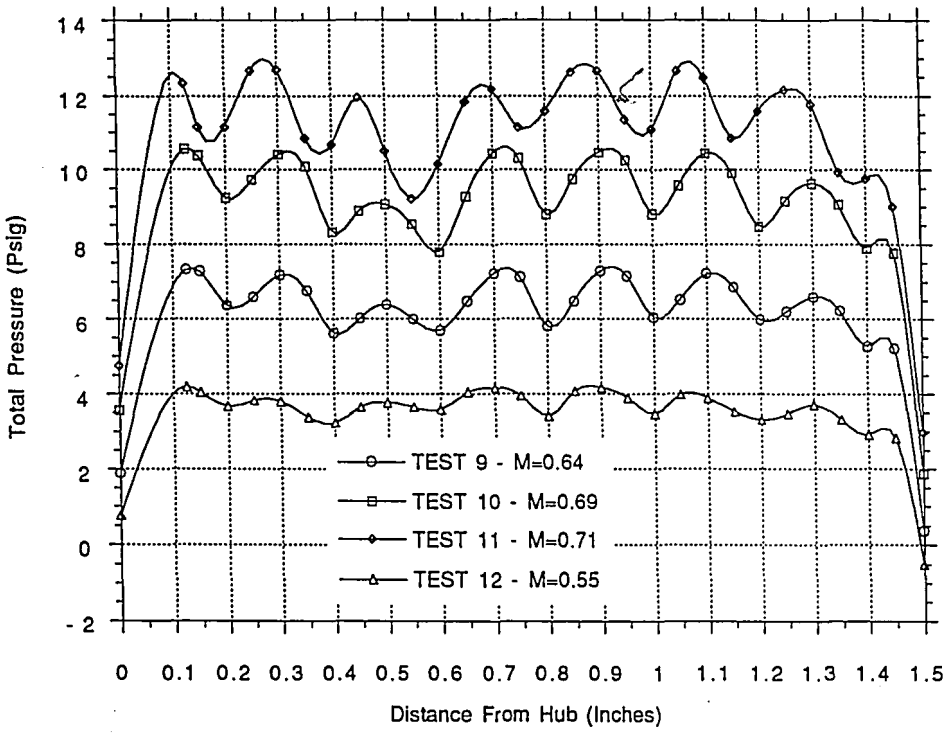

TRAVERSE NO 6
GENERIC MODEL CONFIGURATION 9
W/ SCREEN W/ GUIDE VANE

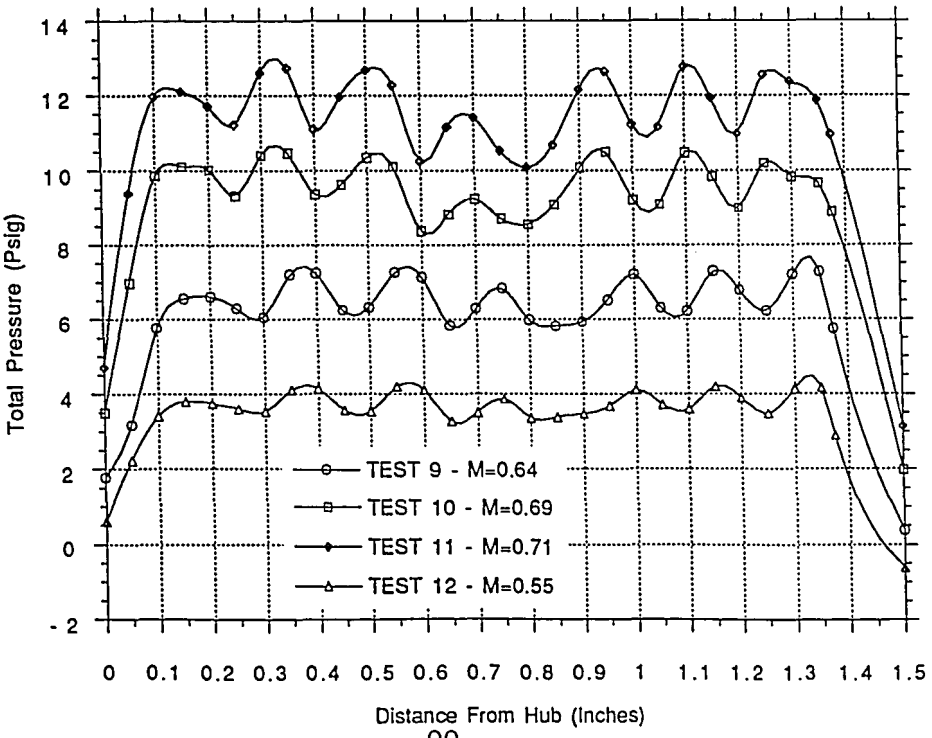

TRAVERSE NO 7
GENERIC MODEL CONFIGURATION 9
W/ SCREEN W/ GUIDE VANE

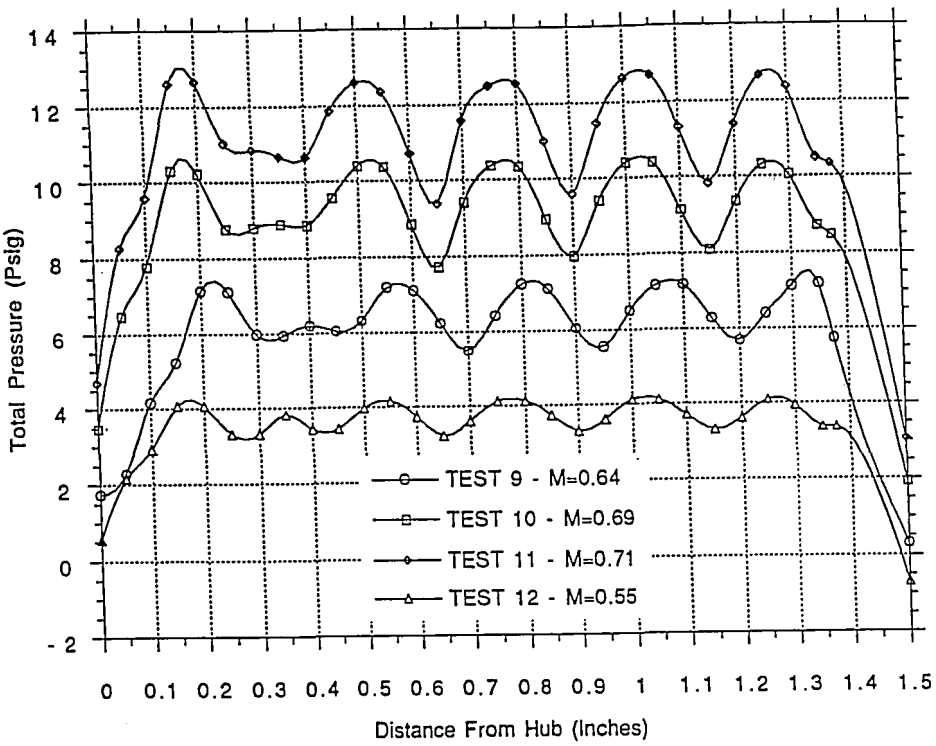

TRAVERSE 1
GENERIC MODEL CONFIGURATION 9B
W/O SCREEN W/ GUIDE VANE

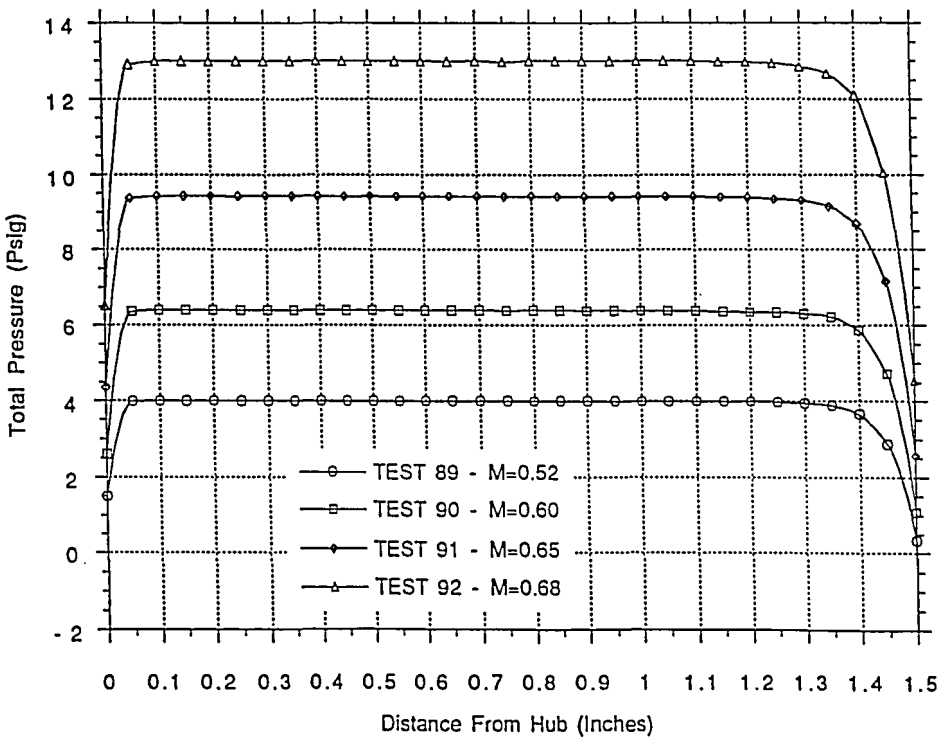

TRAVERSE NO 2
GENERIC MODEL CONFIGURATION 9B
W/O SCREEN W/ GUIDE VANE

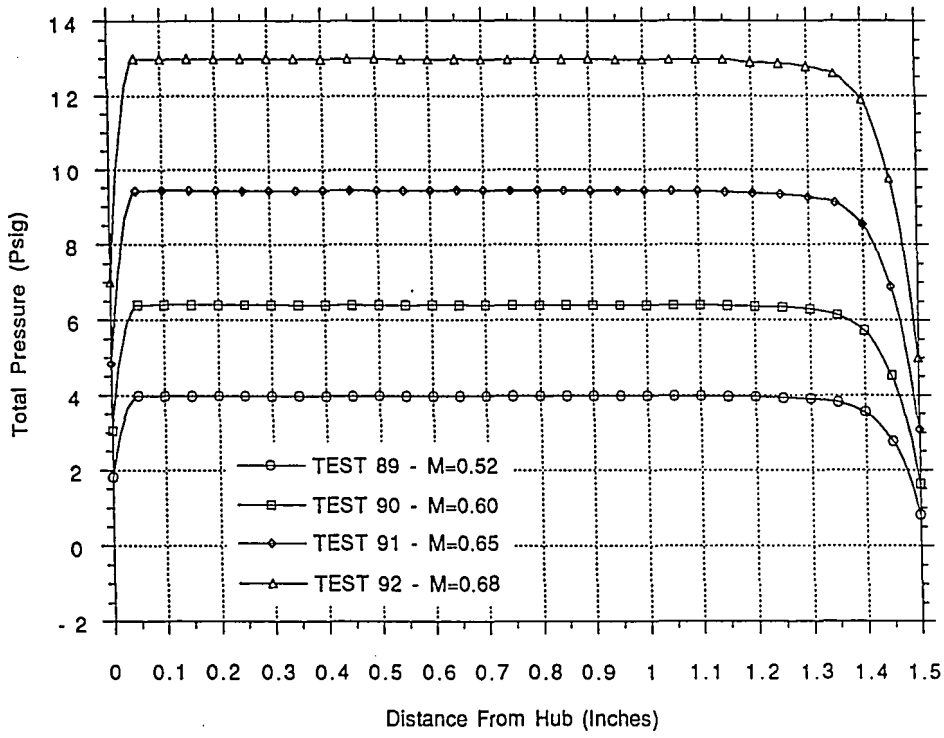

TRAVERSE NO 3
GENERIC MODEL CONFIGURATION 9B
W/O SCREEN W/ GUIDE VANE

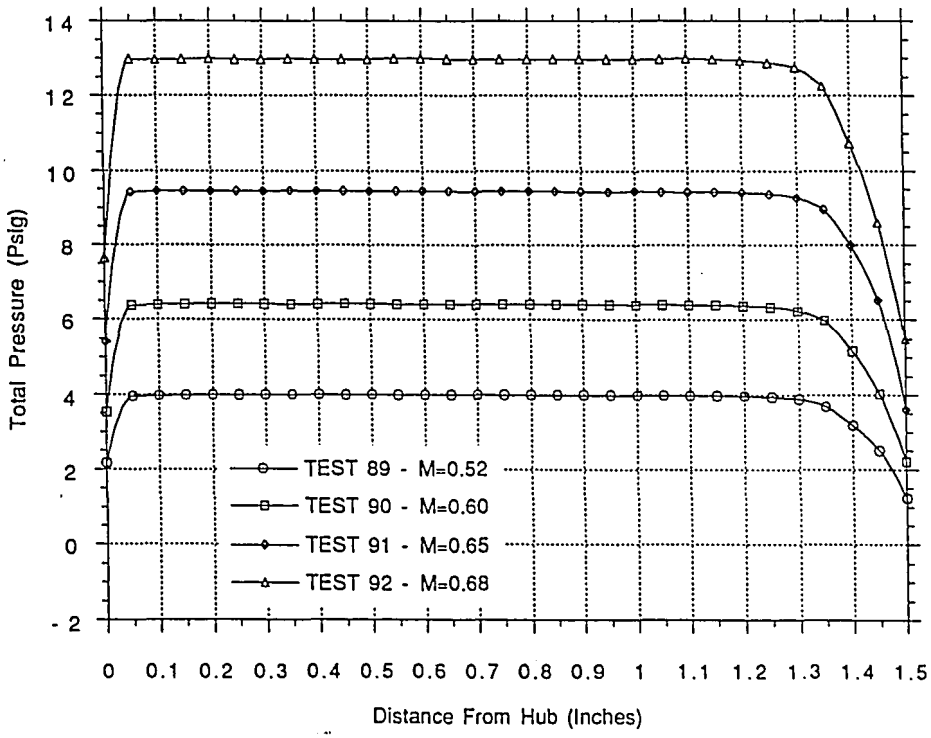

TRAVERSE NO 4
GENERIC MODEL CONFIGURATION 9B
W/O SCREEN W/ GUIDE VANE

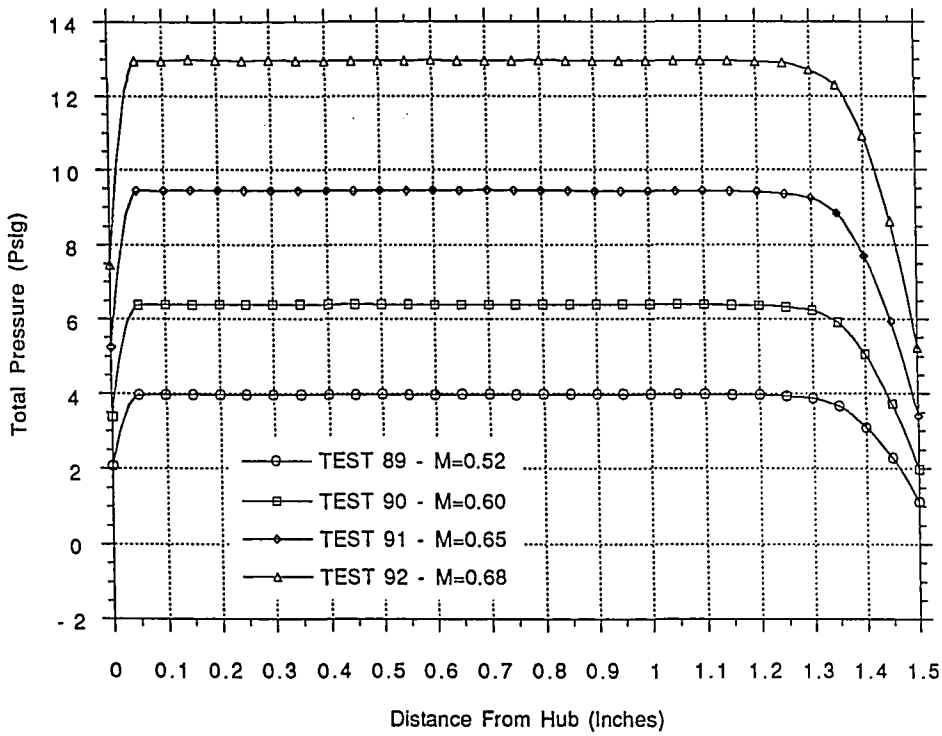

TRAVERSE NO 5
GENERIC MODEL CONFIGURATION 9B
W/O SCREEN W/ GUIDE VANE

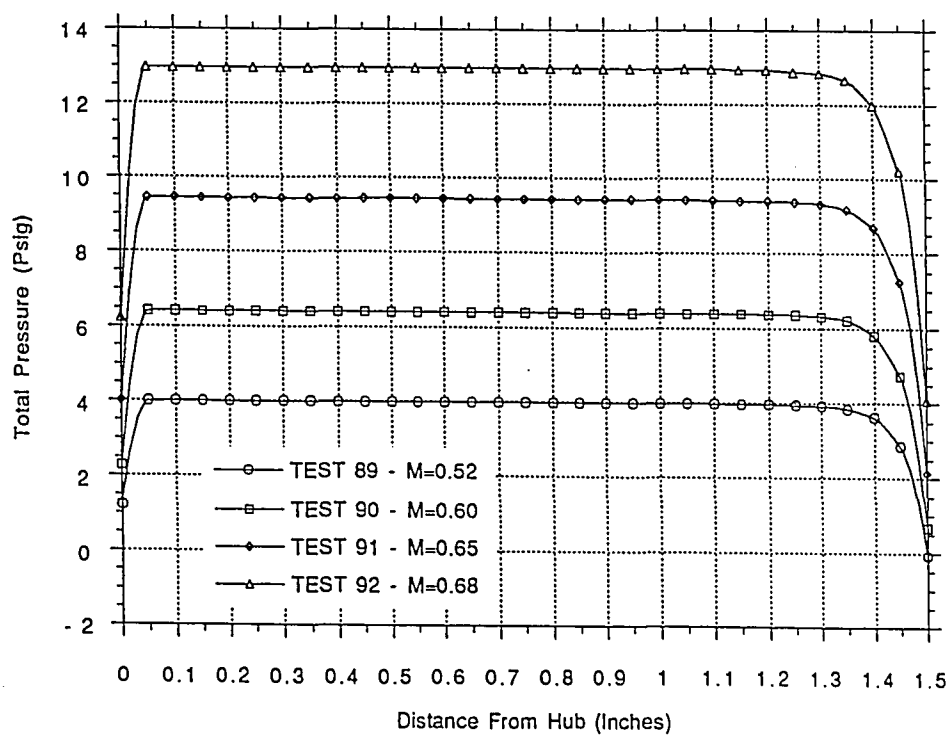

TRAVERSE NO 6
GENERIC MODEL CONFIGURATION 9B
W/O SCREEN W/ GUIDE VANE

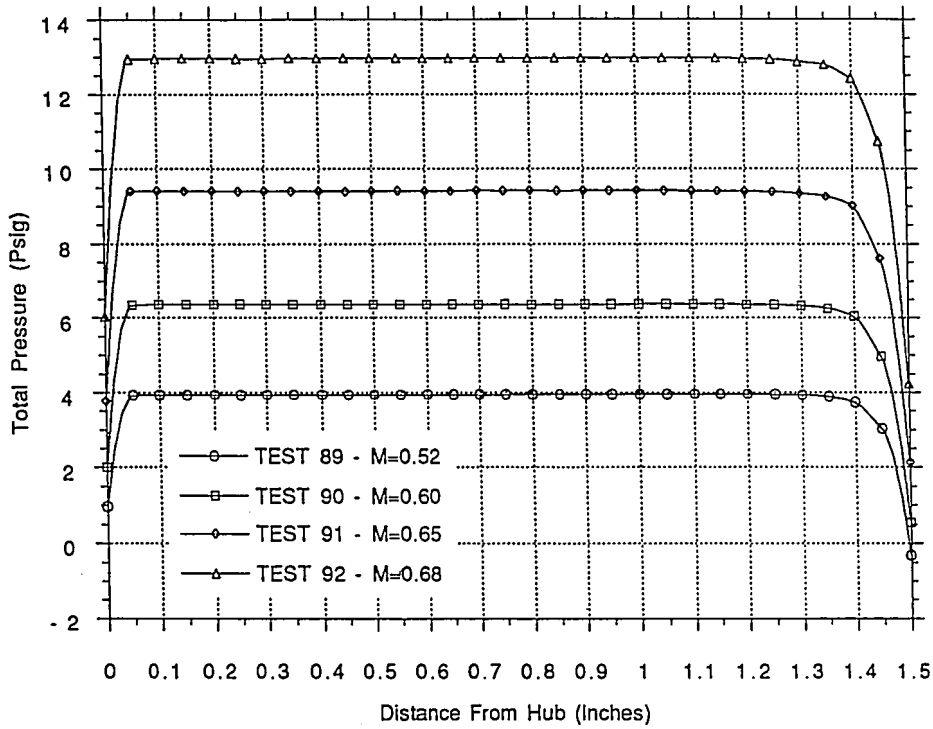

TRAVERSE NO 7
GENERIC MODEL CONFIGURATION 9B
W/O SCREEN W/ GUIDE VANE

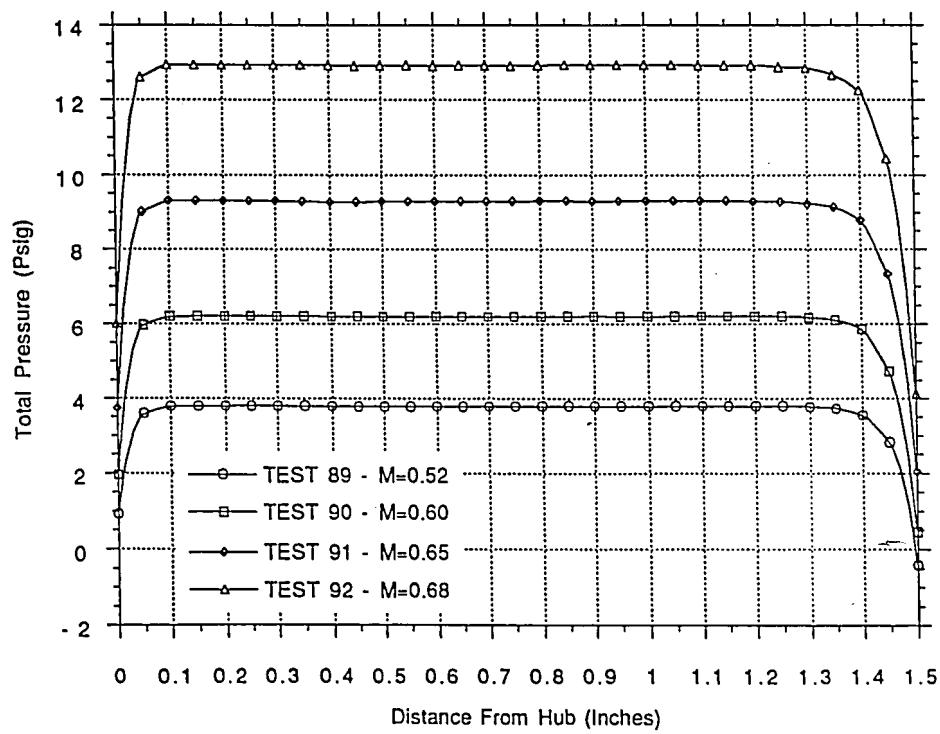

TRAVERSE NO 1
GENERIC MODEL CONFIGURATION 9C
W/O SCREEN W/O GUIDE VANE

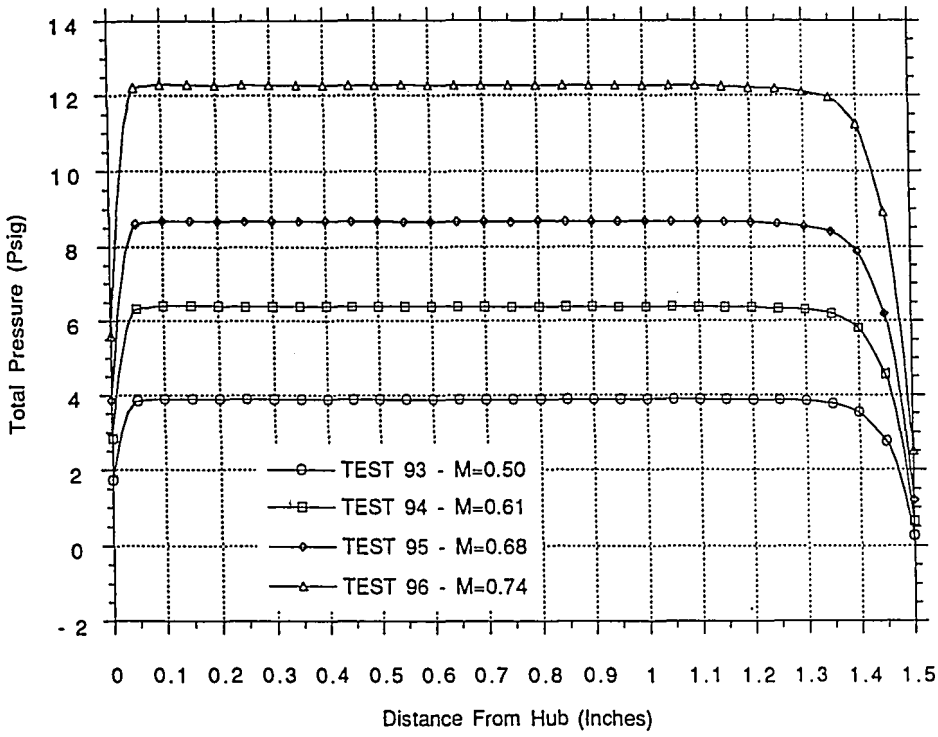

TRAVERSE NO 2
GENERIC MODEL CONFIGURATION 9C
W/O SCREEN W/O GUIDE VANE

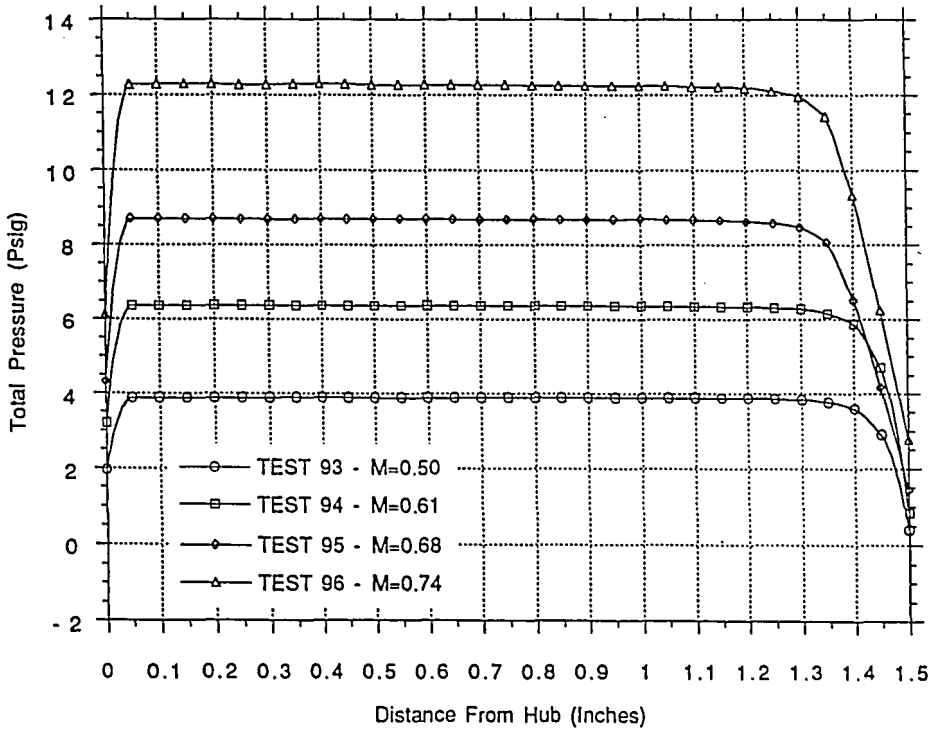

TRAVERSE NO 3
GENERIC MODEL CONFIGURATION 9C
W/O SCREEN W/O GUIDE VANE

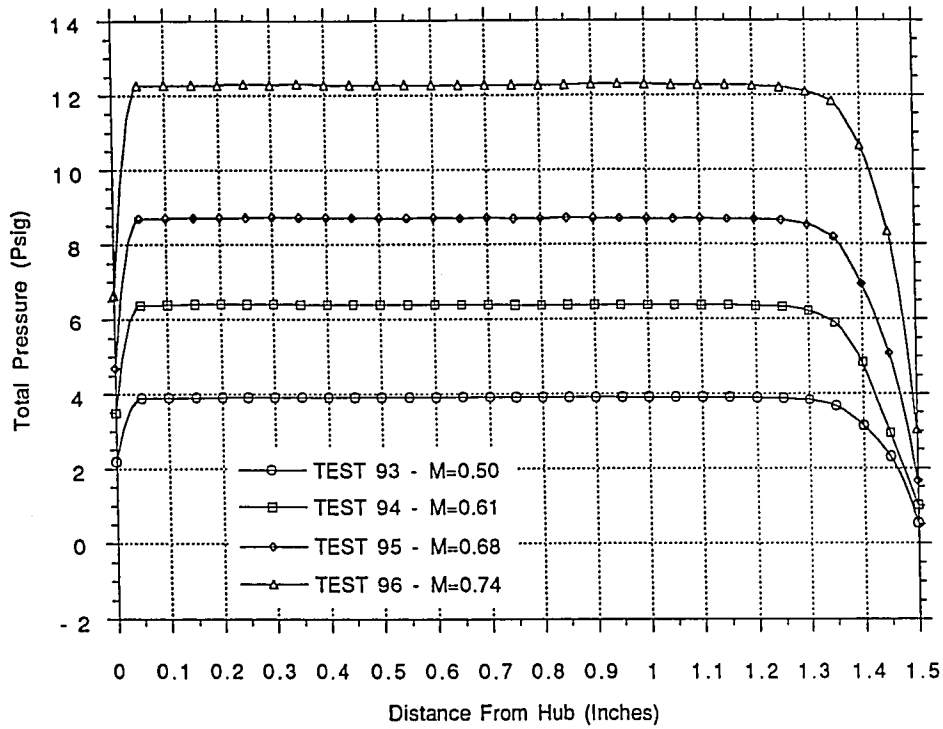

TRAVERSE NO 4
GENERIC MODEL CONFIGURATION 9C
W/O SCREEN W/O GUIDE VANE

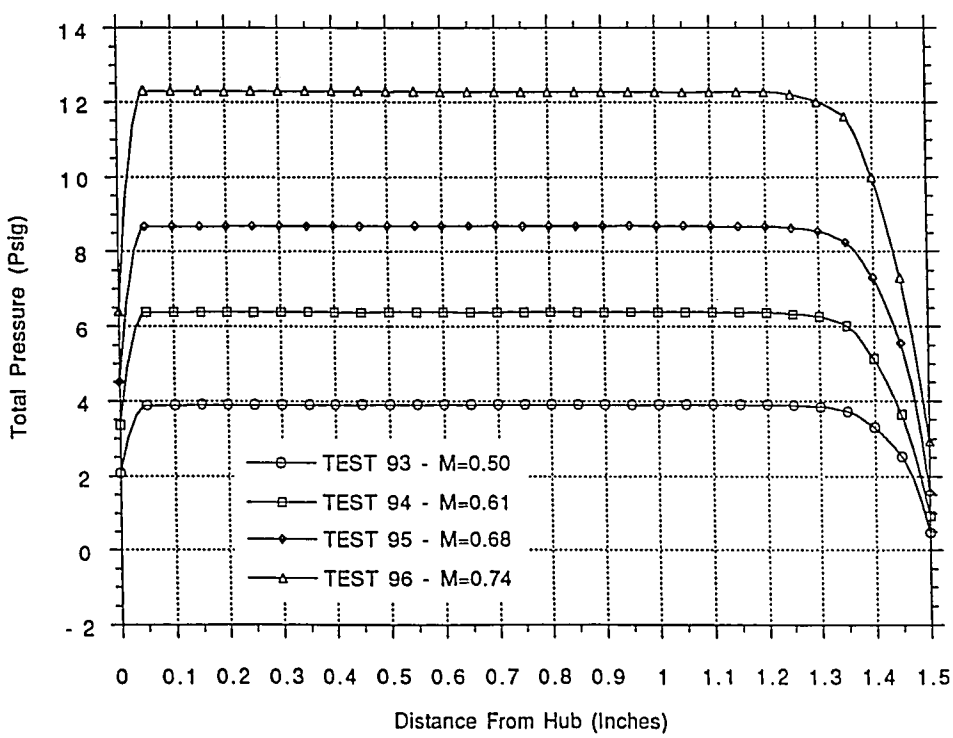

TRAVERSE NO 5
GENERIC MODEL CONFIGURATION 9C
W/O SCREEN W/O GUIDE VANE

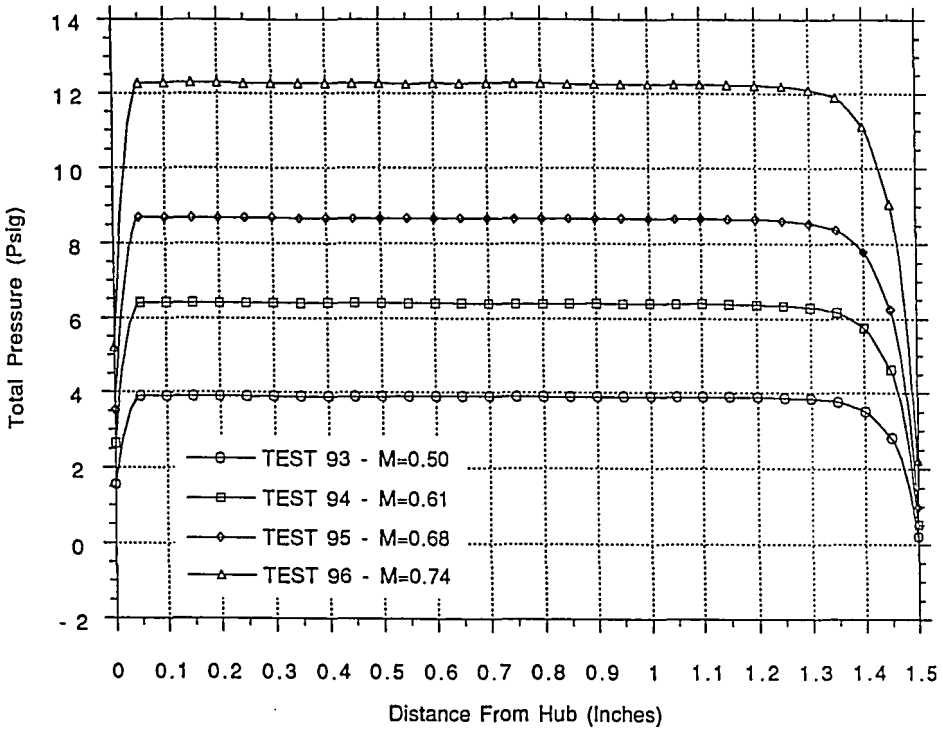

TRAVERSE NO 6
GENERIC MODEL CONFIGURATION 9C
W/O SCREEN W/O GUIDE VANE

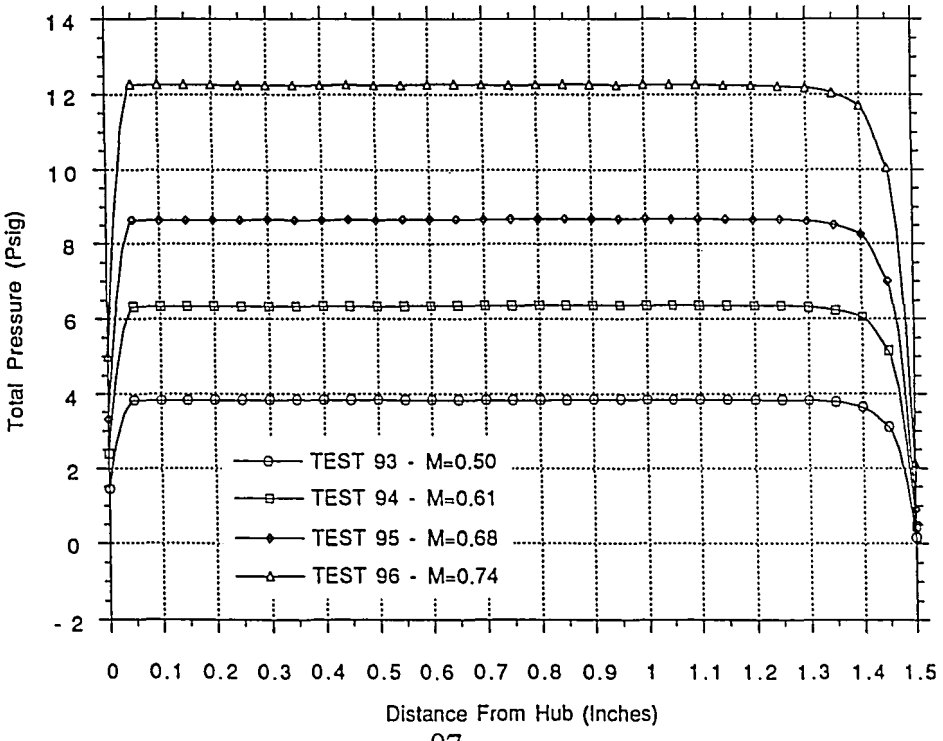

TRAVERSE NO 7
GENERIC MODEL CONFIGURATION 9C
W/O SCREEN W/O GUIDE VANE

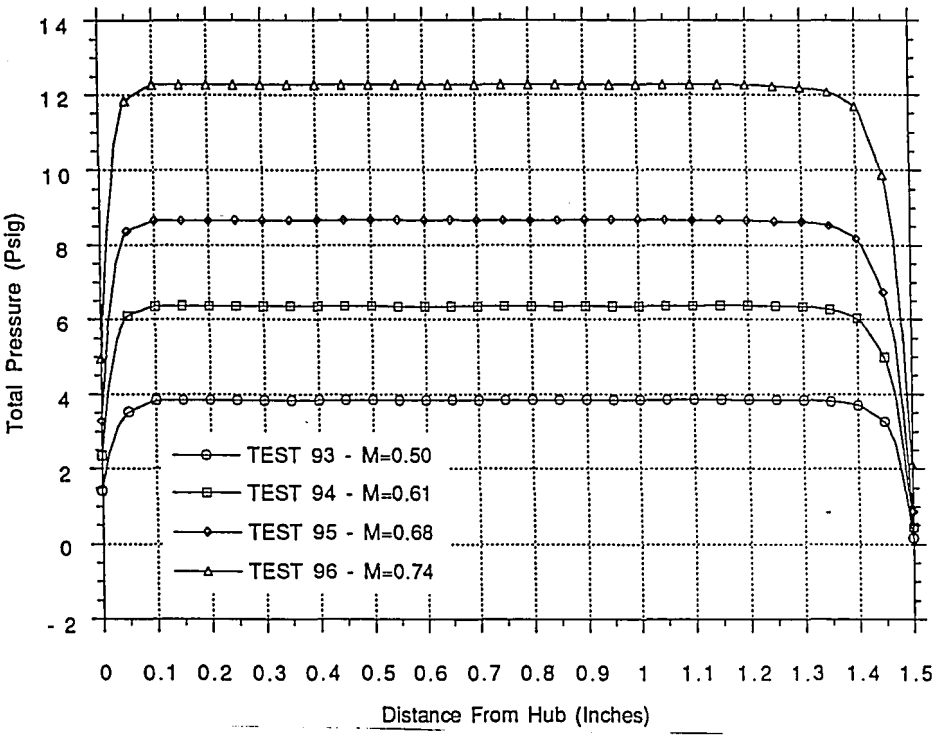

TRAVERSE NO 1
GENERIC MODEL CONFIGURATION 9D
W/ SCREEN W/O GUIDE VANE

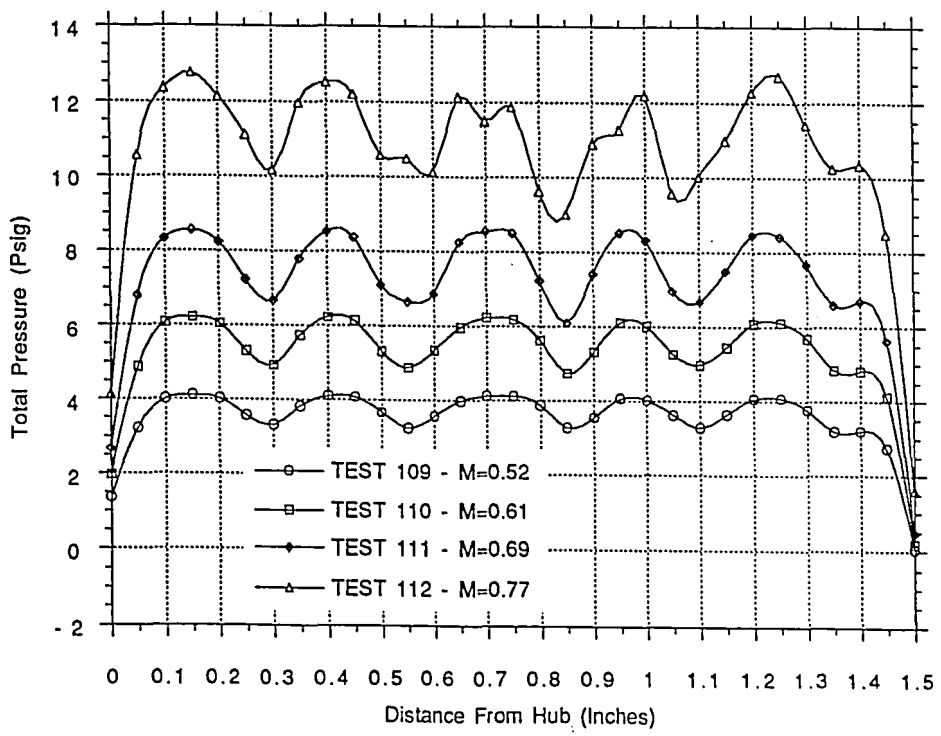

TRAVERSE NO 2
GENERIC MODEL CONFIGURATION 9D
W/ SCREEN W/O GUIDE VANE

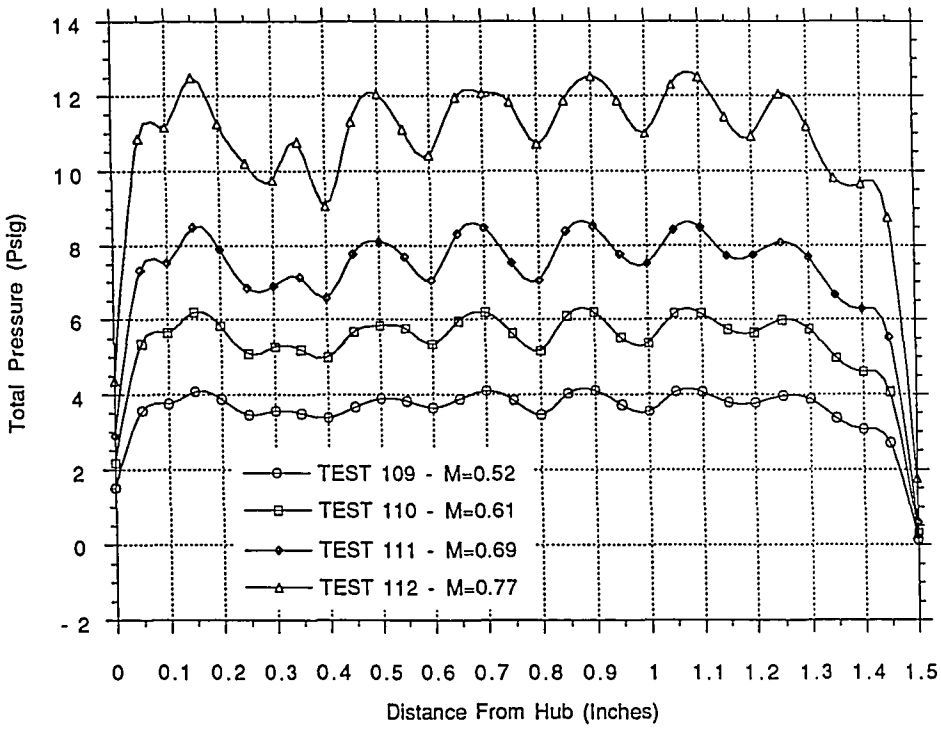

TRAVERSE NO 3
GENERIC MODEL CONFIGURATION 9D
W/ SCREEN W/O GUIDE VANE

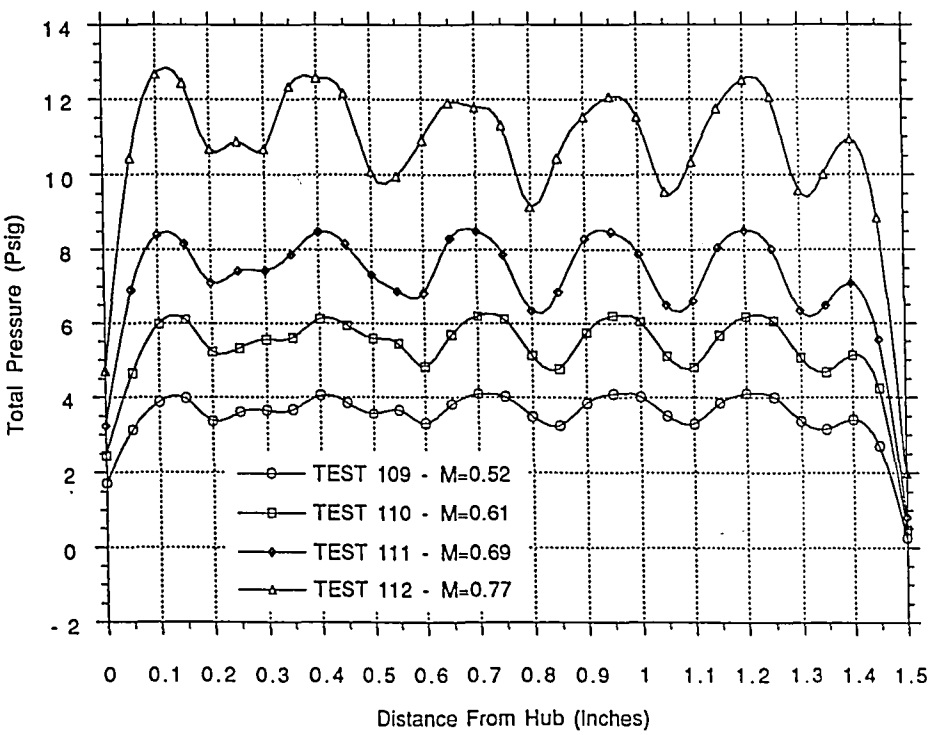

TRAVERSE NO 4
GENERIC MODEL CONFIGURATION 9D
W/ SCREEN W/O GUIDE VANE

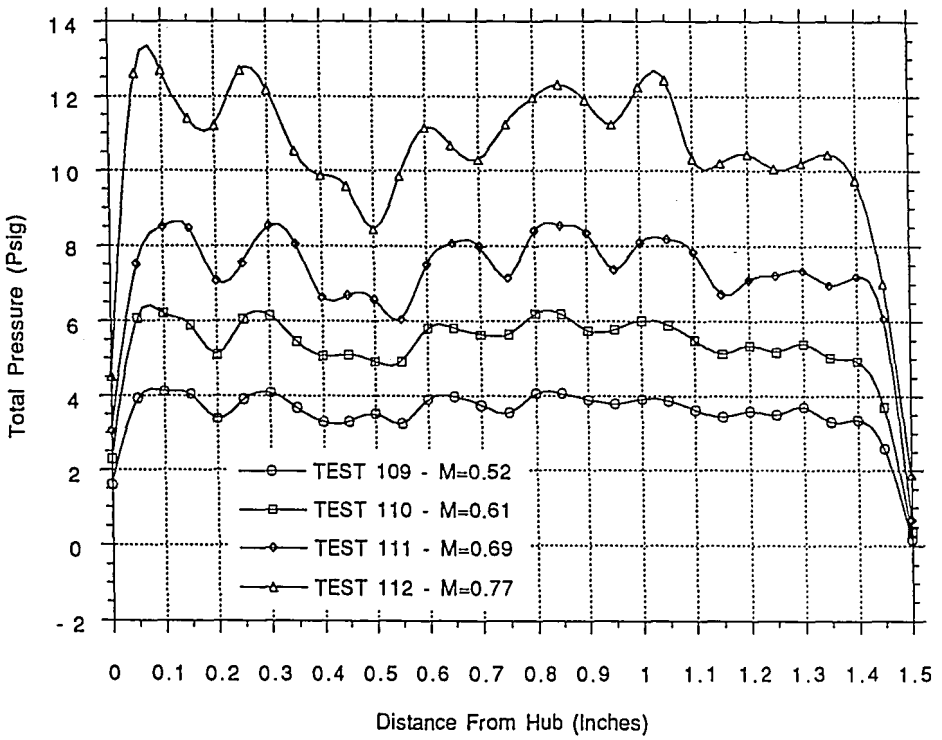

TRAVERSE NO 5
GENERIC MODEL CONFIGURATION 9D
W/ SCREEN W/O GUIDE VANE

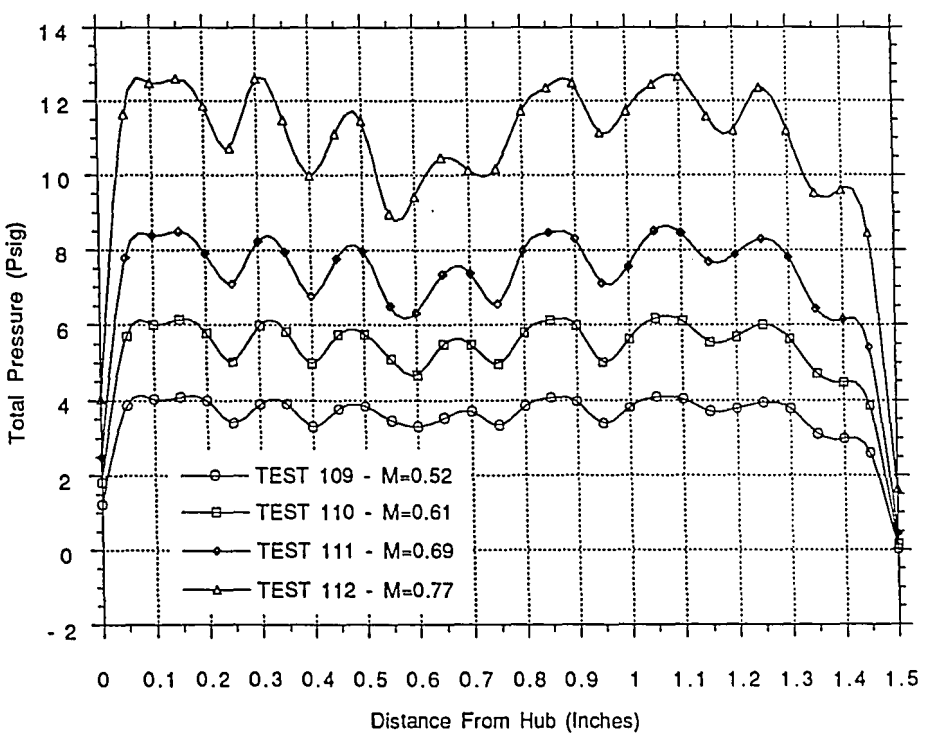

TRAVERSE NO 6
GENERIC MODEL CONFIGURATION 9D
W/ SCREEN W/O GUIDE VANE

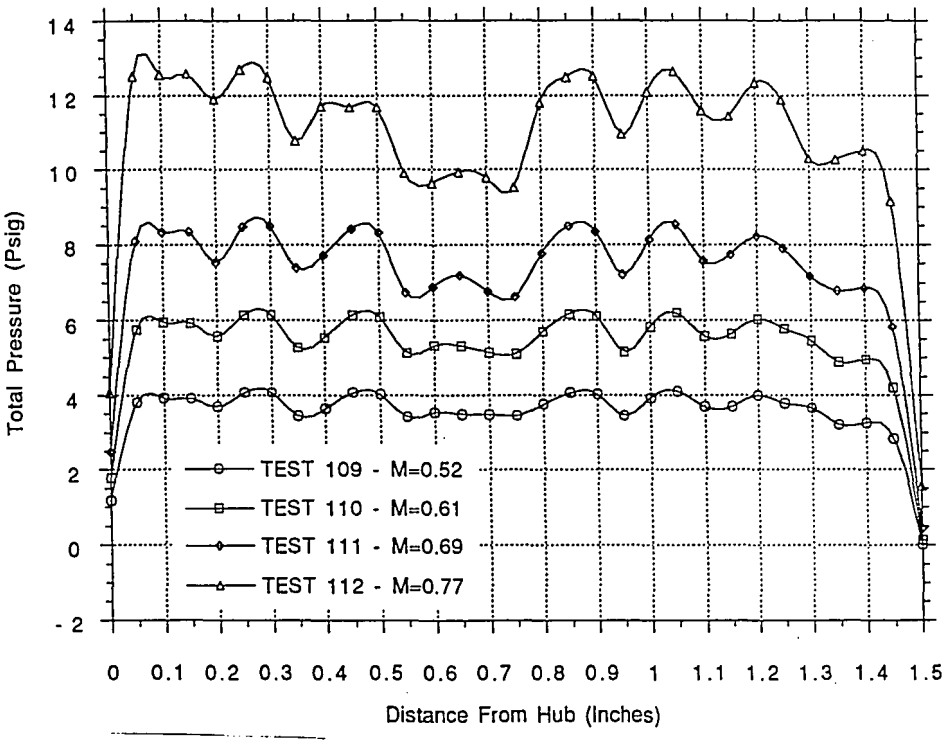

TRAVERSE NO 7
GENERIC MODEL CONFIGURATION 9D
W/ SCREEN W/O GUIDE VANE

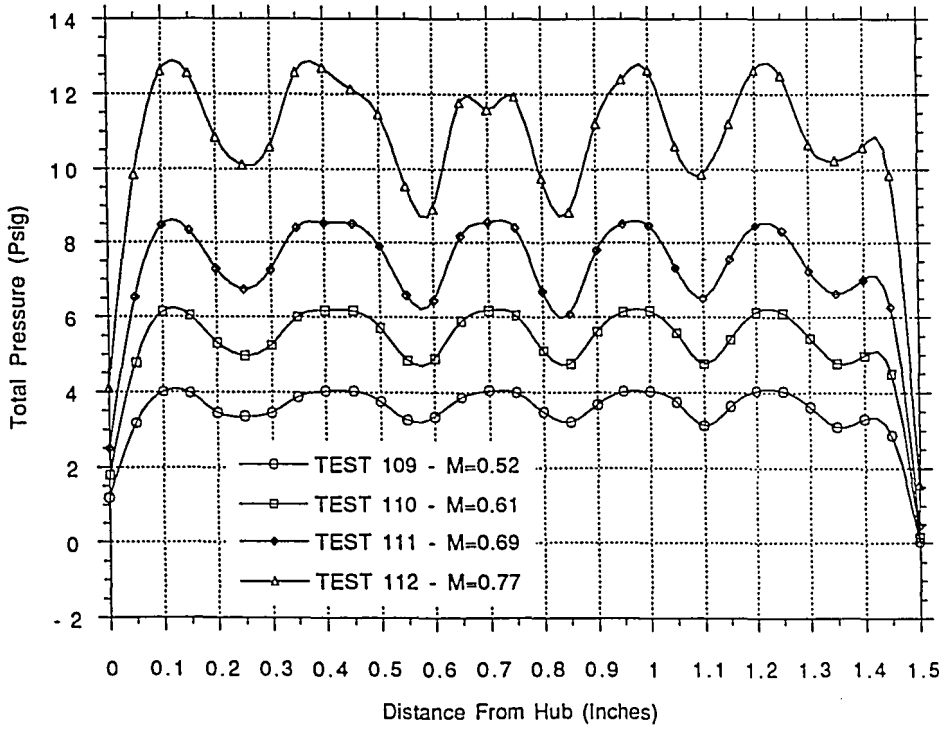

APPENDIX C - SAMPLE CALCULATIONS

- Raw Data Sheets for Test 89 of Configuration 9B
- Fortran Program Used for Averaging the Static and Total Pressure in the Annulus
- Input Sheets for Test 89 of Configuration 9B
- Output Sheet for Test 89 of Configuration 9B
- Sample Mass Flow Rate Calculations for the Venturi Meter
- Charts

Raw Data Sheets for Test 89 of Configuration 9B

DATA SHEET

TEST NO: 89 (1st TEST OF CONFIG 9B)
CONFIGURATION NO: 9B (W/O SCREEN)
MODEL: GENERIC
COMP.SPEED (RPM):
FLOW RATE:

TEST DATE: 7/23/92
TIME(START): 9am
TIME(END):

BAROMETRIC PRES: 29.425" Hg
BAROMETRIC TEMP: 74°F
DRY BULB: 84°F
WET BULB: 71°F
RELATIVE HUMIDI: 52%

	935am	950am	1008am	Average
	29.42 in Hg	29.42 in Hg	29.425 in Hg	29.422 in Hg
	75°F	74°F	75°F	74.5°F

TIME:		9:12	9:23am	9:33am	9:50am	10:05am	Average
VENTURI TEMP:	(F)	101.	103.	99.	100.	100.	100.5
VENTURI INLET PRES:	(PSIG)	3.97	3.98	3.98	3.98	3.98	3.978
ΔP ACROSS VENTURI:	"WATER	6.93	6.90	6.90	6.90	6.90	6.90
MODEL INLET TEMP:	(F)	99.1	101.8	98.2	99.3	99.3	99.54
COMP. DISCHARGE TEMP:	(F)	204.9	212.7	216.9	220.1	219.2	

DATA SHEET

TEST NO: 91 (1st TEST OF CONFIG 9B)
CONFIGURATION NO: 9B (W/O SCREEN)
MODEL: GENERIC

TEST DATE: 7/23/92

2.5 PSID SC. VALVE	CORRESP. PRES TAP	TIME 9:13 PSTAT (Volts)	TIME 10:04 PSTAT (Volts)	PSTAT (Volts)
1	CN 1	.532	.534	
2	CN 2	-.534	-.548	
3	CN 3	-.186	-.188	
4	CN 4	.263	.272	
5	CN 5	.329	.335	
6	CN 6	-.152	-.156	
7	CN 7	-.464	-.466	
8	CN 8	.292	.294	
9	CN 9	.212	.216	
10	CN 10	-.304	-.317	
11	CN 11	-.728	-.726	
12	CN 12	-.370	-.374	
13	CN 13	.250	.255	
14	CN 14	-.162	-.160	
15	CN 15	-.182	-.170	

2.5 PSID SC. VALVE	CORRESP. PRES TAP	TIME 9:17 PSTAT (Volts)	TIME 10:11 PSTAT (Volts)	PSTAT (Volts)
16	CN 16	-.047	-.054	
17	CN 17	-.052	-.050	
18	CN 18	.305	.310	
19	CN 19	.388	.395	
20	CN 20	-.063	-.064	
21	CN 21	-.105	-.106	
22	CN 22	-.222	-.214	
23	CN 23	-.228	-.230	
24	CN 24	.474	.467	
25	CN 25	-.404	-.414	
26	CN 26	-.918	-.918	
27	CN 27	-.330	-.334	
28	CN 28	.306	.304	

DATA SHEET

TEST NO: 89 (1st TEST OF CONFIG 9B)
CONFIGURATION NO: 9B (W/O SCREEN)
MODEL: GENERIC

TEST DATE: 7/27/92

15 PSID SC. VALVE	CORRESP. PRES TAP	TIME 9:13 PSTAT (Volts)	TIME 10:04 PSTAT (Volts)	PSTAT (Volts)
16				
17	US 1	0.825	0.824	
18	US 2	0.815	0.814	
19	US 3	0.811	0.811	
20	US 4	0.818	0.817	
21				
22	H 1	0.344	0.342	
23	H 2	0.436	0.435	
24	H 3	0.550	0.548	
25	H 4	0.658	0.656	
26	H 5	0.722	0.721	
27	H 6	0.718	0.718	
28	H 7	0.658	0.656	
29	H 8	0.550	0.546	
30	H 9	0.446	0.444	
31	H 10	0.360	0.360	
32	H 11	0.314	0.312	
33	H 12	0.308	0.307	

15 PSID SC. VALVE	CORRESP. PRES TAP	TIME 9:17 PSTAT (Volts)	TIME 10:11 PSTAT (Volts)	PSTAT (Volts)
34				
35	S 1	-0.082	-0.083	
36	S 2	0.034	0.034	
37	S 3	0.194	0.193	
38	S 4	0.356	0.356	
39	S 5	////		
40	S 6	0.430	0.428	
41	S 7	0.322	0.320	
42	S 8	0.252	illegible	
43	S 9	0.036	0.034	
44	S 10	-0.082	-0.084	
45	S 11	-0135	-0.137	
46	S 12	-0.132	-0.138	
47				

TEST NO: 09 (1st TEST OF CONFIG 9B)
CONFIGURATION NO: 9B (W/O SCREEN)
MODEL: GENERIC
COMP.SPEED(RPM):
FLOW RATE:

TEST DATE: 7/23/92
TIME(START): 9:20 am
TIME(END): 10:06 "

		TRAVERSE 1		TRAVERSE 2		TRAVERSE 3		TRAVERSE 4		TRAVERSE 5		TRAVERSE 6		TRAVERSE 7			
		Position (Inch)	Ptot (1) (Volts)	Position (Inch)	Ptot (2) (Volts)	Position (Inch)	Ptot (3) (Volts)	Position (Inch)	Ptot (4) (Volts)	Position (Inch)	Ptot (5) (Volts)	Position (Inch)	Ptot (4) (Volts)	Position (Inch)	Ptot (3) (Volts)		
SHR	1	1.500	.329	1.500	.470	1.500	.465	1.500	.390	1.500	.352	1.500	.555	1.500	.457	1	SHR
	2	1.450	.954	1.450	.919	1.450	.828	1.450	.756	1.450	.952	1.450	1.003	1.450	.936	2	
	3	1.400	1.212	1.400	1.176	1.400	1.052	1.400	1.026	1.400	1.206	1.400	1.236	1.400	1.176	3	
	4	1.350	1.287	1.350	1.266	1.350	1.224	1.350	1.218	1.350	1.276	1.350	1.287	1.350	1.236	4	
	5	1.300	1.306	1.300	1.294	1.300	1.290	1.300	1.286	1.300	1.303	1.300	1.303	1.300	1.252	5	
	6	1.250	1.317	1.250	1.304	1.250	1.308	1.250	1.307	1.250	1.310	1.250	1.306	1.250	1.260	6	
	7	1.200	1.322	1.200	1.314	1.200	1.317	1.200	1.316	1.200	1.316	1.200	1.310	1.200	1.260	7	
	8	1.150	1.322	1.150	1.315	1.150	1.321	1.150	1.319	1.150	1.318	1.150	1.310	1.150	1.260	8	
	9	1.100	1.323	1.100	1.319	1.100	1.321	1.100	1.320	1.100	1.321	1.100	1.3095	1.100	1.260	9	
	10	1.050	1.322	1.050	1.319	1.050	1.323	1.050	1.321	1.050	1.322	1.050	1.309	1.050	1.260	10	
	11	1.000	1.323	1.000	1.321	1.000	1.323	1.000	1.320	1.000	1.321	1.000	1.309	1.000	1.259	11	
	12	0.950	1.324	0.950	1.320	0.950	1.325	0.950	1.321	0.950	1.322	0.950	1.308	0.950	1.260	12	
	13	0.900	1.324	0.900	1.321	0.900	1.325	0.900	1.321	0.900	1.323	0.900	1.308	0.900	1.260	13	
	14	0.850	1.324	0.850	1.320	0.850	1.325	0.850	1.320	0.850	1.322	0.850	1.308	0.850	1.260	14	
	15	0.800	1.323	0.800	1.319	0.800	1.325	0.800	1.320	0.800	1.324	0.800	1.308	0.800	1.260	15	
	16	0.750	1.324	0.750	1.320	0.750	1.325	0.750	1.319	0.750	1.322	0.750	1.307	0.750	1.257	16	
	17	0.700	1.324	0.700	1.320	0.700	1.326	0.700	1.320	0.700	1.323	0.700	1.306	0.700	1.258	17	
	18	0.650	1.325	0.650	1.320	0.650	1.326	0.650	1.320	0.650	1.325	0.650	1.306	0.650	1.256	18	
	19	0.600	1.324	0.600	1.321	0.600	1.327	0.600	1.319	0.600	1.323	0.600	1.306	0.600	1.257	19	
	20	0.550	1.323	0.550	1.321	0.550	1.327	0.550	1.319	0.550	1.325	0.550	1.305	0.550	1.256	20	
	21	0.500	1.325	0.500	1.322	0.500	1.328	0.500	1.320	0.500	1.325	0.500	1.305	0.500	1.256	21	
	22	0.450	1.325	0.450	1.320	0.450	1.327	0.450	1.319	0.450	1.325	0.450	1.304	0.450	1.256	22	
	23	0.400	1.325	0.400	1.321	0.400	1.328	0.400	1.319	0.400	1.325	0.400	1.304	0.400	1.258	23	
	24	0.350	1.326	0.350	1.322	0.350	1.328	0.350	1.319	0.350	1.326	0.350	1.304	0.350	1.259	24	
	25	0.300	1.326	0.300	1.321	0.300	1.329	0.300	1.318	0.300	1.327	0.300	1.304	0.300	1.261	25	
	26	0.250	1.326	0.250	1.322	0.250	1.327	0.250	1.318	0.250	1.327	0.250	1.303	0.250	1.261	26	
	27	0.200	1.328	0.200	1.322	0.200	1.327	0.200	1.3175	0.200	1.326	0.200	1.304	0.200	1.260	27	
	28	0.150	1.327	0.150	1.321	0.150	1.323	0.150	1.318	0.150	1.328	0.150	1.303	0.150	1.258	28	
	29	0.100	1.327	0.100	1.321	0.100	1.316	0.100	1.317	0.100	1.328	0.100	1.303	0.100	1.257	29	
	30	0.050	1.323	0.050	1.322	0.050	1.310	0.050	1.314	0.050	1.326	0.050	1.300	0.050	1.192	30	
HUB	31	0.000	1.149	0.000	1.176	0.000	1.238	0.000	1.309	0.000	1.154	0.000	1.003	0.000	.886	31	HUB

Program Used for Averaging the Static and Total Pressures

in the Annulus

```
C     THIS PROGRAM CALCULATES AVERAGE TOTAL PRESSURE &  AVERAGE PRESSURE
C     RATIO IN THE ANNULUS. IT ALSO GIVES THE MACH NUMBER AND THE MASS
C     FLOW RATE BASED ON THE AVERAGE PRESSURE RATIO.
C     THIS PROGRAM IS FOR THE TEST MODEL ONLY. IT SHOULD NOT BE USED
C     FOR OTHER MODELS OR FOR OTHER TEST PROCEDURES.
C
      REAL PT1(31),PT2(31),PT3(31),PT4(31),PT5(31),PT6(31),PT7(31),TATM
C
C     PT1 TO PT7 REPRESENTS THE RAW DATA OBTAINED IN SEVEN TRAVERSES.
C     THE UNIT IS IN VOLTS.(INPUT)
C
C     TATM REPRESENTS THE ATMOSPHERIC TEMPERATURE IN TEST ROOM IN F
C     ATMOSPHERIC TEMPERATURE IS USED FOR THE CORRECTIONS IN SPECIFIC
C     WEIGHT OF MERCURY.(INPUT)
C
     +,PATMHG,PATM,TCAL(18),SWHG(18),PSIG(19),V(19),TT,DUMMY,DUMMY3,
C
C     PATMHG REPRESENTS THE ATMOSPHERIC PRESSURE IN INCHES OF MERCURY(INPUT)
C
C     PATM REPRESENTS THE ATMOSPHERIC PRESSURE IN PSIA UNITS
C
C     TCAL AND SWHG FORMS THE SPECIFIC WEIGHT OF MERCURY VERSUS TEMPERATURE
C     TABLE.THIS IS A PERMENANT INPUT FILE('HGTAB.INP') AND IS USED FOR
C     THE CORRECTION IN SPECIFIC WEIGHT OF MERCURY.
C
C     PSIG AND V FORMS THE CALIBRATION CHART WHICH CONVERTS THE UNITS OF
C     PRESSURE FROM VOLTS TO PSIG.THIS FILE('CALIB.INP') CAN BE UPDATED
C     WHEN A NEW CALIBRATION TEST FOR THE EQUIPMENT IS  DONE.
C
C     TT REPRESENTS THE TOTAL TEMPERATURE AT THE INLET TO THE MODEL
C     THIS IS AN INPUT (IN F).
C     DUMMY IS USED FOR ARRANGING THE INPUT FORMAT.
C
     +PV(7,31),PT(12,31),P(12,31),A(31),MAR(12,31),PTAVE,PSTAT,PFL,
C
C     PV REPRESENTS THE TOTAL PRESSURE READINGS IN VOLTS
C     PT REPRESENTS THE TOTAL PRESSURE READINGS IN PSIA.
C     P REPRESENTS THE STATIC PRESSURE READINGS IN PSIA.
C     A REPRESENTS THE AREA SEGMENTS CORRESPONDING TO THE DATA POINTS.
C     MAR REPRESENTS THE MASS FLOW RATE PER UNIT AREA.
C     PTAVE REPRESENTS THE AVERAGE TOTAL PRESSURE IN THE ANNULUS.
C
     +DSUM,DSUM1,DSUM2,DR,R,D(12,31),DD(12,31),SNUM,SDENOM,STANUM,
     +DDD(12,31),MACH,SSUM,SSUM1,SSUM2,PRATIO,NSUM,NSUM1,NSUM2,
C
C     PRATIO REPRESENTS THE AVERAGE PRESSURE RATIO IN ANNULUS.
C     MACH REPRESENTS THE MACH NUMBER IN THE ANNULUS BASED ON THE
C     AVERAGE PRESSURE RATIO.
C
     +PSH1(12),PSH2(12),PSS1(12),PSS2(12),PSH(12),PSS(12),DUMMY2,HUB(7),
     +SHR(7),X(7,31),PS(7,31),PFL1(28),PFL2(28),LOSSCF,DYN,CP,MVENT,CP2,
     +MACH2,HLCF2,PRAT2,PSTA2,DYN2,MASPAR,MPAR(18),MAHPAR(18),
     +PSTA(12,31),PTOTAL(12,31),CPR,CPR2,DIST(31),PSHV(2,12),PSHG(2,12)
     +,PCOEF(2,12),MASSF
C
C     THE OTHER VARIABLES USED IN THE PROGRAM IS EXPLAINED AT THE POSITIONS
C     WHERE THEY ARE USED.
C
      INTEGER IRUN,IP,IM,N(31)
C     IRUN IS AN INPUT WHICH REPRESENTS THE NUMBER OF THE TEST .
```

```
C     IT IS USED TO IDENTIFY THE TEST DATA.
      CHARACTER*24DATE,CONN
C     DATE IS AN INPUT WHICH GIVES THE DATE OF THE TEST
      OPEN(UNIT=1,FILE='HGTAB.INP')
C
C     'HGTAB.INP' IS THE PERMENANT INPUT FILE WHICH GIVES THE TEMPERATURE
C     VERSUS SPECIFIC WEIGHT OF MERCURY CHART.
C
      OPEN(UNIT=2,FILE='CALIB.INP')
C
C     'CALIB.INP' IS THE INPUT FILE WHICH GIVES THE CALIBRATION CHART
C     WHICH IS USED TO CONVERT PRESSURE DATA FROM VOLTS TO PSIG UNITS.
C     THIS FILE CAN BE MODIFIED WHEN THE CALIBRATION IS UPDATED.
C
      OPEN(UNIT=3,FILE='G9B89I1.INP')
      OPEN(UNIT=4,FILE='G9B89I2.INP')
      OPEN(UNIT=9,FILE='G9B89I3.INP')
C
C     THESE FILES REPRESENT THE INPUT DATA SHEETS.
C     IN THIS CASE 'G9B90I1.INP' REPRESENTS THE INPUT SHEET # 1
C     FOR THE GENERIC MODEL CONFIGURATION #:9B, TEST NO 90
C
      OPEN(UNIT=7,FILE='G9B89.OUT')
C
C     THIS WILL BE THE OUTPUT FILE OF THE PROGRAM
C
C
C     ************READING THE DATA***************
C
C     TEMPERATURE VERSUS SPECIFIC WEIGHT OF Hg IS READ FROM FILE:'HGTAB.INP'
C
      DO 10 I=1,18
      READ(1,100)TCAL(I),SWHG(I),MPAR(I),MAHPAR(I)
10    CONTINUE
C
C     CALIBRATION CHART (VOLTS VERSUS PSIG) IS READ FROM FILE:'CALIB.INP'
C
      DO 15 I=1,19
      READ(2,150)V(I),PSIG(I)
15    CONTINUE
C
C     ATMOSPHERIC TEMPERATURE IN THE TEST ROOM IN F (TATM),
C     ATMOSPHERIC PRESSURE IN THE TEST ROOM IN INCHES OF Hg (PATMHG),
C     TOTAL TEMPERATURE AT THE MODEL INLET IN F(TT)
C     ARE READ FROM THE FILE:'G9B90I1.INP' (INPUT SHEET # 1)
C
      READ(3,200)TATM,PATMHG,TT
C
C     TOTAL TEMPERATURE IS CONVERTED TO R
C
      TT=TT+459.67
C
C     TOTAL PRESSURE DATA IN VOLTS FOR SEVEN TRAVERSES ARE READ FROM
C     THE FILE:'G9B90I1.INP' (INPUT SHEET # 1)
C
      DO 20 I=1,31
      READ(3,250)PT1(I),PT2(I),PT3(I),PT4(I)
20    CONTINUE
      READ(3,270)DUMMY
      DO 21 I=1,31
```

```
      READ(3,300)PT5(I),PT6(I),PT7(I)
21    CONTINUE
C
C     STATIC PRESSURE READINGS AT THE HUB AND SHROUD (IN VOLTS) ARE READ
C     FROM THE FILE 'G9B90I2.INP' (INPUT SHEET # 2)
C     PSH1 AND PSS1 REPRESENTS THE HUB AND SHROUD READINGS AT THE BEGINNING
C     OF THE TEST , WHERE PSH2 AND PSS2 REPRESENTS THE READINGS TAKEN AT
C     THE END OF THE TEST.
C
      READ(4,160)DUMMY2
      DO 22 I=1,12
      READ(4,170)PSH1(I),PSH2(I),PSS1(I),PSS2(I)
C
C     THE TWO READINGS ARE AVERAGED .
C     PSH AND PSS REPRESENTS THE AVERAGE STATIC PRESSURE (in volts) AT THE
C     HUB AND SHROUD RESPECTIVELY.
C
      PSH(I)=(PSH1(I)+PSH2(I))/2.0
      PSS(I)=(PSS1(I)+PSS2(I))/2.0
22    CONTINUE
      READ(9,160)DUMMY3
      SUMFL=0.0
      DO 23 I=1,28
      READ(9,180)PFL1(I),PFL2(I)
      SUMFL=SUMFL+PFL1(I)+PFL2(I)
23    CONTINUE
      PFL=(SUMFL/56.0)*0.5
C
C     FROM THE HUB AND SHROUD READINGS THE WALL STATIC PRESSURES AT
C     THE TRAVERSE LOCATIONS ARE ESTIMATED(in volts).
C     HUB AND SHR (1 TO 7) REPRESENTS THE WALL STATIC PRESSURES IN VOLTS
C     CORRESPONDING TO THE SEVEN TRAVERSE LOCATIONS.
C
      HUB(1)=(PSH(2)+PSH(3))/2.0
      SHR(1)=(PSS(2)+PSS(3))/2.0
      HUB(2)=(PSH(3)+PSH(4))/2.0
      SHR(2)=(PSS(3)+PSS(4))/2.0
      HUB(3)=(PSH(5)+PSH(6))/2.0
      SHR(3)=(PSS(5)+PSS(6))/2.0
      HUB(4)=(PSH(6)+PSH(7))/2.0
      SHR(4)=(PSS(6)+PSS(7))/2.0
      HUB(5)=(PSH(9)+PSH(10))/2.0
      SHR(5)=(PSS(9)+PSS(10))/2.0
      HUB(6)=(PSH(12)+PSH(1))/2.0
      SHR(6)=(PSS(12)+PSS(1))/2.0
      HUB(7)=(PSH(12)+PSH(11))/2.0
      SHR(7)=(PSS(12)+PSS(11))/2.0
      DO 26 I=1,12
      PSHV(1,I)=PSH(I)
      PSHV(2,I)=PSS(I)
26    CONTINUE
C
C     X(J,I) GIVES THE DATA POINTS WHERE TOTAL PRESSURES ARE READ.
C     31 POINTS FOR EACH 7 TRAVERSES.
C
      DO 27 J=1,7
      DO 27 I=1,31
      X(J,I)=((I-1)*0.050)
27    CONTINUE
C
```

```
C     THE STATIC PRESSURE AT THE POINTS WHERE TOTAL PRESSURE ARE READ,
C     IS ESTIMATED BY A STRAIGHT LINE INTERPOLATION BETWEEN THE VALUES
C     AT THE WALLS(HUB AND SHROUD) CORRESPONDING TO THAT TRAVERSE.
C     PS(J,I) REPRESENTS THE STATIC PRESSURE VALUS in volts CORRESPONDING
C     TO EACH DATA POINT.(31 POINTS FOR EACH SEVEN TRAVERSES).
C
      DO 28 J=1,7
      DO 28 I=1,31
      PS(J,I)=((HUB(J)-((X(J,I)/1.5)*(HUB(J)-SHR(J)))))
28    CONTINUE
C
C     ATMOSPHERIC PRESSURE IS CALCULATED IN PSIA.
C     USING THE ATMOSPHERIC TEMPERATURE INPUT THE CORRESPONDING
C     SPECIFIC WEIGHT OF Hg IS INTERPOLATED FROM THE CHART AND
C     BY MULTIPLYING THAT SPECIFIC WEIGHT(lb/in3) AND THE ATMOSPHERIC
C     PRESSURE INPUT IN INCHES OF Hg , THE ATMOSPHERIC PRESSURE IS
C     CALCULATED IN PSIA.
C
      IP=1
30    IF (TATM .EQ. TCAL(IP))THEN
      PATM=PATMHG*SWHG(IP)
      GO TO 40
      END IF
      IF (TATM .GT. TCAL(IP) .AND. TATM .LT. TCAL(IP+1))THEN
      PATM=PATMHG*((((TCAL(IP+1)-TATM)/(TCAL(IP+1)-TCAL(IP)))*(SWHG(IP)-
     +SWHG(IP+1)))+SWHG(IP+1))
      ELSE
      IP=IP+1
      GO TO 30
      END IF
40    PFL=PFL+PATM
C
C     PV REPRESENTS THE TOTAL PRESSURE DATA IN VOLTS .
C     THIS ARRAY REPRESENTS THE 31 DATA POINTS FOR 7 TRAVERSES.
C
C     WALL STATIC PRESSURES ARE TAKEN AS TOTAL PRESSURES AT HUB AND SHROUD
C     AS VELOCITY IS ZERO AT THE WALL.
C
      DO 45 J=1,7
      PV(J,1)=PS(J,1)
      PV(J,31)=PS(J,31)
45    CONTINUE
      DO 50 I=2,30
      PV(1,I)=PT1(I)
      PV(2,I)=PT2(I)
      PV(3,I)=PT3(I)
      PV(4,I)=PT4(I)
      PV(5,I)=PT5(I)
      PV(6,I)=PT6(I)
      PV(7,I)=PT7(I)
50    CONTINUE
C
C     THE STATIC PRESSURE DATA IS CONVERTED TO PSIA USING THE CALIBRATION CHART.
C     THE CORRESPONDING PSIG VALUE IS INTERPOLATED FROM THE CHART FOR EACH
C     STATICL PRESSURE DATA IN VOLTS AND THEN THE ATMOSPHERIC PRESSURE IN PSI
C     IS ADDED TO THAT VALUE TO GIVE THE TOTAL PRESSURE IN PSIA.
C
      DO 52 J=1,7
      DO 51 I=1,31
      K=1
```

```
53     IF (K .EQ. 19) THEN
       P(J,I)=(PS(J,I)*3.0)+PATM
       GO TO 51
       END IF
       IF ( PS(J,I) .EQ. V(K)) THEN
       P(J,I)=PSIG(K)+PATM
       GO TO 51
       END IF
       IF ( PS(J,I) .LT. V(K) .AND. PS(J,I) .GT. V(K+1) ) THEN
       P(J,I)=PSIG(K)-(((V(K)-PS(J,I))/(V(K)-V(K+1)))*(PSIG(K)-PSIG(K+1)
      +))
       P(J,I)=P(J,I)+PATM
       ELSE
       K=K+1
       GO TO 53
       END IF
51     CONTINUE
52     CONTINUE
       DO 57 J=1,2
       DO 54 I=1,12
       K=1
58     IF (K .EQ. 19) THEN
       PSHG(J,I)=(PSHV(J,I)*3.0)
       GO TO 54
       END IF
       IF ( PSHV(J,I) .EQ. V(K)) THEN
       PSHG(J,I)=PSIG(K)
       GO TO 54
       END IF
       IF ( PSHV(J,I) .LT. V(K) .AND. PSHV(J,I) .GT. V(K+1) ) THEN
       PSHG(J,I)=PSIG(K)-(((V(K)-PSHV(J,I))/(V(K)-V(K+1)))*(PSIG(K)-PSIG(
      +K+1)))
       ELSE
       K=K+1
       GO TO 58
       END IF
54     CONTINUE
57     CONTINUE
C
C      THE TOTAL PRESSURE DATA IS CONVERTED TO PSIA USING THE CALIBRATION CHART.
C      THE CORRESPONDING PSIG VALUE IS INTERPOLATED FROM THE CHART FOR EACH
C      TOTAL PRESSURE DATA IN VOLTS AND THEN THE ATMOSPHERIC PRESSURE IN PSI
C      IS ADDED TO THAT VALUE TO GIVE THE TOTAL PRESSURE IN PSIA.
C
       DO 60 J=1,7
       DO 55 I=1,31
       K=1
65     IF (K .EQ. 19) THEN
       PT(J,I)=(PV(J,I)*3.0)+PATM
       GO TO 55
       END IF
       IF ( PV(J,I) .EQ. V(K)) THEN
       PT(J,I)=PSIG(K)+PATM
       GO TO 55
       END IF
       IF ( PV(J,I) .LT. V(K) .AND. PV(J,I) .GT. V(K+1) ) THEN
       PT(J,I)=PSIG(K)-(((V(K)-PV(J,I))/(V(K)-V(K+1)))*(PSIG(K)-PSIG(K+1)
      +))
       PT(J,I)=PT(J,I)+PATM
       ELSE
```

```
      K=K+1
      GO TO 65
      END IF
55    CONTINUE
60    CONTINUE
C
C     THE NUMBER OF THE TEST IS ASKED AND READ AS AN INPUT FROM THE KEYBORD
C     WHEN THE PROGRAM IS RUNNING.
C
      WRITE(6,350)
      READ(5,360)IRUN
C
C     THE TEST DATE IS ASKED AND READ AS AN INPUT FROM THE KEYBORD
C     WHEN THE PROGRAM IS RUNNING.
C
      WRITE(6,365)
      READ(5,380)CONN
      WRITE(6,370)
      READ(5,380)DATE
      WRITE(6,375)
      READ(5,385)MVENT
C
      SNUM=0.0
      STANUM=0.0
      SDENOM=0.0
C
C     PT AND P REPRESENTS THE ARRAYS WHICH STORES THE TOTAL AND STATIC
C     DATA IN PSIA FOR THE 31 POINTS FOR 12 SECTIONS.REFER TO THE
C     DRAWING OF THE ANNULUS WHICH SHOWS THE 12 SECTIONS.
C     DUE TO SYMMETRY SOME OF THE SECTIONS ARE NOT TRAVERSED .
C     FOR THE SECTIONS 8,9,10,11 & 12 THE DATA OBTAINED FROM THE
C     TRAVERSES 4,2,1,6 & 5 ARE USED RESPECTIVELY.
C
      DO 80 J=1,12
      DO 90 I=1,31
      IF (J .GT. 7) GO TO 81
      GO TO 82
81    PT(8,I)=PT(4,I)
      P(8,I)=P(4,I)
      PT(9,I)=PT(2,I)
      P(9,I)=P(2,I)
      PT(10,I)=PT(1,I)
      P(10,I)=P(1,I)
      PT(12,I)=PT(5,I)
      P(12,I)=P(5,I)
      PT(11,I)=PT(6,I)
      P(11,I)=P(6,I)
C
C     DR REPRESENTS THE RADIAL INCREMENT USED FOR THE TRAVERSES(0.050 inches)
C     THIS IS USED AS DIFFERENTIAL RADIUS WHEN CALCULATING THE AREAS OF THE
C     SEGMENTS(0.050 inches except the walls)
C
82    DR=0.050
C
C     R REPRESENTS THE RADIAL DISTANCE TO THE DATA POINT(except the walls)
C     RADIAL DISTANCE TO HUB IS 1.5 inches
C     RADIAL DISTANCE TO SHROUD IS 3.0 inches
C
      R=(1.50+((I-1)*0.050))
C
```

```
C     ************************************************************************
C     *******THE TOTAL PRESSURE DATA AT THE WALLS ARE MODIFIED BY EXTRAPOLATING
C     ***THE VALUES TO THE WALL STATIC PRESSURE VALUES.************************
C     ************************************************************************
C
C
C     A REPRESENTS THE AREAS (in squared feet) FOR 31 AREA SEGMENTS
C     CORRESPONDING TO 31 DATA POINTS.
C
86    A(I)=(3.141592654/6.0)*R*DR/144.0
C
C     MAR REPRESENTS THE MASS FLOW RATE (lb/s) PER UNIT AREA (squared feet)
C     FOR EACH SEGMENT.
C
85    MAR(J,I)=111.8273*(PT(J,I)/SQRT(TT))*SQRT(7.0*(((P(J,I)/PT(J,I))**
     +(2.0/1.4))-((P(J,I)/PT(J,I))**(2.4/1.4))))
C
C     D REPRESENTS THE MASS FLOW RATE (lb/s) FOR EACH SEGMENT
C
      D(J,I)=MAR(J,I)*A(I)
C
C     DD REPRESENTS MASS FLOW RATE (lb/s) TIMES THE TOTAL PRESSURE (psia)
C     FOR EACH SEGMENT
C
      DD(J,I)=MAR(J,I)*A(I)*PT(J,I)
C
C     DDD REPRESENTS MASS FLOW RATE (lb/s) TIMES THE PRESSURE RATIO
C     FOR EACH SEGMENT
C
      DDD(J,I)=MAR(J,I)*A(I)*(P(J,I)/PT(J,I))
90    CONTINUE
80    CONTINUE
C
C     TOTAL PRESSURE AND PRESSURE RATIO ARE MASS AVERAGED USING SIMPSONS
C     METHOD.
C
      DO 95 J=1,12
      DSUM1=0.0
      DSUM2=0.0
      NSUM1=0.0
      NSUM2=0.0
      SSUM1=0.0
      SSUM2=0.0
      DSUM=0.0
      NSUM=0.0
      SSUM=0.0
      DO 96 I=2,30,2
      DSUM1=DSUM1+(4.0*D(J,I))
      NSUM1=NSUM1+(4.0*DD(J,I))
      SSUM1=SSUM1+(4.0*DDD(J,I))
96    CONTINUE
      DO 97 I=3,29,2
      DSUM2=DSUM2+(2.0*D(J,I))
      NSUM2=NSUM2+(2.0*DD(J,I))
      SSUM2=SSUM2+(2.0*DDD(J,I))
97    CONTINUE
      DSUM=((1.0/3.0)*(DSUM1+DSUM2+D(J,1)+D(J,31)))
      NSUM=((1.0/3.0)*(NSUM1+NSUM2+DD(J,1)+DD(J,31)))
      SSUM=((1.0/3.0)*(SSUM1+SSUM2+DDD(J,1)+DDD(J,31)))
      SNUM=SNUM+NSUM
```

```
      SDENOM=SDENOM+DSUM
      STANUM=STANUM+SSUM
95    CONTINUE
      PTAVE=SNUM/SDENOM
      PRATIO=STANUM/SDENOM
      PSTAT=PRATIO*PTAVE
      MASSF=111.8273*(PTAVE/(TT**0.5))*((7.0*((PRATIO**(2.0/1.4))-(PRATI
     +O**(2.4/1.4))))**0.5)*(3.141592654*((3.0**2.0)-(1.5**2.0))/144.0)
      LOSSCF=((PRATIO**(0.4/1.4))-((PFL/PTAVE)**(0.4/1.4)))/(1.0-(PRATIO
     +**(0.4/1.4)))
C
C     MACH NUMBER IN THE ANNULUS IS CALCULATED BASED ON THE AVERAGE
C     PRESSURE RATIO.
C
      MACH=((2.0/0.4)*(((PRATIO)**((-0.4)/1.4))-1.0))**0.5
      DYN=(1.4*(MACH**2.0))/(2.0*((1.0+(0.2*(MACH**2.0)))**3.5))
      CP=(PSTAT-PFL)/(DYN*PTAVE)
      CPR=(PFL-PSTAT)/(PTAVE-PSTAT)
      MASPAR=((16.46793*PTAVE)/(MVENT*(TT**0.5)))
      IM=1
98    IF (MASPAR .EQ. MPAR(IM))THEN
      MACH2=MAHPAR(IM)
      GO TO 99
      END IF
      IF (MASPAR .LT. MPAR(IM) .AND. MASPAR .GT. MPAR(IM+1))THEN
      MACH2=((((MPAR(IM)-MASPAR)/(MPAR(IM)-MPAR(IM+1)))*(MAHPAR(IM+1)-MA
     +HPAR(IM)))+MAHPAR(IM))
      ELSE
      IM=IM+1
      GO TO 98
      END IF
99    PRAT2=(1.0+(0.2*(MACH2**2.0)))**(-1.4/0.4)
      PSTA2=PRAT2*PTAVE
      HLCF2=((PRAT2**(0.4/1.4))-((PFL/PTAVE)**(0.4/1.4)))/(1.0-(PRAT2**(
     +0.4/1.4)))
      DYN2=(1.4*(MACH2**2.0))/(2.0*((1.0+(0.2*(MACH2**2.0)))**3.5))
      CP2=(PSTA2-PFL)/(DYN2*PTAVE)
      CPR2=(PFL-PSTA2)/(PTAVE-PSTA2)
      DO 101 J=1,12
      DO 101 I=1,31
      PSTA(J,I)=P(J,I)-PATM
      PTOTAL(J,I)=PT(J,I)-PATM
101   CONTINUE
C
C     OUTPUTS ARE PRINTED ON THE OUTPUT FILE
C
      WRITE(7,390)CONN,IRUN,DATE
      WRITE(7,410)PATM
      WRITE(7,420)TATM
      WRITE(7,450)TT
      WRITE(7,500)PTAVE
      WRITE(7,560)PSTAT
      WRITE(7,550)PRATIO
      WRITE(7,565)PFL
      WRITE(7,567)
      WRITE(7,570)MACH
      WRITE(7,575)LOSSCF
      WRITE(7,580)CP
      WRITE(7,590)CPR
      WRITE(7,600)MASSF
```

```
      WRITE(7,587)
      WRITE(7,570)MACH2
      WRITE(7,575)HLCF2
      WRITE(7,580)CP2
      WRITE(7,590)CPR2
      WRITE(7,610)MVENT
      WRITE(7,670)
      DO 102 I=1,31
      N(I)=32-I
      DIST(I)=(I-1)*0.05
      WRITE(7,700)N(I),DIST(I),PTOTAL(1,I),PTOTAL(2,I),PTOTAL(3,I),
     +PTOTAL(4,I)
102   CONTINUE
      WRITE(7,675)
      DO 103 I=1,31
      WRITE(7,750)N(I),DIST(I),PTOTAL(5,I),PTOTAL(6,I),PTOTAL(7,I)
103   CONTINUE
      WRITE(7,690)
      DO 104 I=1,31
      WRITE(7,700)N(I),DIST(I),PSTA(1,I),PSTA(2,I),PSTA(3,I),PSTA(4,I)
104   CONTINUE
      WRITE(7,695)
      DO 105 I=1,31
      WRITE(7,750)N(I),DIST(I),PSTA(5,I),PSTA(6,I),PSTA(7,I)
105   CONTINUE
      WRITE(7,710)
      DO 106 I=1,12
      PCOEF(1,I)=(PSHG(1,I)+PATM-PFL)/(PTAVE*DYN)
      PCOEF(2,I)=(PSHG(2,I)+PATM-PFL)/(PTAVE*DYN)
      WRITE(7,720)I,PSHG(1,I),PSHG(2,I),PCOEF(1,I),PCOEF(2,I)
106   CONTINUE
100   FORMAT(F5.1,1X,F8.6,7X,F6.4,4X,F7.5)
150   FORMAT(F5.3,3X,F6.3)
160   FORMAT(//////,F5.3)
170   FORMAT(5X,F6.3,4X,F6.3,4X,F6.3,5X,F6.3)
180   FORMAT(6X,F6.3,4X,F6.3)
200   FORMAT(/,29X,F6.3,/,37X,F6.3,/,38X,F7.3,////////)
250   FORMAT(22X,F7.4,3X,F7.4,3X,F7.4,3X,F7.4)
270   FORMAT(F5.3,///////)
300   FORMAT(22X,F7.4,3X,F7.4,3X,F7.4)
350   FORMAT(' ENTER THE RUN NO')
360   FORMAT(I3)
365   FORMAT(' ENTER THE CONFIGURATION NO')
370   FORMAT(' ENTER THE DATE (MO/DA/YEAR) ')
375   FORMAT(' ENTER MASS FLOW RATE (VENTURI) IN (lbm/sec) ')
380   FORMAT(A24)
385   FORMAT(F6.3)
390   FORMAT(' GENERIC MODEL CONFIGURATION NO ',A24,/,' TEST NO: ',I3,
     +3X,'DATE : ',A12)
400   FORMAT(F10.4)
410   FORMAT(//,' ATMOSPHERIC PRESSURE IN THE TEST ROOM IS : ',F6.3,' lbf
     +/sqi')
420   FORMAT(/, ' ATMOSPHERIC TEMPERATURE IN THE TEST ROOM IS : ',F5.2,'
     + F')
450   FORMAT(//,' TOTAL TEMPERATURE IS : ',F6.2,' R')
500   FORMAT(//,' AVERAGE TOTAL PRESSURE IN THE ANNULUS IS CALCULATED AS
     + : ',F6.3,' lbf/sqi')
550   FORMAT(/,' AVERAGE PRESSURE RATIO IN THE ANNULUS IS CALCULATED AS
     +: ',F5.3)
560   FORMAT(/,' AVERAGE STATIC PRESSURE IN THE ANNULUS IS CALCULATED AS
```

```
     + : ',F6.3,' lbf/sqi')
565   FORMAT(///,' AVERAGE STATIC PRESSURE AT THE EXIT FLANGE IS : ',F6.3
     +,' lbf/sqi')
567   FORMAT(//,' FIRST SET OF RESULTS ',/,' BASED ON THE AVERAGE TOTAL
     + AND STATIC PRESSURES IN THE ANNULUS')
570   FORMAT(/,' CALCULATED AVERAGE MACH NUMBER IN THE ANNULUS IS : ',F5
     +.3)
575   FORMAT(/,' HOOD LOSS COEFFICIENT IS : ',F5.3)
580   FORMAT(/,' PRESSURE COEFFICIENT Cp IS : ',F5.3)
587   FORMAT(//,' SECOND SET OF RESULTS : BASED ON THE MASS FLOW RATE(FR
     +OM VENTURI),',/,' AVERAGE TOTAL PRESSURE AND TOTAL TEMPERATURE')
590   FORMAT(/,' PRESSURE COEFFICIENT (Second Definition) Cpr IS: ',F6.3
     +)
600   FORMAT(/,' CALCULATED MASS FLOW RATE IS : ',F6.3,' lbm/sec')
610   FORMAT(/,' MASS FLOW RATE (FROM VENTURI) IS : ',F6.3,' lbm/sec')
670   FORMAT(/////////////,13X,' TOTAL PRESSURE VALUES FOR TRAVERSE POIN
     +TS',//,1X,'DATA NO', 2X,'DISTANCE',3X,'TRAVERSE 1',5X,'TRAVERSE 2'
     +,5X,'TRAVERSE 3',5X,'TRAVERSE 4',/,10X,'FROM HUB',/,10X,'(inches)'
     +,5X,'(psig)',9X,'(psig)',9X,'(psig)',9X,'(psig)',/)
675   FORMAT(////////////////////////,10X,' TOTAL PRESSURE VALUES FOR TR
     +AVERSE POINTS',//,1X,'DATA NO', 2X,'DISTANCE',3X,'TRAVERSE 5',5X,'
     +TRAVERSE 6',5X,'TRAVERSE 7',/,10X,'FROM HUB',/,10X,'(inches)',5X,'
     +(psig)',9X,'(psig)',9X,'(psig)',/)
690   FORMAT(////////////////////////,13X,' STATIC PRESSURE VALUES FOR TR
     +AVERSE POINTS',//,1X,'DATA NO', 2X,'DISTANCE',3X,'TRAVERSE 1',5X,'
     +TRAVERSE 2',5X,'TRAVERSE 3',5X,'TRAVERSE 4',/,10X,'FROM HUB',/,10X
     +,'(inches)',5X,'(psig)',9X,'(psig)',9X,'(psig)',9X,'(psig)',/)
695   FORMAT(////////////////////////,10X,' STATIC PRESSURE VALUES FOR TRA
     +VERSE POINTS',//,1X,'DATA NO', 2X,'DISTANCE',3X,'TRAVERSE 5',5X,'T
     +RAVERSE 6',5X,'TRAVERSE 7',/,10X,'FROM HUB',/,10X,'(inches)',5X,'(
     +psig)',9X,'(psig)',9X,'(psig)',/)
700   FORMAT(4X,I2,6X,F5.3,6X,F6.3,9X,F6.3,9X,F6.3,9X,F6.3)
710   FORMAT(////,' CIRCUMFERENTIAL STATIC PRESSURE VARIATION',//,'PRESS
     +URE TAP NO',5X,'Ps (HUB)',5X,'Ps (SHROUD)',4X,'Cp (HUB)',5X,'Cp (S
     +HROUD)',/,21X,'(psig)',8X,'(psig)',/)
720   FORMAT(6X,I2,13X,F6.3,8X,F6.3,8X,F6.3,8X,F6.3)
750   FORMAT(4X,I2,6X,F5.3,6X,F6.3,9X,F6.3,9X,F6.3)
      STOP
      END
```

Input Sheets for Test 89 of Configuration 9B

ATMOSPHERIC TEMPERATURE IN F:74.5
ATMOSPHERIC PRESSURE IN INCHES OF Hg:29.423
TOTAL TEMPERATURE IN F AT MODEL INLET:99.54

TOTAL PRESSURE TRAVERSES FOR TEST 89 OF CONFIGURATION NO 9B

DATA NO	DISTANCE FROM HUB (inches)	TRAV 1 (volts)	TRAV 2 (volts)	TRAV 3 (volts)	TRAV 4 (volts)
31	0.000	1.1440	1.1760	1.2380	1.3090
30	0.050	1.3230	1.3220	1.3100	1.3140
29	0.100	1.3270	1.3210	1.3160	1.3170
28	0.150	1.3270	1.3210	1.3230	1.3180
27	0.200	1.3280	1.3220	1.3270	1.3170
26	0.250	1.3260	1.3220	1.3270	1.3180
25	0.300	1.3260	1.3210	1.3290	1.3180
24	0.350	1.3260	1.3220	1.3280	1.3190
23	0.400	1.3250	1.3210	1.3280	1.3190
22	0.450	1.3250	1.3200	1.3270	1.3190
21	0.500	1.3250	1.3220	1.3280	1.3200
20	0.550	1.3230	1.3210	1.3270	1.3190
19	0.600	1.3240	1.3210	1.3270	1.3190
18	0.650	1.3250	1.3200	1.3260	1.3200
17	0.700	1.3240	1.3200	1.3260	1.3200
16	0.750	1.3240	1.3200	1.3250	1.3190
15	0.800	1.3230	1.3190	1.3250	1.3200
14	0.850	1.3240	1.3200	1.3250	1.3200
13	0.900	1.3240	1.3210	1.3250	1.3210
12	0.950	1.3240	1.3200	1.3250	1.3210
11	1.000	1.3230	1.3210	1.3230	1.3200
10	1.050	1.3220	1.3190	1.3230	1.3210
9	1.100	1.3230	1.3190	1.3210	1.3200
8	1.150	1.3220	1.3150	1.3210	1.3190
7	1.200	1.3220	1.3140	1.3170	1.3160
6	1.250	1.3170	1.3040	1.3080	1.3070
5	1.300	1.3060	1.2940	1.2900	1.2860
4	1.350	1.2870	1.2660	1.2240	1.2180
3	1.400	1.2120	1.1760	1.0520	1.0260
2	1.450	0.9540	0.9190	0.8280	0.7560
1	1.500	0.6000	0.7000	0.6000	0.5400

TOTAL PRESSURE TRAVERSES FOR TEST 89 OF CONFIGURATION NO 9B

DATA NO	DISTANCE FROM HUB (inches)	TRAV 5 (volts)	TRAV 6 Svolts)	TRAV 7 (volts)
31	0.000	1.1540	1.0030	0.8860
30	0.050	1.3260	1.3000	1.1920
29	0.100	1.3280	1.3030	1.2570
28	0.150	1.3280	1.3030	1.2580
27	0.200	1.3260	1.3040	1.2600
26	0.250	1.3270	1.3030	1.2610
25	0.300	1.3270	1.3040	1.2610
24	0.350	1.3260	1.3040	1.2590
23	0.400	1.3250	1.3040	1.2580
22	0.450	1.3250	1.3040	1.2560
21	0.500	1.3250	1.3050	1.2560
20	0.550	1.3250	1.3050	1.2560
19	0.600	1.3230	1.3060	1.2570
18	0.650	1.3250	1.3060	1.2560
17	0.700	1.3230	1.3060	1.2580
16	0.750	1.3220	1.3070	1.2570
15	0.800	1.3240	1.3080	1.2600
14	0.850	1.3220	1.3080	1.2600
13	0.900	1.3230	1.3080	1.2600
12	0.950	1.3220	1.3080	1.2600
11	1.000	1.3210	1.3090	1.2590
10	1.050	1.3220	1.3090	1.2600
9	1.100	1.3210	1.3090	1.2600
8	1.150	1.3180	1.3100	1.2600
7	1.200	1.3160	1.3100	1.2600
6	1.250	1.3100	1.3060	1.2600
5	1.300	1.3030	1.3030	1.2520
4	1.350	1.2760	1.2870	1.2360
3	1.400	1.2060	1.2360	1.1760
2	1.450	0.9520	1.0030	0.9360
1	1.500	0.5000	0.6000	0.5000

TEST 89 OF CONFIGURATION 9B
STATIC PRESSURE READINGS

	HUB (1.DATA) (Volts)	HUB (2.DATA) (Volts)	SHROUD (1.DATA) (Volts)	SHROUD (2.DATA) (Volts)
1	0.344	0.342	-0.082	-0.083
2	0.436	0.435	0.034	0.034
3	0.550	0.548	0.194	0.193
4	0.658	0.656	0.356	0.356
5	0.722	0.721	0.396	0.396
6	0.718	0.718	0.430	0.428
7	0.658	0.656	0.322	0.320
8	0.550	0.546	0.180	0.180
9	0.446	0.444	0.036	0.034
10	0.360	0.360	-0.082	-0.084
11	0.314	0.312	-0.135	-0.137
12	0.308	0.307	-0.132	-0.138

TEST 89 OF CONFIGURATION 9B
STATIC PRESSURE READINGS AT THE FLANGE

	PSTAT (1.DATA) (Volts)	PSTAT (2.DATA) (Volts)
1	0.532	0.534
2	-0.534	-0.548
3	-0.186	-0.188
4	0.363	0.372
5	0.332	0.335
6	-0.152	-0.156
7	-0.464	-0.466
8	0.392	0.396
9	0.212	0.216
10	-0.304	-0.317
11	-0.728	-0.726
12	-0.370	-0.374
13	0.256	0.252
14	-0.162	-0.160
15	-0.182	-0.178
16	-0.047	-0.054
17	-0.052	-0.050
18	0.308	0.310
19	0.388	0.396
20	-0.063	-0.064
21	-0.105	-0.106
22	-0.222	-0.214
23	-0.228	-0.230
24	0.474	0.463
25	-0.404	-0.414
26	-0.818	-0.818
27	-0.330	-0.334
28	0.306	0.304

Output Sheets for Test 89 of Configuration 9B

GENERIC MODEL CONFIGURATION NO 9B W/O SCREEN W/ GV
TEST NO: 89 DATE : 7/23/92

ATMOSPHERIC PRESSURE IN THE TEST ROOM IS : 14.389 lb/sqi

ATMOSPHERIC TEMPERATURE IN THE TEST ROOM IS : 74.50 F

TOTAL TEMPERATURE IS : 559.21 R

AVERAGE TOTAL PRESSURE IN THE ANNULUS IS CALCULATED AS : 18.261 lbf/sqi

AVERAGE STATIC PRESSURE IN THE ANNULUS IS CALCULATED AS : 15.234 lbf/sqi

AVERAGE PRESSURE RATIO IN THE ANNULUS IS CALCULATED AS : 0.834

AVERAGE STATIC PRESSURE AT THE EXIT FLANGE IS : 14.352 lbf/sqi

FIRST SET OF RESULTS
BASED ON THE AVERAGE TOTAL AND STATIC PRESSURES IN THE ANNULUS

CALCULATED AVERAGE MACH NUMBER IN THE ANNULUS IS : 0.516

HOOD LOSS COEFFICIENT IS : 0.318

PRESSURE COEFFICIENT Cp IS : 0.311

PRESSURE COEFFICIENT (Second Definition) Cpr IS: -0.291

CALCULATED MASS FLOW RATE IS : 6.641 lbm/sec

SECOND SET OF RESULTS : BASED ON THE MASS FLOW RATE(FROM VENTURI),
AVERAGE TOTAL PRESSURE AND TOTAL TEMPERATURE

CALCULATED AVERAGE MACH NUMBER IN THE ANNULUS IS : 0.509

HOOD LOSS COEFFICIENT IS : 0.351

PRESSURE COEFFICIENT Cp IS : 0.343

PRESSURE COEFFICIENT (Second Definition) Cpr IS: -0.322

MASS FLOW RATE (FROM VENTURI) IS : 6.578 lbm/sec

TOTAL PRESSURE VALUES FOR TRAVERSE POINTS

DATA NO	DISTANCE FROM HUB (inches)	TRAVERSE 1 (psig)	TRAVERSE 2 (psig)	TRAVERSE 3 (psig)	TRAVERSE 4 (psig)
31	0.000	1.482	1.812	2.163	2.065
30	0.050	3.986	3.983	3.947	3.959
29	0.100	3.998	3.980	3.965	3.968
28	0.150	3.998	3.980	3.986	3.971
27	0.200	4.001	3.983	3.998	3.968
26	0.250	3.995	3.983	3.998	3.971
25	0.300	3.995	3.980	4.004	3.971
24	0.350	3.995	3.983	4.001	3.974
23	0.400	3.992	3.980	4.001	3.974
22	0.450	3.992	3.977	3.998	3.974
21	0.500	3.992	3.983	4.001	3.977
20	0.550	3.986	3.980	3.998	3.974
19	0.600	3.989	3.980	3.998	3.974
18	0.650	3.992	3.977	3.995	3.977
17	0.700	3.989	3.977	3.995	3.977
16	0.750	3.989	3.977	3.992	3.974
15	0.800	3.986	3.974	3.992	3.977
14	0.850	3.989	3.977	3.992	3.977
13	0.900	3.989	3.980	3.992	3.980
12	0.950	3.989	3.977	3.992	3.980
11	1.000	3.986	3.980	3.986	3.977
10	1.050	3.983	3.974	3.986	3.980
9	1.100	3.986	3.974	3.980	3.977
8	1.150	3.983	3.962	3.980	3.974
7	1.200	3.983	3.959	3.968	3.965
6	1.250	3.968	3.929	3.941	3.938
5	1.300	3.935	3.899	3.887	3.875
4	1.350	3.878	3.814	3.688	3.670
3	1.400	3.652	3.543	3.170	3.091
2	1.450	2.873	2.767	2.491	2.273
1	1.500	0.341	0.811	1.235	1.116

TOTAL PRESSURE VALUES FOR TRAVERSE POINTS

DATA NO	DISTANCE FROM HUB (inches)	TRAVERSE 5 (psig)	TRAVERSE 6 (psig)	TRAVERSE 7 (psig)
31	0.000	1.203	0.958	0.914
30	0.050	3.995	3.917	3.592
29	0.100	4.001	3.926	3.787
28	0.150	4.001	3.926	3.790
27	0.200	3.995	3.929	3.796
26	0.250	3.998	3.926	3.799
25	0.300	3.998	3.929	3.799
24	0.350	3.995	3.929	3.793
23	0.400	3.992	3.929	3.790
22	0.450	3.992	3.929	3.784
21	0.500	3.992	3.932	3.784
20	0.550	3.992	3.932	3.784
19	0.600	3.986	3.935	3.787
18	0.650	3.992	3.935	3.784
17	0.700	3.986	3.935	3.790
16	0.750	3.983	3.938	3.787
15	0.800	3.989	3.941	3.796
14	0.850	3.983	3.941	3.796
13	0.900	3.986	3.941	3.796
12	0.950	3.983	3.941	3.796
11	1.000	3.980	3.944	3.793
10	1.050	3.983	3.944	3.796
9	1.100	3.980	3.944	3.796
8	1.150	3.971	3.947	3.796
7	1.200	3.965	3.947	3.796
6	1.250	3.947	3.935	3.796
5	1.300	3.926	3.926	3.772
4	1.350	3.844	3.878	3.724
3	1.400	3.634	3.724	3.543
2	1.450	2.867	3.022	2.818
1	1.500	-0.072	-0.326	-0.406

STATIC PRESSURE VALUES FOR TRAVERSE POINTS

DATA NO	DISTANCE FROM HUB (inches)	TRAVERSE 1 (psig)	TRAVERSE 2 (psig)	TRAVERSE 3 (psig)	TRAVERSE 4 (psig)
31	0.000	1.482	1.812	2.163	2.065
30	0.050	1.444	1.780	2.132	2.034
29	0.100	1.407	1.747	2.101	2.002
28	0.150	1.369	1.714	2.070	1.971
27	0.200	1.328	1.682	2.039	1.940
26	0.250	1.288	1.649	2.008	1.909
25	0.300	1.248	1.617	1.977	1.878
24	0.350	1.208	1.584	1.947	1.847
23	0.400	1.168	1.551	1.916	1.816
22	0.450	1.128	1.519	1.885	1.785
21	0.500	1.088	1.486	1.855	1.754
20	0.550	1.047	1.453	1.824	1.723
19	0.600	1.007	1.421	1.794	1.691
18	0.650	0.967	1.388	1.763	1.660
17	0.700	0.930	1.354	1.733	1.629
16	0.750	0.893	1.319	1.702	1.598
15	0.800	0.857	1.284	1.672	1.567
14	0.850	0.820	1.250	1.641	1.536
13	0.900	0.783	1.215	1.611	1.505
12	0.950	0.747	1.180	1.580	1.474
11	1.000	0.710	1.145	1.550	1.443
10	1.050	0.674	1.110	1.519	1.412
9	1.100	0.637	1.075	1.489	1.381
8	1.150	0.600	1.041	1.458	1.348
7	1.200	0.568	1.006	1.428	1.315
6	1.250	0.531	0.971	1.397	1.282
5	1.300	0.493	0.938	1.366	1.248
4	1.350	0.455	0.907	1.333	1.215
3	1.400	0.417	0.875	1.300	1.182
2	1.450	0.379	0.843	1.268	1.149
1	1.500	0.341	0.811	1.235	1.116

STATIC PRESSURE VALUES FOR TRAVERSE POINTS

DATA NO	DISTANCE FROM HUB (inches)	TRAVERSE 5 (psig)	TRAVERSE 6 (psig)	TRAVERSE 7 (psig)
31	0.000	1.203	0.958	0.914
30	0.050	1.158	0.916	0.871
29	0.100	1.113	0.874	0.828
28	0.150	1.068	0.832	0.785
27	0.200	1.022	0.790	0.742
26	0.250	0.977	0.748	0.699
25	0.300	0.934	0.706	0.656
24	0.350	0.893	0.664	0.613
23	0.400	0.852	0.622	0.574
22	0.450	0.811	0.580	0.530
21	0.500	0.770	0.542	0.485
20	0.550	0.728	0.498	0.440
19	0.600	0.687	0.455	0.396
18	0.650	0.646	0.412	0.351
17	0.700	0.605	0.368	0.307
16	0.750	0.568	0.325	0.262
15	0.800	0.525	0.281	0.218
14	0.850	0.482	0.238	0.173
13	0.900	0.440	0.195	0.128
12	0.950	0.397	0.151	0.084
11	1.000	0.354	0.108	0.039
10	1.050	0.312	0.064	-0.005
9	1.100	0.269	0.021	-0.050
8	1.150	0.227	-0.022	-0.094
7	1.200	0.184	-0.066	-0.139
6	1.250	0.141	-0.109	-0.184
5	1.300	0.099	-0.153	-0.228
4	1.350	0.056	-0.196	-0.273
3	1.400	0.013	-0.239	-0.317
2	1.450	-0.029	-0.283	-0.362
1	1.500	-0.072	-0.326	-0.406

CIRCUMFERENTIAL STATIC PRESSURE VARIATION

PRESSURE TAP NO	Ps (HUB) (psig)	Ps (SHROUD) (psig)	Cp (HUB)	Cp (SHROUD)
1	1.014	-0.247	0.371	-0.074
2	1.308	0.102	0.475	0.049
3	1.651	0.581	0.596	0.218
4	1.973	1.055	0.710	0.386
5	2.168	1.183	0.778	0.431
6	2.158	1.288	0.775	0.468
7	1.973	0.945	0.710	0.347
8	1.648	0.540	0.595	0.204
9	1.339	0.105	0.486	0.050
10	1.068	-0.249	0.390	-0.075
11	0.922	-0.408	0.339	-0.131
12	0.906	-0.405	0.333	-0.130

SAMPLE MASS FLOW RATE CALCULATIONS

FOR THE VENTURI METER

Generic Model, Configuration 9, Test 89

Specific Humidity

$$S = 0.622 \frac{P_v}{P_{LAB} - P_v}$$

$P_{LAB} = 14.389$ psia (29.4225 inches of Hg at 74.5 °F)

$T_{dry\ bulb} = 84$ °F

$\phi = 0.52$

P_g (at $T_{dry\ bulb}$) $= 0.5771$ psia

$\Rightarrow P_v = \phi\ P_g = 0.3001$ psia

$\Rightarrow \underline{S = 0.0132485}$

$$\rho_1 = 2.6991\ (1+S)\ \frac{P_{vent\ inlet} - P_v}{T_{vent}}$$

$P_{vent\ inlet} = 3.978$ psig $= 18.367$ psia

$T_{vent} = 100.6$ °F $= 560.27$ °R

$\Rightarrow \underline{\rho_1 = 0.08819\ lb_m/ft^3}$

$\Delta P_{vent} = 6.90$ inches of H_2O

$\Delta P_{vent} = 6.90$ inches of H_2O x 0.036062 lb_f/in^3 of H_2O $= 0.24883$ psia

$C = 0.99$

$Y = 0.99$ ($\Delta P/P_1 = 0.014$)

$F_a = 1.00045$

$$W(lb_m/sec) = 45.285 \times C \times Y \times F_a \times \sqrt{\rho_1\ (lb_m/ft^3) \times \Delta P_{vent}\ (psi)}$$

$$\Rightarrow W(lb_m/sec) = 45.285 \times 0.99 \times 0.99 \times 1.00045 \times \sqrt{0.08819 \times 0.2488278}$$

$$\Rightarrow \underline{W(lb_m/sec) = 6.578}$$

THE SPECIFIC WEIGHTS OF MERCURY AND WATER

	Specific Weight	
Temperature, °F	Mercury (lb/in^3)	Water (lb/in^3)
52	0.490164	0.036113
56	0.489966	0.036104
60	0.489769	0.036092
64	0.489572	0.036078
68	0.489375	0.036062
72	0.489178	0.036045
76	0.488981	0.036026
80	0.488784	0.036005

NON DIMENSIONAL MASS FLOW RATE vs MACH NUMBER

$\frac{P_{T,AN}A_{AN}}{W\sqrt{RT_{T,AN}}}$	Mach Number
2.0498	0.46922
1.9928	0.48749
1.9420	0.50536
1.8550	0.54009
1.7836	0.57372
1.7242	0.60650
1.6744	0.63862
1.6323	0.67022
1.5967	0.70144
1.5666	0.73240
1.5412	0.76318
1.5200	0.79389

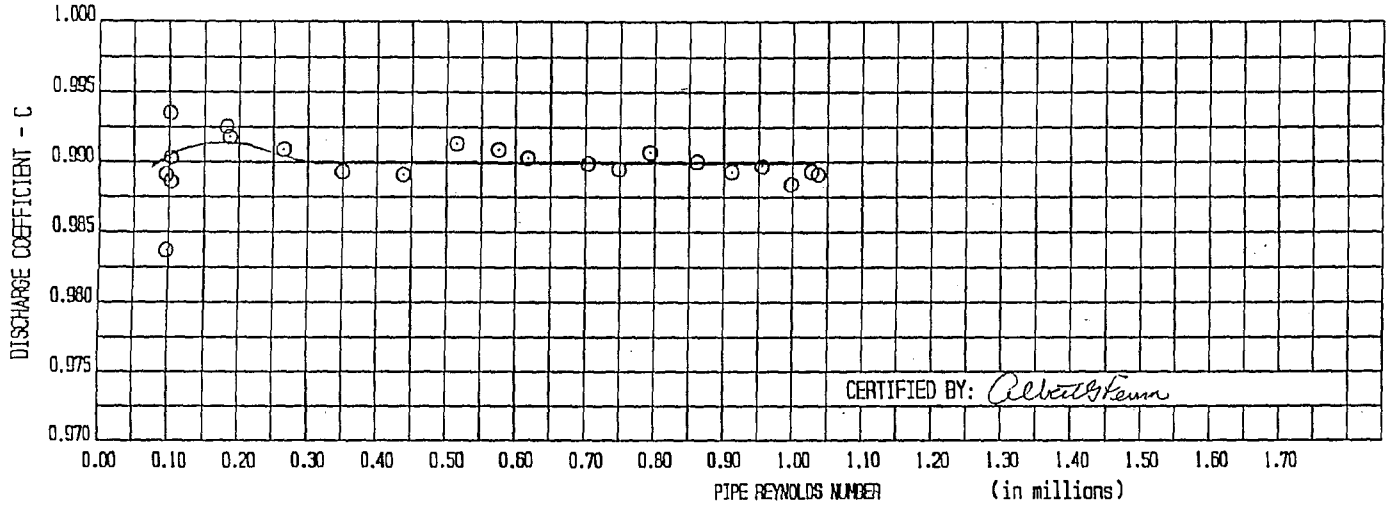

$$q_a = C F_a K_M \sqrt{h}$$

q_a = Actual Flow Rate (ft^3/sec)	
C = Discharge Coefficient (Dimensionless)	
h = Pressure Differential (Feet of Water at Run Temperature)	
K_M = Meter Constant = $\frac{F_a\, a\sqrt{2g}}{\sqrt{1-\beta^4}}$	3.7742
F_a = Thermal Expansion Factor	
a = Throat Area (ft^2) =	0.4519
g = Local Acceleration of Gravity (ft/sec^2)	32.1630
β = Ratio of Throat to	
Pipe Diameter (Dimensionless) =	0.5281
Upstream Diameter (inches) =	17.2340
Throat Diameter (inches) =	9.1020
Dimensions By: FLUIDIC	

MEAN - 0.9899 ABOVE PIPE REYNOLDS #200000

REFERENCES

1. Owczarek, J.A., and Warnock, A.S., "Improvement of a Low Pressure Turbine Exhaust End Performance at Indian Point Unit No. 2 Model Experiments", Energy Research Center Report, Lehigh University, 1989.
2. Howard, J.H.G., Henseler, H.J., and Thornton-Trump, A.B., "Performance and Flow Regimes for Annular Diffusers", ASME Paper No. 67-WA/FE-21, 1967.
3. Kline, J.S., "On the Nature of Stall", ASME Trans., Journal of Basic Engineering, Vol. 81, September 1959, pp. 305-320.
4. Sovran, G., and Klomp, E.D., "Experimentally Determined Optimum Geometries for Rectilinear Diffusers with Rectangular, Conical or Annular Cross-section", New York: Elsevier Publishing Co., 1967.
5. Hoffman, J.A., and Gonzales, G., "Effects of Small Scale, High Intensity Inlet Turbulence on Flow in a Two Dimensional Diffuser", ASME Trans., Journal of Fluids Engineering, Vol. 106, June 1984, pp. 121-124.
6. Seglem C.E., and Brown R.O., "Turbine Exhaust Hood Losses", ASME Paper No. 60-PWR-7,1960.
7. Bean, Howard S., "Fluid Meters, Their Theory and Application", 6th ed., New York, ASME, 1971.
8. Turegun, Behzat, "Design of an Air Test Loop and Turbine Exhaust Hood Models for Performance Improvement Study ", MS Thesis, Lehigh University,

June 1991.

9. Owczarek, J.A., and Warnock, A.S., "Proposal for Research Project, Part 2: Improvement of LP Turbine Hood Performance", Energy Research Center, Lehigh University, 1989.

10. Rodes, N., "The Prediction of Turbine Exhaust Performance", ASME Trans., Latest Advances in Steam Turbine Design, Blading, Repairs, Condition Assessment, and Condenser Interaction, PWR-Vol. 7, 1989, pp. 99-105.

11. Gray, L., Sandhu, S.S., Davids, J., and Southall, L.R., " Technical Considerations in Optimizing Blade-Exhaust Hood Performance for LP Steam Turbines", ASME Trans., Latest Advances in Steam Turbine Design, Blading, Repairs, Condition Assessment, and Condenser Interaction, PWR-Vol. 7, 1989, pp. 99-97.

12. Drakanov, A.M., and Zeryankin, A.E., " Investigating the Joint Operation of a Turbine Stage and a Diffuser Exhaust Hood", Teploenergetika, Vol. 19, No. 2, 1972, pp. 66-69.

13. Von Karman Institude for Fluid Dynamics, "Steam Turbines for Large Power Outputs", Lecture Series 1980-6, 1980.

14. Owczarek, J.A., "Fundamentals of Gas Dynamics", International Textbook Co., Scranton, PA., 1964.

15. Takehira, A., Tanaka, M., Kawashima, T., and Hanabusa, H., "An Experimental Study of the Annular Diffusers in Axial Flow Compressors and Turbines", Proceedings of the 1977 Tokyo Joint Gas Turbine Congress, 1977,

pp. 319-329.

16. Senoo, Y., and Nishi, M., " Improvement of the Performance of Conical Diffusers by Vortex Generators", ASME Trans., Journal of Fluids Engineering, Vol. 96, 1974, pp. 4-10

17. Stevens, S.J, and Williams, G.J., " The Influence of Inlet Conditions on the Performance of Annular Diffusers with Conical Walls", ASME Trans., Journal of Fluids Engineering, Vol. 102, September 1980, pp. 357-363.

18. McDonald, A.T., Fox, R.W., and Van Dewoestine, R.V., " Effect of Swirling Flow on Pressure Recovery in Conical Diffusers", AIAA Paper No. 71-84, 1984

19. Lohmann, R.P., Markowsky, S.J., and Brookman, E.T., " Swirling Flow Through Annular Diffusers with Conical Walls", ASME Trans., Journal of Fluids Engineering, Vol. 101, June 1979, pp. 224-229.

20. Chesmejef, S., " Aerodynamic Testing of a Low Stimulus, Efficient Exhaust Hood-Industrial Turbines", ASME Paper No. 77-JPGC-Pwr-2, 1977.

21. Migai, V.K., Gudkov, E.I., and Nosova, I.S., " Increasing the Efficiency of Diffusers of Steam Turbine Exhausts", Teploenergetika, Vol. 21, No. 12, 1974, pp. 46-50.

VITA

Sinan Çelen was born in Elazığ, Turkey on April 10, 1969. He obtained his high school degree from T.E.D. Ankara High School. He received his B.S. degree in Mechanical Engineering from Middle East Technical Universitty in June 1990. Upon graduation, he enrolled in the graduate program in Mechanical Engineering at the same university, and worked there as a research assistant for one year. In June 1991, he came to Mechanical Engineering Department of Lehigh University to continue his graduate studies. During his graduate studies at Lehigh, he worked as a research and teaching assistant.

END

OF

TITLE